SHIP

SCIENCE & TECHNOLOGY

CIENCIA & TECNOLOGÍA DE BUQUES

COTECMAR
COLOMBIA

ISSN 1909-8642 (Impreso)
ISSN 2619-645X (Online)

Vol. 11 - n.° 22
(1 - 96) January 2018

SHIP
SCIENCE & TECHNOLOGY
CIENCIA & TECNOLOGÍA DE BUQUES

Volume 11, Number 22 - January 2018 ISSN 1909-8642 (Impreso) - ISSN 2619-645X (Online)

COTECMAR

President
Rear Admiral **Javier Díaz Reina**

Vice President of Technology and Operations
Captain **Henry Helman Goyeneche Wilches**

Manager of Science, Technology and Innovation
Captain (R) **Carlos Eduardo Gil De los Ríos**

Editor in Chief
Captain (R) **Carlos Eduardo Gil De los Ríos**

Editorial Board

VADM Jorge Enrique Carreño Ph.D
COTECMAR, Colombia

Oscar Tascón Muñoz Ph.D
Armada Nacional de Colombia, Colombia

Hassan Ghassemi, Ph.D
Amirkabir University of Technology, Iran

Marcos Salas Inzunza Ph.D
Universidad Austral de Chile, Chile

Adan Vega Saenz Ph.D
Universidad Tecnológica de Panamá, Panamá

Marcos San Juan Ph.D
Universidad del Norte, Colombia

Jairo Useche Vivero Ph.D
Universidad Tecnológica de Bolívar, Colombia

Antonio Bula Silvera Ph.D
Universidad del Norte, Colombia

Juan Contreras Montes Ph.D
Escuela Naval de Cadetes Almirante Padilla, Colombia

Scientific Committee

Richard Luco Salman Ph.D
Universidad Austral de Chile, Chile

Luís Pérez Rojas Ph.D
Universidad Politecnica de Madrid, España

Rui Carlos Botter Ph.D
Universidad de Sao Paulo, Brasil

Wilson Adarme Jaimes Ph.D
Universidad Nacional de Colombia, Colombia

José María Riola Ph.D
Armada Española, España

Jairo Cabrera Tovar Ph.D
Universidad Tecnológica de Bolívar, Colombia

Diego Hernandez Lozada Ph.D
Universidad Nacional de Colombia, Colombia

Carlos Cano Restrepo M. Sc
COTECMAR, Colombia

Jymmy Saravia Arenas M.Sc
COTECMAR, Colombia

Ship Science & Technology is a specialized journal in topics related to naval architecture, and naval, marine and ocean engineering. Every six months, the journal publishes scientific papers that constitute an original contribution in the development of the mentioned areas, resulting from research projects of the Science and Technology Corporation for the Naval, Maritime and Riverine Industries, and other institutions and researchers. It is distributed nationally and internationally by exchange or subscription.

A publication of

Corporación de Ciencia y Tecnología para el Desarrollo de la Industria Naval, Marítima y Fluvial - COTECMAR
Electronic version: www.shipjournal.co

COTECMAR
COLOMBIA

Editorial Coordinator
Karen Dominguez Martínez M.Sc.;
Adriana Lucía Salgado Martínez M.Sc (C)

Layout and design Mauricio Sarmiento Barreto

Cover image designed by Vladimir González Castiblanco

Printed by C&D Publicidad & Marketing. Bogotá, D.C.

SHIP

SCIENCE & TECHNOLOGY

CIENCIA & TECNOLOGÍA DE BUQUES

Volume 11, Number 22 - January 2018 ISSN 1909-8642 (Impreso) - ISSN 2619-645X (Online)

SHIP
SCIENCE & TECHNOLOGY
CIENCIA & TECNOLOGÍA DE BUQUES

Editorial Note

Cartagena de Indias, January 18th, 2018.

In 2017, Cotecmar achieves important results in science, technology and innovation for the development of the naval, maritime and fluvial industry. As stated in our previous edition, one of the most important results was the fifth version of the International Ship Design and Naval Engineering Congress, described as a great success because it managed to bring together the scientific and technological community of this industry.

Likewise, international networks were strengthened by complying with the technology transfer plan between the ASMAR-SISDEF Alliance from Chile and COTECMAR, with the “LINK CO Project” for the co-development of a new technology in a Naval Tactical Network- Data Link. Great advances were obtained with the results of the Amazon River Patrol Project with EMGEPRON from Brazil and SIMA from Peru, and the completion of the preliminary design of the OPV 93, a vessel completely designed by the engineers of our Design and Engineering area. We close the year with the pride of had been recognized again with a new award as "Innovative Organization of the Year", delivered by the Simon Bolívar Award for Business Merit 2017; All this achievements thanks to our teamwork, oriented to the generation of value, the application of knowledge and innovation.

In this edition we open with an article for a reflection on naval and oceanic engineering, followed by a nomoto model of river support vessels. Two hydrodynamic works, the first of the OPV using CFD and the second on propellers and their effects. Methodology for the Experimental Analysis of Offshore Systems in Deep Water, Development of Materials for Maritime, Fluvial and Military Applications, and closing with an article on a Shipyard Model in Industry 4.0.

Finally, we invite our readers to join us in recognition to our first editor of the journal Number 01 Volume 01 of July 21th, 2007, Mr. Vice Admiral Jorge Enrique Carreño Moreno, President of Cotecmar in the period 2014 - 2017, who had the vision of fulfilling the social purpose of disseminating and appropriating science, technology and innovation as the main components for the development of the industry, and that today allows this journal to continue articulating knowledge networks and sharing the results of research and original contributions to science from the design and naval engineering. Thank you Mr. Vice Admiral Carreño, we wish you "Fair Winds and Following Seas".

Captain (Ret) CARLOS EDUARDO GIL DE LOS RÍOS
Ship Science and Technology Journal Editor

SHIP
SCIENCE & TECHNOLOGY
CIENCIA & TECNOLOGÍA DE BUQUES

Nota Editorial

Cartagena de Indias, 18 de Enero de 2018.

Cotecmar fiel a su misión obtiene en el año 2017 importantes logros en ciencia, tecnología e innovación para el desarrollo de la industria naval, marítima y fluvial, tal y como fue expuesto en nuestra edición anterior. Uno de los resultados más importantes fue la quinta versión del Congreso Internacional de Diseño e Ingeniería Naval, calificado como un gran éxito al lograr agrupar a la comunidad científica y tecnológica que representa esta industria en torno de un evento académico y de divulgación de primer nivel.

De igual manera se fortalecen las redes internacionales cumpliendo con el plan de transferencia tecnológica fruto de la Alianza entre la Unión Temporal ASMAR-SISDEF de Chile y COTECMAR, en el marco del Proyecto Red Táctica Naval Data Link – LINK CO, en el codesarrollo de nuevas tecnológicas de Comando y Control. Se obtienen grandes avances con los resultados del Proyecto Regional del Patrullero Amazónico en alianza con EMGEPRON de Brasil y SIMA de Perú y el hito de la culminación del diseño preliminar de la nueva Patrullera de Zona Económica Exclusiva denominada OPV 93, embarcación diseñada en su totalidad por el personal de la Gerencia de Diseño e Ingeniería; y cerrando el año con broche de oro al haber sido nuevamente reconocidos con un premio como “Organización Innovadora”, recibiendo el Premio Simón Bolívar al Mérito Empresarial 2017; todo esto gracias a la convicción de trabajar en equipo orientados a la generación de valor, la aplicación de conocimiento y la innovación.

En esta edición les presentamos artículos sobre la Ingeniería naval y oceánica, un modelo nomoto de embarcaciones de apoyo fluvial, dos trabajos de hidrodinámica; el primero, sobre la optimización de las formas de casco de la OPV usando CFD; y el segundo sobre hélices y sus efectos en la hidrodinámica del buque, Metodología para el Análisis Experimental de Sistemas Offshore en Aguas Profundas, Desarrollo de Materiales para Aplicaciones Marítimas, Fluviales y Militares, para cerrar con el artículo de Modelo de Astillero Industria 4.0.

Finalmente invito a nuestros lectores a unirnos en nuestro agradecimiento al primer editor de la revista No. 01 Vol. 01 del 21 de Julio de 2007, el Señor Vicealmirante Jorge Enrique Carreño Moreno, Presidente de Cotecmar en el periodo 2014 – 2017, quien tuvo la visión de cumplir con el propósito social de divulgar y apropiar la ciencia, la tecnología y la innovación como los principales componentes para el desarrollo de la industria, y que hoy nos permite disponer de este producto para continuar articulando redes de conocimiento y compartir los resultados de las investigaciones y aportes a la ciencia desde el diseño y la ingeniería naval. Muchas gracias señor Almirante por todos sus aportes, le deseamos buen viento y buena mar en sus próximos derroteros.

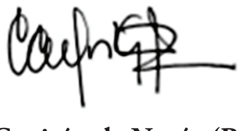

Capitán de Navío (RA) CARLOS EDUARDO GIL DE LOS RÍOS
Editor revista Ciencia y Tecnología de Buques

Naval and Oceanic Engineering: more than Ships and Offshore

Ingeniería Naval y Oceánica: más que Buques y Offshore

DOI: https://doi.org/10.25043/19098642.159

Marcos Salas [1]
Cristian Cifuentes [2]
Richard Luco [3]
Astrid Santander [4]
Gonzalo Tampier [5]
Claudio Troncoso [6]
Federico Zilic [7]

Abstract

Traditionally, Naval and Oceanic Engineering has been focused on research in surface and submarine ships; and fixed and floating offshore structures. More than 90% of world trade is transported by sea, so it is not surprising that most research efforts have been focused on making merchant ships more efficient and safer. Something similar is happening in the offshore industry driven by the demand for energy. Despite the evident need to perform research in the traditional fields of Naval and Oceanic Engineering, new challenges have caused universities and research centers to tackle new fields of research. This paper presents some of the research and innovations developed at the Institute of Naval and Maritime Sciences (ICNM) of the Austral University of Chile (UACH). These new frontiers for research address problems as diverse as the capturing of energy from waves and currents [1], the development of structures and systems for aquaculture [2], the design of autonomous underwater vehicles [3], the use of solar energy for the propulsion of small boats [4] and the design of floating ports for remote areas [5].

Key words: Innovation, Naval Engineering, Ocean Engineering.

Resumen

Tradicionalmente la Ingeniería Naval y Oceánica ha estado enfocada a la investigación en naves de superficie y submarinas; y estructuras offshore fijas y flotantes. Más del 90% del comercio mundial es transportado vía marítima por lo que no es de sorprender que la mayoría de los esfuerzos de investigación hayan sido enfocados a hacer los buques mercantes más eficientes y seguros. Algo similar ocurre en la industria offshore impulsada por la demanda de energía. No obstante la evidente necesidad de investigar en los campos tradicionales de la Ingeniería Naval y Oceánica, nuevos desafíos han hecho que las universidades y centros de investigación aborden nuevos campos de investigación. Este trabajo presenta algunas de las investigaciones e innovaciones desarrolladas en el Instituto de Ciencias Navales y Marítimas (ICNM) de la Universidad Austral de Chile (UACH). Estas nuevas fronteras para la investigación abordan problemas tan diversos como la captación de energía de olas y corrientes [1], el desarrollo de estructuras y sistemas para la acuicultura [2], el diseño de vehículos autónomos submarinos [3], el aprovechamiento de la energía solar para propulsión de pequeñas embarcaciones [4] y el diseño de puertos flotantes para zonas remotas [5].

Palabras claves: Innovación, Ingeniería Naval, Ingeniería Oceánica.

Date Received: June 2nd 2017 - *Fecha de recepción: Junio 2 de 2017*
Date Accepted: November 23th 2017 - *Fecha de aceptación: Noviembre 23 de 2017*

[1] Instituto de Ciencias Navales y Marítimas. Universidad Austral de Chile. Email: msalas@uach.cl
[2] Instituto de Ciencias Navales y Marítimas. Universidad Austral de Chile. Email: cristiancifuentes@uach.cl
[3] Instituto de Ciencias Navales y Marítimas. Universidad Austral de Chile. Email: rluco@uach.cl
[4] Instituto de Ciencias Navales y Marítimas. Universidad Austral de Chile. Email: astridsantander@uach.cl
[5] Instituto de Ciencias Navales y Marítimas. Universidad Austral de Chile. Email: gonzalo.tampier@uach.cl
[6] Instituto de Ciencias Navales y Marítimas. Universidad Austral de Chile. Email: claudio.troncoso@uach.cl
[7] Instituto de Ciencias Navales y Marítimas. Universidad Austral de Chile. Email: efe011@gmail.com

Introduction

The Institute of Naval and Maritime Sciences has a long history of research and innovation. It has several laboratories, including its own hydrodynamic test channel. Many of its research efforts make use of experimental methodologies using scale models. Traditionally, test channels have been used to determine vessel resistance and wave behavior, however, with the right instruments it can be used in objectives as diverse as measuring the efficiency of wave energy converters [6] or tidal turbine forces. The experimental tests are also compared with computer simulations made with CFD tools.

Marine Energies

The ICNM is part of the recently created Center for Research and Innovation of Marine Energy (MERIC), a consortium composed of Universities and Research Centers funded by the Government of Chile with the express objective of promoting research in the field of non-conventional renewable energies (NCRE). The work of the ICNM in this field specifically consists of investigating the devices that capture wave energy [6], the so-called WEC (Wave Energy Converter) mechanisms and the capture of tidal energy [7].

Chile's energy demand has been growing in the last decades and it is expected to continue increasing with the development of the country. Conventional sources of renewable energy, such as traditional hydroelectric power plants, are almost fully exploited or exposed to strong opposition from environmental groups. In the current situation, more than half of the electricity required by Chile is produced by thermal power plants that burn oil, coal or gas. The Chilean government is fully aware of this vulnerability and is making efforts to increase the contribution of other sources of renewable energy; it is intended that by 2025, 20% of the energy consumed in the country will come from NCRE.

The wave energy potential in Chile is among the largest in the world, with an energy potential that has been estimated between 164 and 240 GW [8]. Although significant advances have been made in the development of wave energy converters (WEC) over recent years, they are still considered to be at an early stage of development, compared to other NCRE technologies, such as wind, hydroelectric or solar energy.

The region of the Chilean fjords, between the 41º 30` and 55º parallels, is perhaps the most suitable for tidal projects, not only because the currents are strong and predictable, but also because there is almost no efficient alternative. In this region there are many small towns and hundreds of fish farming centers, isolated and without access to the electricity grid. Here electricity is produced mainly by generators, sometimes during limited hours of the day.

This section shows the evaluation of a WEC, with a scale model, in which its response was measured under different wave conditions in the test channel, as shown in Fig. 1. The experimental configuration for the converter WEC consisted of two ultrasonic measuring instruments for incident waves and WEC movement, an adjustable damper connected to a load cell to measure force and data acquisition software (LabView). The experimental results were compared with the numerical results obtained by WAMIT in the form of transfer function and output power. The comparative are in accordance with the variation of the set of wave frequency parameters, wave height and damping factors as shown in Fig. 2. These developments are the first steps towards the specialization of this tank in

Fig. 1. WEC in Canal tests

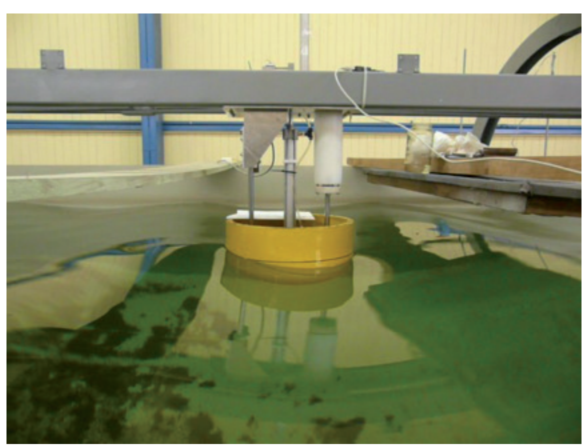

Fig. 2. FEM turbine analysis

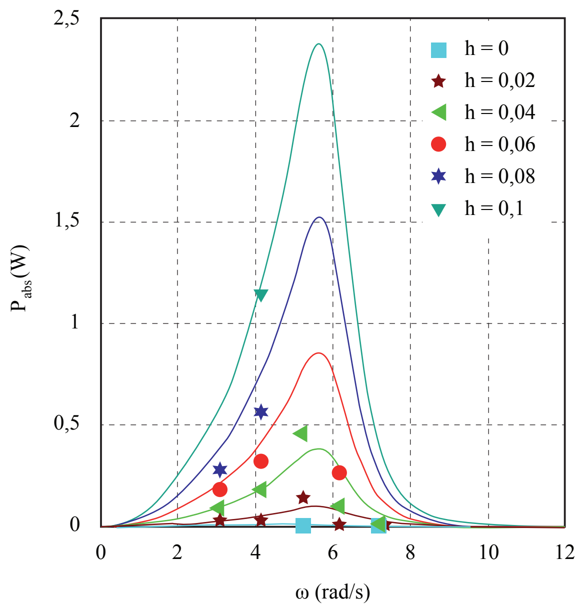

Experimental hydrodynamics of marine renewable energy technologies.

In another aspect of marine energy research, the development of a hydrokinetic rotor is included in the evaluation of a horizontal axis rotor using NACA profiles, as well as NREL profiles (National Renewable Energy Laboratory). Different configurations of the profile along the propeller blades were used for the design of these rotors. Configurations were evaluated in terms of efficiency, structural integrity, and cavitation. The investigation consisted of a fluid-dynamic evaluation of the hydrokinetic rotor blades, considering the rotor running inside a diffuser. The performance evaluation was carried out using the blade element method and in the structural evaluation, using the finite element method. For the selection of the design, an optimization process was defined to determine the configuration of profiles that best meet the established design requirements. The results of this work show the need for design profiles that consider the exclusive requirements of its use in a hydrokinetic rotor.

For the realization of the fluid-dynamic analysis of the rotor, the Qblade program was used, a program that integrates XFOIL in a rotor design and analysis environment using the blade element momentum method (BEM), allowing the design and dynamic calculation of the rotor blades. XFOIL is a free computer program that allows the distribution of pressures on the faces of the profile to be calculated together with its performance coefficients. The results obtained allow NREL profiles to be established with the characteristics that allow more efficient rotors to be designed in comparison with the NACA profiles. Figs. 3 and 4 show the results for both rotors.

Fig. 3. Power Coefficient

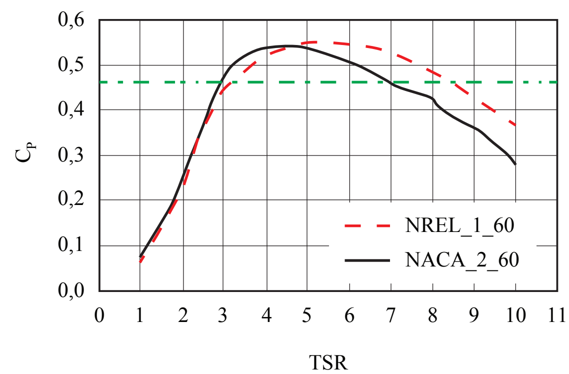

Fig. 4. Thrust Coefficient

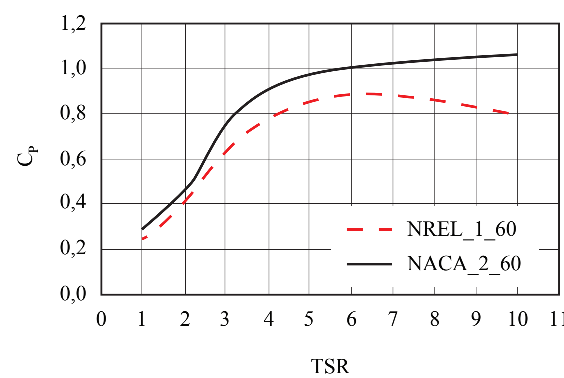

Engineering Applications in Aquaculture

The development of large-scale aquaculture in countries such as Norway and Chile has led naval architects and ocean engineers to develop studies, both numerical and experimental, to determine the forces and corresponding deformation of flexible structures such as the nets used in floating cages. The culture centers, mainly for salmon, operate with square or circular shape cages (Fig. 5), installed in protected areas such as bays and inside channels and fjords, to avoid the effect of waves and currents present in the open sea. The feeding of the fish is done by automated systems installed on a pontoon as shown in Fig. 6. The basic components of the cages are: a float that acts as a flotation reserve to support the weight of the net and shapes the same, the net, which encloses the production volume where the fish and the ballast system are found, which extend the net and help to control the deformation of the same when faced with current loads.

Fig. 5. Farming center in southern Chile (www.sermar.cl)

Fig. 6. Feeder and control pontoon

The study of the hydrodynamic behavior of raft cages is complex due to the dependence between the drag force on the nets and the deformation of the same. In the same way, for circular cages constructed out of HDPE (High Density Polyethylene), the rings that form the surface float deform when facing wave loads, directly influencing the tensions in the mooring lines.

Additionally, the reduction of current speed when crossing networks, a phenomenon known as the shadow effect, adds complexity to numerical and experimental modeling. This effect has a direct impact on the volume available inside the cages [9]. Several studies, including those covering the behavior of the fish inside the cages, biofouling on the nets and flow into the culture centers have been developed by various specialists to improve production in increasing the safety of these structures.

There are several numerical methods for estimating the hydrodynamic response of cages. The nets have been modeled using consistent bar elements in a finite element model, panel elements and finite element models using bars and buoys that allow the submerged weight of the network to be adjusted to create a reduced model of elements that simulates the mechanical properties and inertial network in the physical model [9]. An example of results obtained by the bar and buoy method can be seen in Fig. 7, which also includes the study of the density of elements in direct comparison with the deformation resulting from experimental tests.

Regarding the response of the cages to waves, it has been determined that the forces on the mooring lines are directly related to the wave height [10]. In the face of combined wave and current effects, depending on the combination of height and wave period and current speed, the effect of wave loading can be of the same importance range as current charging, which implies a careful modeling of both effects.

In exposed areas, fish farms must operate autonomously with minimal human intervention and the cage anchoring system will be shared with the platform that houses equipment and food for the fish. Results obtained for systems exposed to extreme wave and current conditions, both in numerical models and field tests, demonstrate the feasibility of the installation and operation of these structures and open the door for the future development of the industry in exposed areas [11].

Fig. 7. Comparison of deformations in networks subject to current [9]

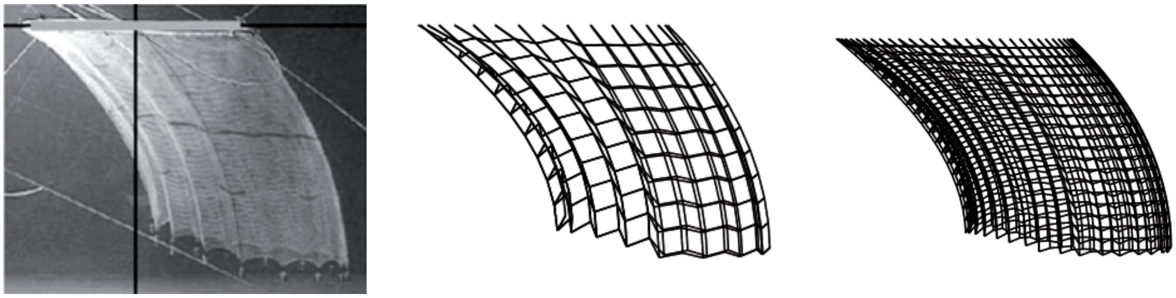

a) Experimental model b) Numeric thick mesh c) Numeric fine mesh

In the open sea conditions are optimal for fish due to the constant exchange of nutrients in the water column. The almost unlimited availability of space would allow the production of a greater volume of fish, in addition to opening up of areas to new species with greater commercial value.

The development of aquaculture depends on an increase in both numerical and experimental research and field research, where naval and oceanic engineers can contribute their knowledge. The use of the knowledge gained in the design, construction and operation of ships and floating structures can and should be transferred to fish farms to ensure sustainable and sustainable development in offshore aquaculture.

Autonomous Submarine Vehicles

Unmanned underwater vehicles are divided into ROVs (Remote Operated Vehicles or remotely operated vehicles), devices connected via a cable to a station or surface vessel; AUVs (Autonomous Underwater Vehicles or autonomous underwater vehicles) that operate autonomously and without physical connection to the surface, which use some form of artificial intelligence; and a third group of hybrid vehicles that is a combination of the previous two.

One of the lines of research in force at the ICNM is the development of an autonomous submarine vehicle or AUV. Design criteria were established based on a proposed oceanographic study for a coastal area of Chile (39º 48'30 ''S 73º14'30''W), which covers the entire continental shelf of said geographical area (4100 Km^2). The maximum distance from the coast is 26 NM, while the minimum distance is 16 NM, with depths reaching up to 200 m. The device must be able to navigate without human intervention from the coast to the limit of the platform, to later return.

The basic design has a length of 2 m with a circular master section of 160 mm in diameter, with a cylindrical central watertight compartment of 1 m in length, watertight lids at its ends and two flooded compartments of 0.5 m at both ends. To date, a prototype tele operated in the Hydrodynamic Test Channel of the Universidad Austral has been tested with successful results in mechanical and hydrodynamic systems tests. A second prototype is currently under construction in accordance with the preliminarily design requirements established and that will be able to perform missions in open and protected waters.

Given the characteristics of the environment, it is extremely difficult to establish communication with a ground station since salt water cancels the electromagnetic signals, while acoustic systems are expensive and limited in their range of operation. Moreover, the signals of the global positioning systems can only be obtained on the surface, so when submerging the AUV must use the other on-board measuring devices to navigate by estimating control signals.

The AUV in development will have an artificial intelligence system to navigate without human intervention and only using an initial programming defined by the user. The basis of this system is

Fig. 8. AUV in Channel tests

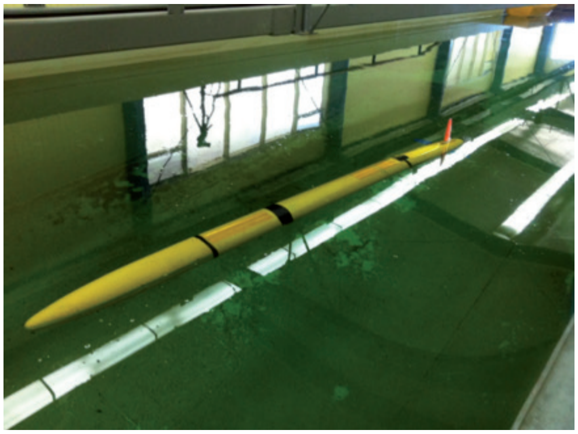

Fig. 9. AUV configuration

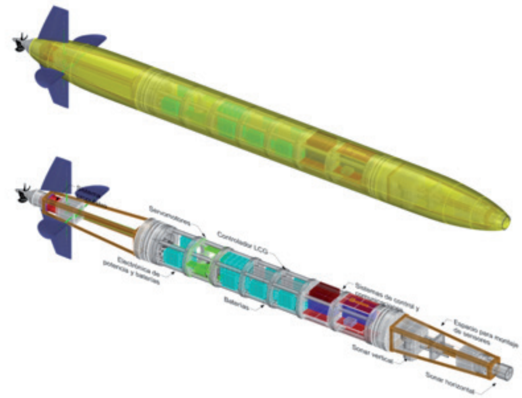

software capable of processing the information coming from sensors (accelerometer, gyroscope, magnetometer, sonar, GPS, etc.) and can, therefore, generate useful control signals to achieve the fulfillment of the mission.

The device has a multipurpose area in the bow for the assembly of measurement equipment, either cameras to capture images or sensors for measuring environmental parameters. This area has been specifically designed so that the device can serve any type of user.

The potential of the platform includes substantially improving the environmental monitoring capabilities sustained over time and greater efficiency, which will benefit aquaculture companies, government entities and port agencies, in addition to others.

Solar energy for small electric propulsion boats

The main disadvantage of electric propulsion systems in smaller ships lies in the limited capacity to store energy on board, due to the large weight and volume of batteries required. For this reason the power of the engine is generally modest and consequently the speed of the boat it is relatively low compared to what could be achieved by a conventional propulsion system based on an internal combustion engine. This is the reason why electric propulsion in smaller vessels is almost exclusively limited to displacement hulls in the low speed range, where the resistance to advancement is minimal.

The advantages of electric propulsion are; a very quiet operation, without the emission of pollutants to the environment and virtually no maintenance of the engines, compared to internal combustion engines, which must be subject to periodic preventive maintenance, in addition to being permanently subject to potential damage of parts due to failure of lubrication, cooling and corrosion, which directly affects the operating costs of the engine. On the other hand, the limited autonomy that depends on the storage capacity of the batteries, can be increased by having on-board photovoltaic panels, normally on flat surfaces in roofs or ceilings. This allows the batteries to be recharged continuously, provided natural light is available.

Having recognized the advantages and disadvantages of electric propulsion, this section shows a vessel in operation for the transport of passengers in the city of Valdivia. Table 1 shows the main characteristics of the boat that was built by Alwoplast shipyards (www.alwoplast.cl). The boat has been designed with the minimum possible displacement and for this purpose the hull is constructed from composite materials. Its main use is the daytime transportation of passengers in the rivers of the city of Valdivia. Trips are limited to a few hours and the battery bank has been sized to provide the necessary energy for each trip, at the end of which the boat returns to its base port in the city.

Table 1. Main characteristics of the solar boat

Total length	9.5 m
Sleeve	3.0 m
Strut	1.4 m
Openwork	0.35 m
Displacement	4.8 t
Passengers (crew)	12
Crew	1
Maximum speed	6 knots
Speed system	displacement
Engine power	4 KW
DC	48V
Solar panels	1.6 KW
Hull material	compounds

Fig. 10. Boat with electric propulsion operating in Valdivia, Chile. [4]

A roof covered with photovoltaic panels has been designed, see Fig. 10, normally placing a heavy weight on deck that could be a problem for the stability of the boat. However, this moderate weight is amply compensated by the greater weight of the battery bank, conveniently located as low as possible. The panels continually recharge the batteries during the trip in daytime conditions. Notwithstanding the above, recharging batteries during the trip is not necessary, if at the beginning of the trip the batteries are at full capacity.

There is also the possibility of recharging the bank during the night connecting a charger to the local electrical network. This is not necessary if the boat stays the next day in port, with the load being achieved through solar panels, without incurring electricity costs. The electric propulsion is extremely silent, which is especially advantageous in a passenger vessel.

Currently there are 3 vessels with solar propulsion operating in Valdivia. The results, after several years of operation have been satisfactory, which means that the costs of maintenance and operation of the propulsion system are practically null. Passengers are extremely satisfied with the silent and non-polluting navigation.

Design of floating ports for remote areas

The south of Chile is an area of extreme difficulty of access, the existence of thousands of islands and canals makes the construction of roads extremely difficult and in many cases maritime transport is the main supply route, and ports and appropriate conditions must be provided to ensure the connectivity of those regions. The Government of Chile has developed a connectivity program for remote regions that, among other solutions, has favored the construction of floating ports.

According to Tsinker [5], it is advisable to install a floating dock where:

- It has protected waters, where the waves generated by the wind or the movement of boats do not exceed 1 to 1.5 m in height,
- Where the soil quality does not allow foundations for fixed structures.
- The change in sea levels is high due to the large difference in tides.
- In seismic zones, since floating docks are less affected by earth movements during an earthquake.

Main components of a floating port

The main components of a floating port are the following:

- Floating pontoon
- Access bridge
- Anchoring and mooring system

The floating pontoon is a naval artifact, which is designed to meet certain functionality requirements (load capacity, vehicle / people traffic, deck area, behavior at sea, others). Depending on the design requirements of the dock, it can be designed using several configurations, including one or more modules joined by a continuous cover or a pivoting mechanism. Although it is a simple hydrostatic problem, careful attention must be paid to the rolling load displacement on the deck, to avoid displacements or rotations of the pontoons that may impede proper operation, see Figs. 11 and 12.

The access bridge is the connection between the pontoon and the coast, which must be designed to provide an effective solution for the traffic of vehicles, cargo and people. Considering that there are variations in the water level (changes of tide in the sea, changes of seasonal levels in lakes and rivers) in the site of the bridge, the use of articulations should be considered in its design, allowing the bridge to vary the position from the end on which it is resting on the pontoon. In addition to its design, special care must be taken in verifying the angle of inclination reached by the bridge in the different water level conditions.

The pontoon mooring system must allow the safe and efficient operation of the floating dock, keeping the dock in a stable relative position with respect to the access bridge. Mooring systems can be composed of elements that are deployed on the coast or offshore, which can be of anchor line type, anchor pillars or articulated beams.

In addition to the static analysis of the load on the pontoons, the dynamic effects must also be considered, environmental loads such as waves or the effect of wind must be considered. The dynamic analysis of the movement of ships is well documented, however, for floating structures the problem has additional variables. Due to the

Fig. 11. Effect of moving a load on pontoons with different buoyancy reserves

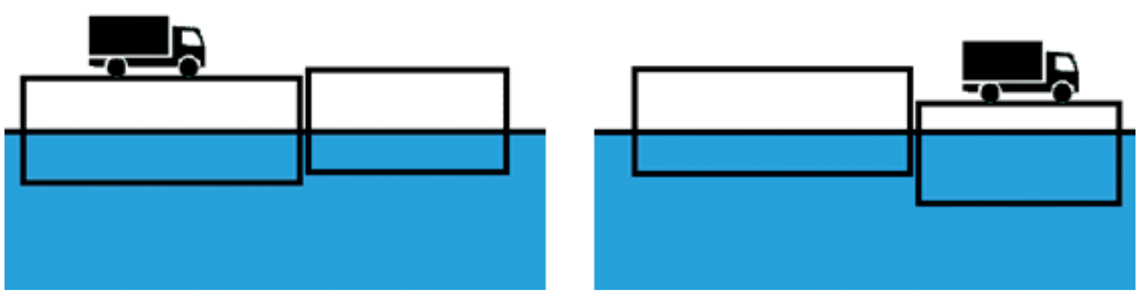

Fig. 12. Effect of positioning a load on a pontoon fixed to another by means of an articulated joint

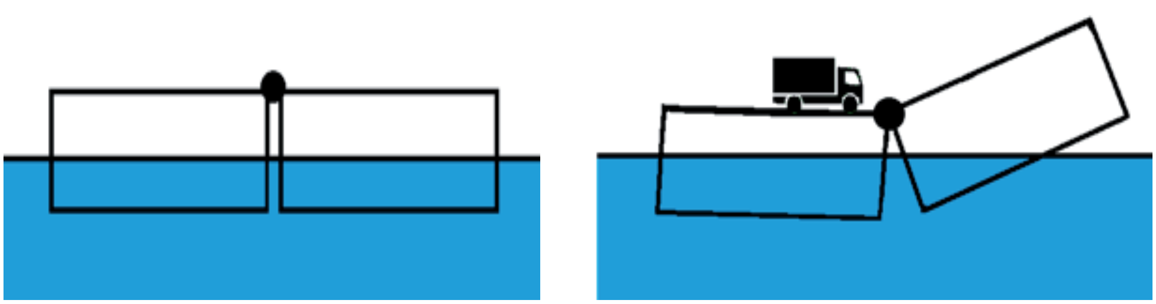

complex interaction between the floating structures, the anchoring and the fluid medium, it is advisable, in addition to the analytical studies and numerical simulations, to carry out experimental tests with scale models, considering the characteristic waves and the bathymetry of the place where a floating port is proposed. It is important to determine the significant wave height and period that determines the closure of the port due to unsafe operating conditions, taking as a criterion the limits that ensure comfortable work on the floating port. for which the limits defined in Table 2 can be taken as an example. In addition to establishing criteria for the closure of port operations, the floating structure must be designed to survive extreme conditions that ensure its useful life, for example, 100 years. Fig. 13 shows wave tests for a floating port in southern Chile, under typical conditions imposed by the zone fetch, 13a, and Fig. 13b shows waves with a return period of 100 years.

Conclusions

It is clear that professional training must be flexible enough to adapt to the new challenges that Naval and Oceanic Engineers needs to address. The experience of the labor market in Chile indicates that the training is comprehensive and appropriate for the requirements of the industry. In Chile there are many Naval Engineers developing vessels and systems for aquaculture, including high speed vessels for transporting personnel, control and habitability pontoons, automatic pneumatic feeding systems capable of feeding hundreds of thousands of fish, wellboats capable of transporting live salmon under controlled PH conditions with optimum temperature and oxygenation. Innovation in aquaculture is through the application of various buoyant materials, new environmentally friendly antifouling systems, safer anchoring systems and the projection of the industry indicates that the

Table 2. Criteria for accelerations and roll angle (NORDSFORK, 1987)

Level	Comfort criteria (rms)			
	Description	**Vertical Acceleration**	**Transverse Acceleration**	**Roll**
I	Light manual work	< 0.20 g	< 0.10 g	< 6.0 º
II	Heavy manual work	< 0.15 g	< 0.05 g	< 4.0 º
III	Intellectual work	< 0.10 g	< 0.05 g	< 3.0 º
IV	Transit of passengers	< 0.05 g	< 0.04 g	< 2.5 º
V	Passengers on cruise ships	< 0.02 g	< 0.03 g	< 2.0 º

Fig. 13a. Wave tests typical condition given by fetch. H1 / 3 = 0.52 m T = 2.99

Fig. 13b. Wave tests return period 100 years. H1 / 3 = 1.38 m T = 4.15 s

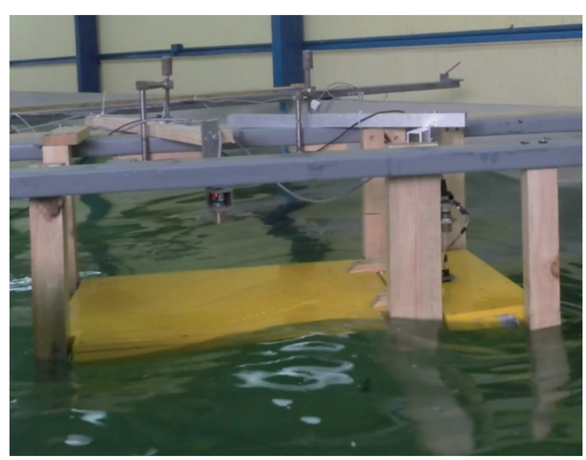

future trend is to develop offshore systems that will be able to withstand exposed sea conditions. More recently, the need to take advantage of new sources of renewable energy makes it possible for Naval Engineers to design systems to obtain energy from the waves and currents generated by the tides in Chilean channels. It is difficult to predict what new challenges will exist for the future generations of Naval and Oceanic Engineers, perhaps the only sure thing to affirm is that Naval and Oceanic Engineering is a profession that must always provide innovative solutions for the benefit of society and the environment.

References

[1] TAMPIER, G.; SALAS, M.; TRONCOSO, C. AND GRÜTER, L. *"Wave Energy Converter and Hydrokinetic Rotor Developments in Chile"*. 10th Annual Energy Harvesting Workshop. Blacksburg, USA, September 13 - 16, 2015.

[2] SALAS, M. AND DI GIROLAMO G. *"Engineering Applications in Chilean Aquaculture"*. Journal of Ocean Technology. Vol. 5 Nº2, 2010.

[3] ZILIC, F.; G. TAMPIER; R. LUCO. *"Desarrollo de Vehículo Submarino Autónomo para Exploración Oceanográfica"*. XXIV Congreso Panamericano de Ingeniería Naval. 18 al 22 de Octubre 2015 , Montevideo, Uruguay.

[4] SALAS, M.; LUCO, R. AND EKDAHL, H. *"Energía Solar para Propulsión de Embarcaciones Fluviales"* First International Conference IDS2013 – Amazonia, 17th-19th July 2013, Iquitos, Peru.

[5] Tsinker, G.P. Floating Ports 1986

[6] TAMPIER, G. AND GRÜTER, L. *"Development of an experimental test bed for Wave Energy Converters"*. WTE'14 -First Workshop on Wave and Tidal Energy, Valdivia, Chile. 29th to 31st October 2014.

[7] TRONCOSO, C. AND TAMPIER, G. *"Design of Hydrokinetic Rotor using NACA and NREL Profiles"*. WTE'14 -First Workshop on Wave and Tidal Energy, Valdivia, Chile. 29th to 31st October 2014.

[8] MONÁRDEZ, P. *et al.*; *"Evaluation of the potential of wave energy in Chile",* OMAE2008 – International Conference on Offshore Mechanics and Arctic Engineering, 2008.

[9] C. CIFUENTES AND M. H. KIM, *"Numerical simulation of wake effect in nets under steady current"*, in Proceedings of the ASME 2015 34th International Conference on Ocean, Offshore and Arctic Engineering OMAE2015, 2015, pp. 1–10.

[10] C. CIFUENTES, *"Dynamic analysis of cage systems under waves and current for offshore applications"*, Texas A&M University, 2016.

[11] C. CIFUENTES AND M. H. KIM, *"Dynamic analysis for the global performance of an SPM-feeder-cage system under waves and currents"*, China Ocean Eng., vol. 29, no. 3, pp. 415–430, 2015.

Obtaining First and Second Order Nomoto Models of a Fluvial Support Patrol using Identification Techniques

Obtención de Modelos de Nomoto de Primer y Segundo Orden de una Patrullera de Apoyo Fluvial empleando Técnicas de Identificación

DOI: 1https://doi.org/10.25043/19098642.160

Sandra Carrillo [1]
Juan Contreras [2]

Abstract

In this paper we present a method for obtaining a second order Nomoto model that describes the yaw dynamic of a Patrol River Boat. This model is obtained from experimental input and output data gathered from the turning circle maneuver. System identifications techniques and a gray box model are employed to find the coefficients of the Nomoto model. The results of the identification process as well as the results of validation process are presented.

Key words: second order Nomoto model, coefficients of Nomoto, maneuverability, system identification, gray box model.

Resumen

Este artículo describe la obtención del modelo de Nomoto de segundo orden para una patrullera de apoyo fluvial PAF a partir de datos experimentales, derivados de pruebas estándares de maniobra realizadas en aguas poco profundas. Se utilizan técncias de identificación de sistemas y un modelo de caja gris que permite extraer los coeficientes del modelo de Nomoto. Se presentan los resultados del proceso de identificación, así como de los procesos de validación utilizando datos de pruebas diferentes a la empleada en la identificación.

Palabras claves: modelo de Nomoto de segundo orden, coeficientes de Nomoto, mabiobrabilidad, identificación de sistemas, modelo de caja gris.

Date Received: July 1st 2017 - *Fecha de recepción: Julio 1 de 2017*
Date Accepted: November 23th 2017 - *Fecha de aceptación: Noviembre 23 de 2017*

[1] Escuela Naval de Cadetes Almirante Padilla, Cartagena, Colombia. Email: spcarrillo@gmail.com
[2] Escuela Naval de Cadetes Almirante Padilla, Cartagena, Colombia. Email: epcontrerasj@ieee.org

Introduction

According to the International Maritime Organization, IMO, the International Association of IMCA Marine Contractors, and other classes of certification societies, a dynamic positioning vessel is related to the automatic control of the position of the vessel and the course with respect to one or more position references for the use of active propellers [1]. Maintaining the course of a vessel is a complex problem due to the vessel's non-linear dynamics, but it has a great impact on the economy, safety and operation of vessels [2,3].

For the description of the dynamics of surface vehicles, the authors have used different types of models, such as the Nomoto model [4,5,6], the Norbin model [7] and others.

For the data of the tests the Patrol Boat of Heavy Fluvial Support "PAF-P" of 3rd generation built by COTECMAR 2009 has been taken as a study model. The ship was subjected to the approval of an evolutionary circle at different approach speeds and rudder angles. , zig-zag and emergency stop in shallow water (H / T = 2.4) and deep water (H / T> 10) [8,9].

Linear Maneuver Model

Equations of rigid body dynamics

The equations that control the dynamics of a ship are derived from the equations of motion of a rigid body with 6 degrees of freedom. These equations are shown below in vector form [10]:

$$M_{RB}\dot{v} + C_{RB}(\dot{v})v = \tau_{RB} \tag{1}$$

Where M_{RB} is the mass matrix, C_{RB} is the centripetal and coriolis matrix, v is the angular and linear velocity vector of the rigid body ($[u, v, w, p,q, r]^T$) and τ_{RB} is the generalized vector of external forces and moments ($[X, Y, Z, K, M, N]^T$).

From equation (1) an expansion of the terms of the 6 degrees of freedom is made [10]:

$$\begin{array}{ll}
m | \dot{u} \quad vr | wq \quad x_G(q^2 | r^2) | y_G(pq \quad \dot{r}) | z_G(pr | \dot{q}) | & X \\
m | \dot{v} \quad wp | ur \quad y_G(r^2 | p^2) | z_G(qr \quad \dot{p}) | x_G(qp | \dot{r}) | & Y \\
m | \dot{w} \quad uq | vp \quad z_G(p^2 | q^2) | x_G(rp \quad \dot{q}) | y_G(rq | \dot{p}) | & Z \\
l_x \dot{p} | (l_z \quad l_y) qr | m | y_C(\dot{w} \quad uq | wp) \quad z_C(\dot{v} \quad wp | ur) | & K \\
l_y \dot{q} | (l_x \quad l_z) rp | m | x_C(\dot{u} \quad vr | wq) \quad x_C(\dot{w} \quad uq | vp) | & M \\
l_z \dot{r} | (l_y \quad l_x) pq | m | x_C(\dot{v} \quad vp | ur) \quad y_C(\dot{u} \quad vr | wq) | & N
\end{array} \tag{2}$$

Where *X, Y, Z* are external and hydrodynamic disturbing forces and *K, M* and *N* are hydrodynamic and external disturbance moments.

To simplify this model of equations of six degrees of freedom to 3 degrees, the following assumptions are made:

1. The ship is symmetric around the *x-z* plane ($I_{xy} = I_{yz} = y_G = 0$) .
2. The vessel has a homogeneous mass distribution.
3. The fixed origin of the body is selected as $r_G = [x_G \;\; 0 \;\; z_G]^T$ (lxz = 0)
4. The tipping, tilt and roll are ignored ($q = w = p = 0$).

This produces three simplified nonlinear equations:

$$\begin{array}{ll}
\textit{surge:} & m(\dot{u} - vr - x_G r^2) = X \\
\textit{sway:} & m(\dot{u} + ur + x_G \dot{r}) = Y \\
\textit{yaw:} & l_z \dot{r} | m x_G(\dot{v} | ur) \quad N
\end{array} \tag{3}$$

The disturbed equations of motion are based on an additional assumption:

- The speed of deviation (sway) v, and the yaw rate r and the rudder angle δ are small.

This implies that the mode of advance (surge) can be dissociated from the yaw and deflection modes assuming that the average speed of advance u_0 is constant for a constant thrust. In the same way, it is assumed that the average yaw and yaw velocities are $v_0 = r_0 = 0$. As such:

$$\begin{array}{lll}
u = u_0 + \Delta u; & v = \Delta v; & r = \Delta r \\
X = X_0 + \Delta X; & Y = \Delta Y; & V = \Delta V
\end{array}$$

Where Δu, Δv and Δr are small disturbances of nominal values u_0, v_0 and r_0 , and ΔX, ΔY and ΔZ

are small disturbances of nominal values $X_{0,}\ Y_0$ and N_0.

Assuming that higher order disturbances can be neglected, the nonlinear equations of motion can be expressed as:

$$\begin{aligned} m\Delta\dot{u} &= X_0 + \Delta X \\ m(\Delta\dot{u} + u_0\Delta r + x_G\Delta\dot{r}) &= \Delta Y \\ l_z\Delta\dot{r} + mx_G(\Delta\dot{u} + u_0\Delta r) &= \Delta N \end{aligned} \tag{4}$$

Note that the governing equations of motion are completely decoupled from the velocity equation.

$$\begin{aligned} &\text{velocity equation:} && m\Delta\dot{u} = X \\ &\text{gobernance equation:} && m(\dot{u} + u_0 r + x_G\dot{r}) = Y \\ & && l_z\dot{r} + mx_G(\dot{u} + u_0 r) = N \end{aligned} \tag{5}$$

The assumption that the average forward speed is constant implies that this model is only valid for small rudder angles.

First-order Nomoto equation

Starting from the governance equation:

$$l_z\dot{r} + mx_G(\dot{u} + u_0 r) = N$$

Reorganizing and replacing the governance time constant $T = lz / mx_G u_0$ and the rudder gain $K = N / \delta_R mx_G u_0$ would be expressed as the First Order Nomoto Equation of the form [11]:

$$T\dot{r} + r = K\delta_R$$

Or alternatively:

$$T\ddot{\psi} + \dot{\psi} = K\delta_R \qquad con\ \dot{\psi} = r \tag{6}$$

Reorganized the equation to the state-space form $x = Ax + Bu$ y $y = Cx$, The First Order Nomoto model becomes:

$$\begin{aligned} \begin{bmatrix}\dot{\psi}\\ r\end{bmatrix} &= \begin{bmatrix}0 & 1\\ 0 & -\frac{1}{T}\end{bmatrix}\begin{bmatrix}\psi\\ r\end{bmatrix} + \begin{bmatrix}0\\ \frac{K}{T}\end{bmatrix}\delta_R \quad \textit{(Constant Time form)} \\ \begin{bmatrix}\dot{\psi}\\ r\end{bmatrix} &= \begin{bmatrix}0 & 1\\ 0 & a_{22}\end{bmatrix}\begin{bmatrix}\psi\\ r\end{bmatrix} + \begin{bmatrix}0\\ b_2\end{bmatrix}\delta_R \quad \textit{(Parametric form)} \end{aligned} \tag{7}$$

Second order Nomoto equation

A second-order deviation-yaw model is obtained from the motion equations with 3 degrees of freedom and uncoupled in advance, assuming small perturbations we have:

Governance equiations

$$m(\dot{u} + u_0 r + x_G\dot{r}) = Y$$

$$l_z\dot{r} + mx_G(\dot{u} + u_0 r) = N$$

Assuming the origin in the center of gravity (x_G = 0). The linear theory suggests that hydrodynamic force and momentum can be modeled as *(Davidson and Schiff, 1946)* [12]:

$$\begin{aligned} Y &= Y_{\dot{v}}\dot{v} + Y_{\dot{r}}\dot{r} + Y_v v + Y_r r + Y_\delta\delta_R \\ N &= N_{\dot{v}}\dot{v} + N_{\dot{r}}\dot{r} + N_v v + N_r r + N_\delta\delta_R \end{aligned} \tag{8}$$

Therefore, we can write the equations of motion in the form of state-space according to:

$$M\dot{v} + N(u_0)\,\dot{v} = b\delta_R$$

and the Nomoto model is obtained:

Where $v = [v,r]^T$ is the state vector, δ_R the rudder angle, and:

$$M = \begin{bmatrix} m - Y_{\dot{v}} & mx_G - Y_{\dot{r}} \\ mx_G - N_{\dot{v}} & l_z - N_{\dot{r}} \end{bmatrix}; \qquad N_{(u_0)} = \begin{bmatrix} -Y_v & mu_0 - Y_r \\ -N_v & mx_G u_0 - N_r \end{bmatrix};$$

$$b = \begin{bmatrix} Y_\delta \\ N_\delta \end{bmatrix}$$

The $N(u_0)$ matrix is obtained by the is obtained by the linear sum of the damping D and the terms of Coriolis $C(u_0)$ and centripetal (additional terms mu_0 and $mx_G u_0$), which means:

$$N_{(u_0)} = C_{(u_0)} + D$$

The corresponding space-state model is obtained, leaving $v = [v,r]^T$ is the state vector and $u = \delta_R$.

As such:

$$\dot{x} = Ax + b_1 u$$

with:

$$A = -M^{-1}N = \begin{bmatrix} a_{11} & a_{12} \\ a_{21} & a_{22} \end{bmatrix}; \qquad b_1 = -M^{-1}b \begin{bmatrix} b_1 \\ b_2 \end{bmatrix}$$

The coefficients are defined as [13]:

$$a_{11} = \frac{(l_z - N_{\dot{r}})\, Y_v - (mx_G - Y_{\dot{r}})\, N_v}{det\ (M)}$$

$$a_{12} = \frac{(l_z - N_{\dot{r}})\, (Y_r - mu_0) - (mx_G - Y_{\dot{r}})(N_{\dot{r}} - mx_G u_0)}{det\ (M)}$$

$$a_{21} = \frac{(m - Y_{\dot{v}})\, N_v - (mx_G - N_{\dot{v}})\, Y_v}{det\ (M)}$$

$$a_{22} = \frac{(m - Y_{\dot{v}})\, (N_r - mx_G u_0) - (mx_G - N_{\dot{v}})\, (Y_{\dot{r}} - mu_0)}{det\ (M)} \tag{9}$$

$$b_1 = \frac{(l_z - N_{\dot{r}})\, Y_\delta - (mx_G - Y_{\dot{r}})\, N_\delta}{det\ (M)}$$

$$b_2 = \frac{(m - Y_{\dot{v}})\, N_\delta - (mx_G - N_{\dot{v}})\, Y_\delta}{det\ (M)}$$

These models are obtained by eliminating the deviation speed from $M\dot{v} + N(u_0)\,\dot{v} = b\delta_R$ to get the Nomoto transfer function between r and δ_R, which is:

$$\frac{r}{\delta_R}(s) = \frac{K_R(1 + T_3 s)}{(1 + \ \ s)\,(1 + T_2 s)} \tag{10}$$

The parameters of the transfer function are the relationships with hydrodynamic derivatives such as:

$$T_1\, T_2 = \frac{det\ (M)}{det\ (N)}$$

$$T_1 + T_2 = \frac{n_{11}m_{22} + n_{22}m_{11} - n_{12}m_{21} - n_{21}m_{12}}{det\ (N)}$$

$$K_R = \frac{n_{21}b_1 - n_{11}b_2}{det\ (N)} \tag{11}$$

$$K_R T_3 = \frac{m_{21}b_1 - m_{11}b_2}{det\ (N)}$$

Where the elements n_{ij}, m_{ij} and b_i are defined as:

$$M = \begin{bmatrix} m - Y_{\dot{v}} & mx_G - Y_{\dot{r}} \\ mx_G - N_{\dot{v}} & l_z - N_{\dot{r}} \end{bmatrix}; \qquad N_{(u_0)} = \begin{bmatrix} -Y_v & mu_0 - Y_r \\ -N_v & mx_G u_0 - N_r \end{bmatrix};$$

$$b = \begin{bmatrix} Y_\delta \\ N_\delta \end{bmatrix}$$

$$M = \begin{bmatrix} m_{11} & m_{12} \\ m_{21} & m_{22} \end{bmatrix}; \qquad N_{(u_0)} = \begin{bmatrix} n_{11} & n_{12} \\ n_{21} & n_{22} \end{bmatrix}; \qquad b = \begin{bmatrix} b_1 \\ b_2 \end{bmatrix}$$

Expressing the equation $\dot{x} = Ax + b_1 u$, it becomes state form - space

$$\begin{bmatrix} \dot{r} \\ \ddot{r} \end{bmatrix} = \begin{bmatrix} 1 & 0 \\ 1 & -\frac{T_1 + T_2}{T_1 T_2} \end{bmatrix} \begin{bmatrix} \dot{r} \\ \ddot{r} \end{bmatrix} + \begin{bmatrix} 0 & 0 \\ K_R & K_R T_3 \end{bmatrix} \begin{bmatrix} \delta_R \\ \dot{\delta}_R \end{bmatrix} \delta_R \tag{12}$$

Identification of Mathematical Models

To obtain a simplified mathematical model (under order) that represents the dynamics in an approximate way, identification techniques were used. In the process of identification and validation of the model that describes the dynamics of the vehicle under study in the horizontal plane, several tests were performed based on the maneuver test of the evolutionary circle. Two (2) of these tests can be seen in Fig. 1 The rudder angle is considered as input and the heading angle as an output.

Obtaining the first order Nomoto model

It was used, as a second identification technique, the use of the method of least squares using as input the rudder angle and as output the variation of the angle of course (yaw rate), in order to achieve a gray box model that would allow to associate the parameters with the coefficients or indices of a first order Nomoto model. The obtained coefficients are: K = -0.0032 and T = 0.4702, with which the first-order Nomoto model is expressed by

$$G(s) = \frac{\psi(s)}{\delta(s)} = \frac{K}{s\,(Ts + 1)} = \frac{-0.0032}{s\,(0.4702s + 1)} \tag{13}$$

Fig. 2 shows the output, or heading angle, generated by the first-order Nomoto model compared to the actual heading angle. The standardized mean squared error was 0.2883.

Fig. 1. Evolution circle maneuver tests used for identification and validation

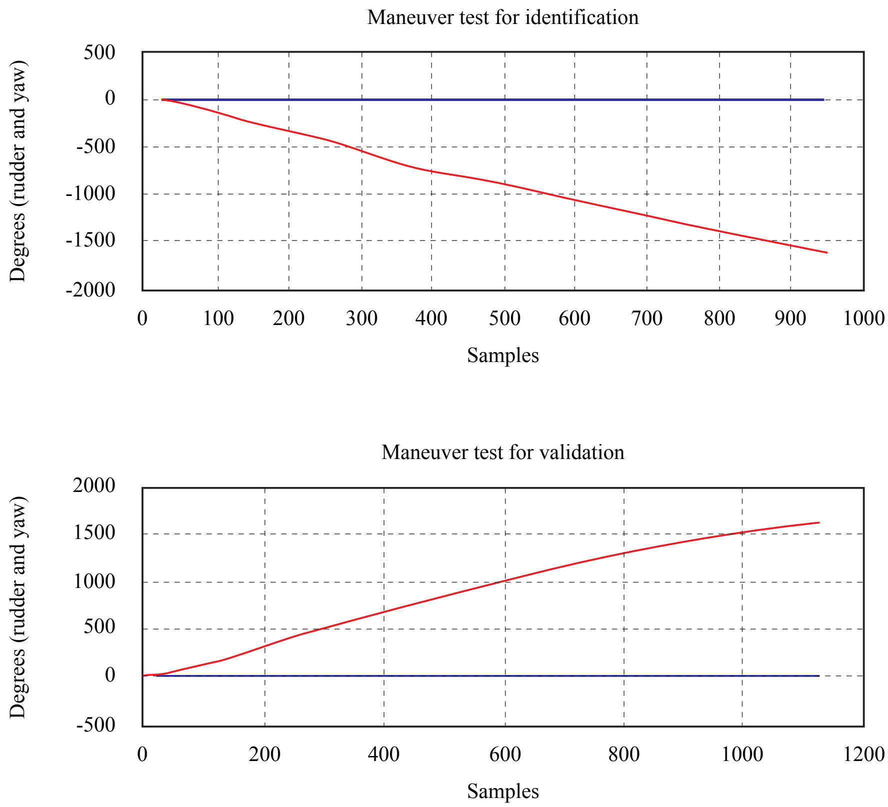

Fig. 2. Comparison between the output of the first order (discontinuous) Nomoto model and the true heading angle

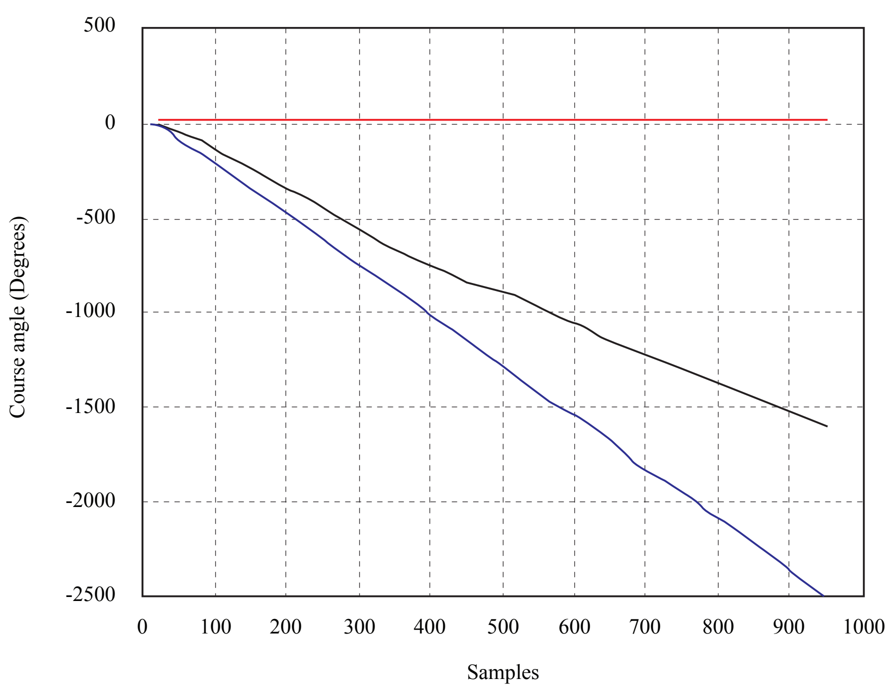

Obtaining second order Nomoto model

The second-order Nomoto model is given by the expression:

$$G(s) = \frac{\psi(s)}{\delta(s)} = \frac{K(T_3 s+1)}{(T_1 s+1)(T_2 s+1)} = \frac{\frac{KT_3}{T_1T_2}\left(s+\frac{1}{T_3}\right)}{\left(s+\frac{1}{T_1}\right)\left(s+\frac{1}{T_2}\right)} \quad (14)$$

If we break down by partial fractions, we have to

$$G(s) = \frac{\psi(s)}{\delta(s)} = \frac{A_1}{\left(s+\frac{1}{T_1}\right)} + \frac{A_2}{\left(s+\frac{1}{T_2}\right)} \quad (15)$$

With which the following is obtained

$$A_1 = \frac{K(T_1-T_3)}{T_1(T_1-T_2)}\,; \qquad A_2 = \frac{K(T_2-T_3)}{T_2(T_2-T_1)} \quad (16)$$

That is, the response in the time domain will be given by

$$\psi(t) = \frac{K(T_1-T_3)}{T_1(T_1-T_2)} * e^{-\frac{1}{T_1}t} + \frac{K(T_2-T_3)}{T_2(T_2-T_1)} * e^{-\frac{1}{T_2}t} \quad (17)$$

Then, in the Z domain

$$G(z) = A_1 \frac{1}{1-e^{-\frac{1}{T_1}T} z^{-1}} + A_2 \frac{1}{1-e^{-\frac{1}{T_2}T} z^{-1}}$$

$$G(z) = \frac{A_1\left(1-e^{-\frac{1}{T_2}T} z^{-1}\right) + A_2\left(1-e^{-\frac{1}{T_2}T} z^{-1}\right)}{\left(1-e^{-\frac{1}{T_1}T} z^{-1}\right)\left(1-e^{-\frac{1}{T_2}T} z^{-1}\right)} \quad (18)$$

$$G(z) = \frac{A_1+A_2-\left(A_1\left(e^{-\frac{1}{T_2}T}\right)+A_2\left(e^{-\frac{1}{T_1}T}\right)\right)z^{-1}}{\left(-1\left(e^{-\frac{1}{T_1}T}+e^{-\frac{1}{T_2}T}\right)z^{-1}+e^{-\left(\frac{1}{T_1}+\frac{1}{T_2}\right)}z^{-2}\right)}$$

Where T is the sampling time.

If we make an analogy with a discrete second-order model expressed by the following equation:

$$G(z) = \frac{b_0 + b_1 z^{-1}}{1 + a_1 z^{-1} + a_2 z^{-2}} \quad (19)$$

We have that:

$$\begin{aligned} b_0 &= A_1 + A_2 \\ b_1 &= \left(A_1\left(e^{-\frac{1}{T_2}T}\right)+A_2\left(e^{-\frac{1}{T_1}T}\right)\right) \\ a_1 &= -\left(e^{-\frac{1}{T_1}T}+e^{-\frac{1}{T_2}T}\right) \\ a_2 &= e^{-\left(\frac{1}{T_1}+\frac{1}{T_2}\right)T} \end{aligned} \quad (20)$$

Where we get:

$$1n(a_2) = \left(\frac{T}{T_1}+\frac{T}{T_2}\right)$$

$$T_2 = \frac{T}{-\frac{T}{T} - 1n(a_2)}$$

$$\begin{aligned} a_1 * e^{\frac{T}{T_1}} &= -e^{\frac{T}{T_1}} * \left(e^{-\frac{1}{T_1}} + e^{-\frac{1}{T_2}}\right) \\ a_1 * e^{\frac{T}{T_1}} &= -e^{\frac{T}{T_1}} * e^{-\frac{1}{T_1}} - e^{-\frac{1}{T_2}} * e^{\left(\frac{T}{T_1}+1n(a_2)\right)} \\ a_1 * e^{\frac{T}{T_1}} &= -1 - a_2 * e^{\frac{2T}{T_1}} \\ a_2 * e^{\frac{2T}{T_1}} &+ a_1 * e^{\frac{T}{T_1}} + 1 = 0 \\ x &= e^{\frac{T}{T_1}} \\ a_2 x^2 &+ a_1 x + 1 = 0 \\ x_{1,2} &= \frac{-a_1 \pm \sqrt{a_1^2 - 4(a_2)(1)}}{2a_2} \\ T_1 &= \frac{T}{1n(x_{1,2})} \end{aligned} \quad (21)$$

We calculate K it from the gain of the model in discrete time (z = 1), as follows:

$$K = \frac{(b_0 + b_1)}{(1 + a_1 + a_2)} \quad (22)$$

Finally we find T_3, as follows:

$$b_0 = A_1 + A_2$$

$$b_0 = \frac{K(T_1 - T_3)}{T_1(T_1 - T_2)} + \frac{K(T_2 - T_3)}{T_2(T_2 - T_1)}$$

$$b_0 = \frac{K * T_3}{T_1 T_2} \quad (23)$$

$$T_3 = \frac{b_0 T_1 T_2}{K}$$

The coefficients obtained are: K = -0.1724, T_1 = 2.0875, T_2 = 0.3179 and T_3 = 0.1830, with which the second-order Nomoto model is expressed by

$$G(s) = \frac{\psi(s)}{\delta(s)} = \frac{K(T_3 s + 1)}{s(T_1 s + 1)(T_2 s + 1)} =$$

$$G(s) = \frac{-0.1724(0.1830s + 1)}{s(2.0875s + 1)(0.3179s + 1)} = \quad (24)$$

$$\frac{-0.3155s - 0.1724}{0.6636s^2 + 2.405s + s}$$

Fig. 3 shows the output, or heading angle, generated by the second-order Nomoto model compared to the actual heading angle. The standardized mean square error obtained was 0.0397.

Fig. 4 shows the output, or heading angle, generated by the first and second order Nomoto models compared to the actual heading angle in the validation exercise. The standardized mean square error obtained with the first order Nomoto model was 0.3826, while with the second order Nomoto model it was 0.0516.

Stability analysis of the second order Nomoto model

Fig. 5 shows the place of the roots of the second order Nomoto model. Three poles are observed: two of them are located on the left side of the plane S, which remains on the negative real axis for system gain levels less than 23.6; the other pole is located at the origin and moves to the right if the gain is incremented, which would generate system instability. This pole located in the origin is the one that generates the movement of evolutionary circle for the entrance (change in the rudder) type step.

Fig. 3. Comparison between the output of the second-order (discontinuous) Nomoto model and the actual heading angle with the identification data

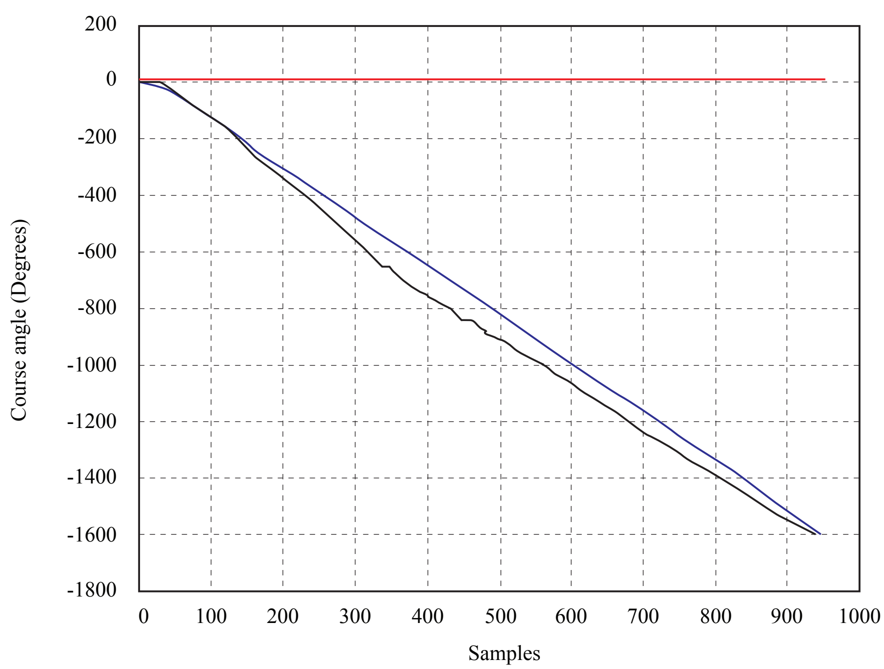

Fig. 4. Comparison between the output of the second-order (discontinuous) Nomoto model and the actual heading angle with the validation data

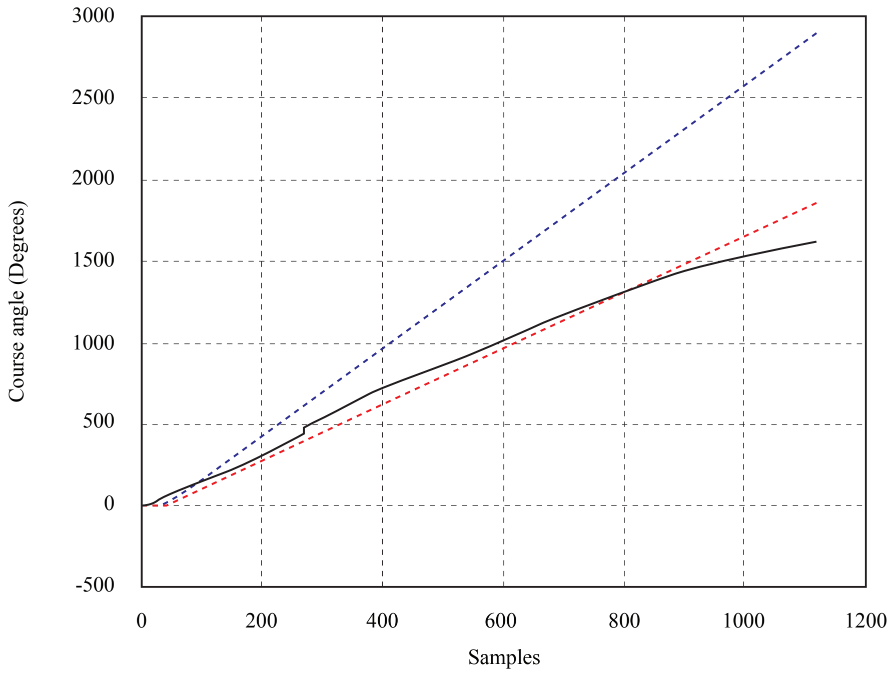

Fig. 5. Place of the roots of the second order Nomoto model

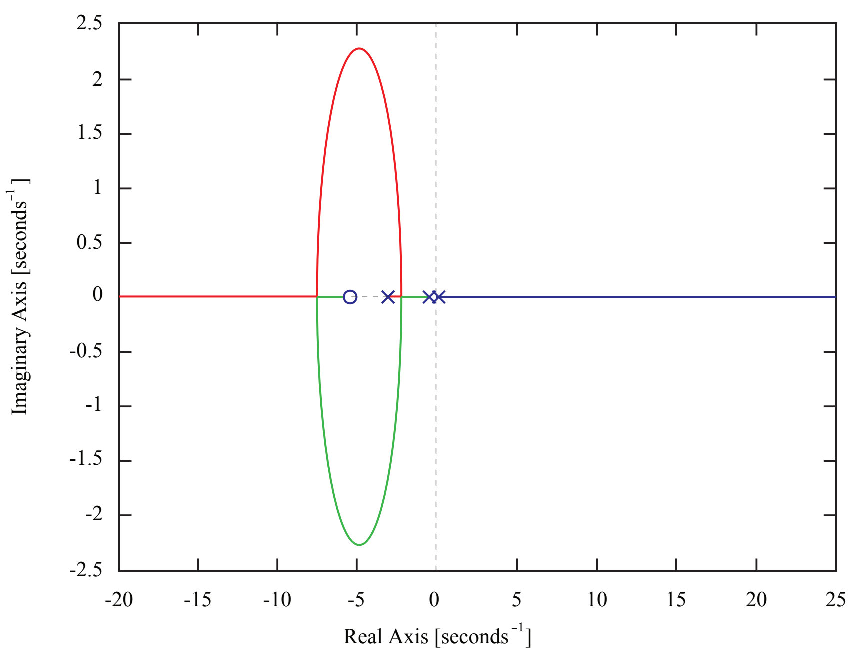

Conclusions

A methodology was presented to obtain the second order Nomoto model of a PAF fluvial support patrol using identification technique and using experimental data from a standard such as the turning circle maneuver. The mathematical model obtained presents a standardized mean square error of 0.0397 in the identification process and 0.0516 in the validation process, which shows a fairly high approximation. The test used for validation was done with a turn to port while the one used for identification was made to starboard.

The analysis of the place of the roots of the Second Order Nomoto model shows the temporal behavior of the system. The pole located at the origin is the one that causes an indefinite turn to port, or starboard, since its location at the origin of the S plane implies an unstable or critically stable behavior.

Acknowledgements

The authors thank Dr. VALM Jorge Enrique Carreño Moreno, who provided important knowledge to carry out the development of this project.

Bibliography

[1] WANG MENG, LI HONG SHENG, MIAO QING and BIAN GUANG RONG. “Intelligent control algorithm for ship dynamic positioning”. Archives of Control Sciences, Vol. 24, No. 4, p.p.: 479–497. 2014.

[2] HAIJUN XU, WEI LI, YANG YU and YONG LIU. “A Novel Adaptive Neural Control Scheme for Uncertain Ship Course-keeping System”. Sensors & Transducers, Vol. 178, No. 9, p.p.: 282-285, 2014.

[3] SK. SHARMA, W. NAEEM, R. SUTTON. “An Autopilot Based on a Local Control Network Design for an Unmanned Surface Vehicle”. The Journal of Navigation. Vol. 65, p.p.: 281–301. 2012.

[4] VELASCO, F.J., REVESTIDO, E., LÓPEZ, E., MOYANO, E., HARO CASADO, M. “Autopilot and Track-Keeping Simulation of an Autonomous In-scale Fast-ferry Model”. 12th WSEAS International Conference on Systems, Heraklion, Greece, July 22-24, 2008.

[5] VELASCO, F.J., REVESTIDO, E., LÓPEZ, E., MOYANO, E., HARO CASADO, M. “Simulation of an Autonomous In-scale Fast-ferry Model”. International Journal of System Applications, Engineering and Development , Vol. 2, No.3, p.p.: 114–121. 2008.

[6] BANAZADEH A, GHORBANI MT. Frequency domain identification of the Nomotomodel to facilitate Kalman filter estimation and PID heading control of a patrolvessel. Ocean Eng 2013;72:344–55.

[7] AULIA ZITI AISJAH, An Analysis Nomoto Gain and Norbin Parameter on Ship Turning Maneuver , IPTEK, The Journal for Technology and Science, Vol. 21, No. 2, May 2010.

[8] CARREÑO, J. E., “Simulación de maniobras de buques con sistemas de propulsión no convencional en aguas poco profundas”, Madrid, España: Universidad Politécnica de Madrid, Tesis doctoral, 2012.

[9] CARREÑO, J. E., MORA, J. D., PÉREZ, F. L., “Mathematical model for maneuverability of a riverine support patrol vessel with a pump-jet propulsion system”, Ocean Engineering, Vol. 63, 2013, pp. 96-104

[10] T. I. FOSSEN, Guidance and Control of Ocean Vehicles, John Wiley and Sons,New York, 1994.

[11] TZENG, C., and CHEN, J., “Fundamental Properties of Linear Ship Steering Dynamic Models,” Journal of Marine Science and Technology, Vol. 7, No. 2, pp 79–88, 1999.

[12] REVESTIDO E., VELASCO F., LÓPEZ E., Diseño de Experimentos para la Estimación de Parámetros de Modelos de Maniobra Lineales de Buques. Elsevier Revista Iberoamericana de Automática e Informática industrial 9 (2012) 123–134.

[13] POLLAND, S. Recursive parameter identification for estimating and displaying Maneuvering vessel path, Thesis 2003.

Hydrodynamic study of the influence of bulbous bow design for an Offshore Patrol Vessel using Computational Fluid Dynamics

Estudio Hidrodinámico de la Influencia de 3 Tipos de Bulbos de proa para un Buque tipo Patrullero Oceánico con Herramientas de Dinámica de Fluidos Computacional (CFD)

DOI: https://doi.org/10.25043/19098642.161

Luis Leal [1]
Edison Flores [2]
David Fuentes [3]
Bharat Verma [4]

Abstract

The resistance of a ship is of vital importance in giving greater viability to the development of a design project, since at lower ship resistance, the power demand to achieve a desired design speed will be lower which will reduce the amount of power to be installed in the ship resulting in lower fuel consumption. The use of computational fluid dynamics to analyze and optimize hull form and its appendages permits the hydrodynamic performance of the ship to be improved from the early design stages, allowing improvements to the hull shape and appendages. This paper shows a qualitative analysis which was performed to reduce the resistance of the OPVMKII (Second Generation Offshore Patrol Vessel) in its preliminary design stage by means of designing and integrating three types of bulbous bow with the ship´s hull and analyzing the resistance curves obtained using computational fluid dynamics.

Key words: Computational Fluid Dynamics (CFD), Appendages, bulbous bow, Ship Resistance, Offshore Patrol Vessel.

Resumen

La resistencia al avance de un buque, es de vital importancia para dar mayor viabilidad al desarrollo de un proyecto de diseño, puesto que a menor resistencia al avance, la demanda de potencia para alcanzar una velocidad de diseño deseada será menor y con esto disminuir la cantidad de potencia instalada en el buque, lo que se traduce en menor consumo de combustible. El uso de la dinámica de fluidos computacionales para analizar y optimizar las formas del buque y sus apéndices permite, desde tempranas etapas del diseño, mejorar el desempeño hidrodinámico del buque, permitiendo generar mejoras a las formas y apéndices del casco. El presente trabajo muestra en su etapa preliminar, el proceso de análisis cualitativo de la reducción de la resistencia al avance del proyecto OPVMKII (Patrullero Oceánico de Segunda Generación) mediante diseño e integración al casco del buque con tres tipos de bulbos de proa, y el análisis de los resultados obtenidos en las curvas de resistencia al avance usando dinámica de fluidos computacionales.

Palabras claves: Dinámica de Fluidos Computacional (CFD), Apéndices, bulbo de proa, Resistencia al avance, Buque Patrullero Oceánico.

Date Received: June 20th 2017 - *Fecha de recepción: Junio 20 de 2017*
Date Accepted: October 18th 2017 - *Fecha de aceptación: Octubre 18 de 2017*

[1] COTECMAR. Cartagena, Colombia. Email: lleal@cotecmar.com
[2] COTECMAR. Cartagena, Colombia. Email: eflores@cotecmar.com
[3] COTECMAR. Cartagena, Colombia. Email: dfuentes@cotecmar.com
[4] COTECMAR. Cartagena, Colombia. Email: bharat@cotecmar.com

Introduction

The Corporation for Science and Technology for the Development of the Maritime and River Naval Industry, Cotecmar has built 3 oceanic patrol vessels (OPVs) that are operated by the Navy of the Republic of Colombia. To comply with new requirements in missions, capacities and growth margins, a design was started from scratch of a second generation OPV type vessel. The preliminary design phase of this vessel is currently under development.

Within the development in the design spiral, this phase of the project seeks to optimize the resistance to the advance of the vessel that as mentioned above, influences the amount of installed power, the weight of engines and fuel consumption. The CFD (Computational Fluid Dynamic) tool is of great importance for the development of analysis of this type of vessel, thanks to the advance in the processors and current computational capacities that allow more accurate simulations to be performed with greater precision. The CFD workshops in Gothenburg, 2010 *(Larsson et al., 2010)* and Tokyo, 2015 show that the CFD methods developed can achieve good results compared to experimental results. RANS methods are currently a common tool used in design departments to support the design process. The accuracy of the CFD analysis is proven to be accurate, and most naval architects use this method for initial design phases instead of channel testing that is tedious, expensive and time consuming.

The analysis of advance resistance is a fundamental initial step in the design of a new vessel, these analyzes are regularly made in a channel of test experiments to refine aspects of resistance reduction, the analysis of the behavior of the ship at sea, optimization of the shape lines of the hull itself, but a good approximation can also be obtained by simulating the aforementioned analyzes through calculations using the CFD tool, although the admissible results of this method is in the order of 5-10% when compared with the results of channel tests. It will always be necessary to confirm these data with a channel test, so this computational analysis provides sufficient information for a good qualitative analysis and can present approximate values.

Description of the problem

Initially, the validation of the computational model will be carried out with a channel tested model and CFD model, with which resistance to advance results will be obtained and the percentages of difference will be compared to the point of having maximums of 10% for the case of qualitative analysis as it is the object of study of this document.

For the correct validation of the model, the hull of the OPVMKII vessel will be analyzed at a design speed of 20 knots as the maximum speed (real scale). The analysis will be carried out in calm and deep waters. 4 speeds were simulated to recreate a curve of advance resistance, this for the bare hull (without appendages). After this 3 types of bulbs will be designed and simulated under the same conditions. At the end we will obtain results of 4 models, for each model a resistance curve with 4 points will be charted and it will be defined if it is efficient to place a bow bulb and if so, which of the 3 types of designed appendages present lower results of advance resistance.

Methodology Implemented

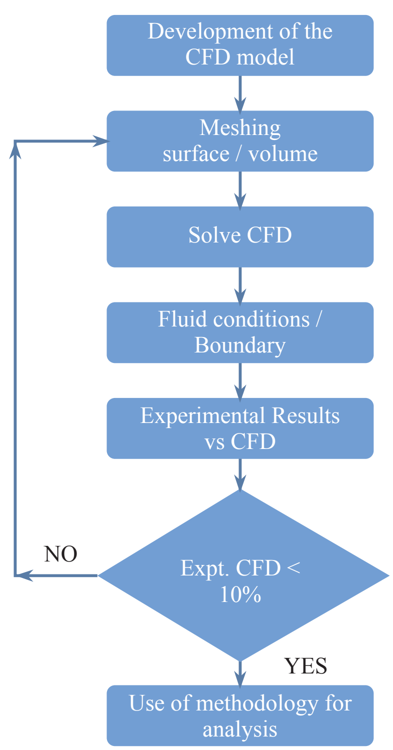

To address the steps considered for the simulation of the computational model, it is necessary to describe some items that are a fundamental part in the construction of the model as follows.

Configuration of the Geometric Model

The governing equations are the RANS equations and the continuity and momentum equations for the average speed of the unstable, three-dimensional and incompressible flow.

To model the fluid flow, the solver used a finite volume method that uses the integral formulation of the Navier-Stokes equations. The RANS solver uses a predictor-corrector approach to link the equations of continuity and momentum.

The turbulence model selected in this study was a standard k-ε model. The use of the turbulence model formulation of the standard k-ε equation is reasonably robust and reliable near solid boundaries and recirculation regions such as ship boundary layers.

The height of the computational domain is 3.5 Lwl and its width is taken as 2 Lwl due to the symmetry of the problem. The entry limit of the domain is at a distance of 1 Lwl in front of the vessel, while the exit limit is 3 Lwl from the stern of the vessel. ITTC recommends that the entry limit should be 1- 2 Lpp and the exit limit should be 3-5 Lpp away from the hull to avoid wave reflections [2].

Fig. 1. 3D model of the hull

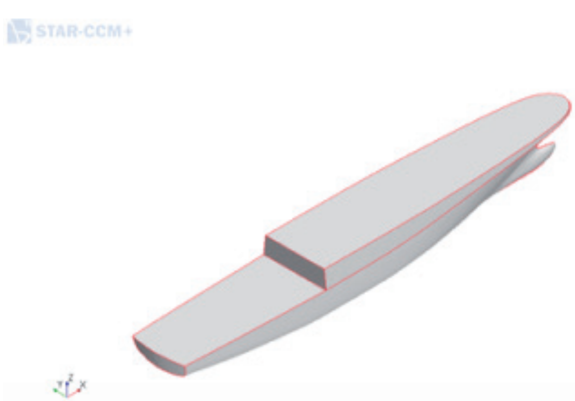

Contour conditions of the model

Inlet

The domain entry was defined as a type of contour; velocity speed (Velocity Inlet) and is the part where the flow will pass from the beginning (direction to the bow of the hull) to the end (aft direction of the hull).

Outlet

The output of the computational domain represents the place where the flow leaves it, this was defined as contour type; Pressure Outlet, represents the plane that is towards the stern of the vessel and with normal in the direction of the negative "x" axis.

Bottom, Side and Top

The bottom, side and top of the domain in this case was defined as contour type; Wall with a sliding option that works allowing the flow of water or air to pass through.

Symmetry Plane

The plane of symmetry works for the cases in which, when simplifying the problem, only half of the computational domain can be used for the symmetry of the model, if the physical phenomenon allows it. In this case the physical model obeys the interaction of the dragging pressures of the ship element and the free surface of the sea, so that having certain assumptions as the condition of the sea that for the model is of calm waters there are no reflections or sums of waves that can change the result of the calculations of the equations in this part of the domain (free surface), which is why the declaration of domain symmetry works. Then the symmetry plane condition only reflects the results of half of the analyzed or simulated domain.

Vessel-Wall

The ship in this case is represented by a wall type element (Wall) that prevents the passage of the flow through it and that has the shape of the vessel, which allows the fluid that passes outside it to be analyzed but not the ship element.

Free Surface

The free surface is the center of attention of the hydrodynamic study, since it captures the effects of the conditions already mentioned in the computational domain that was defined as a free sliding wall. This means that the velocity component parallel to the wall has a finite value (which is calculated), but the normal wall velocity and the shear stress of the wall are set to zero.

Fig. 2. Contour conditions of computational domain

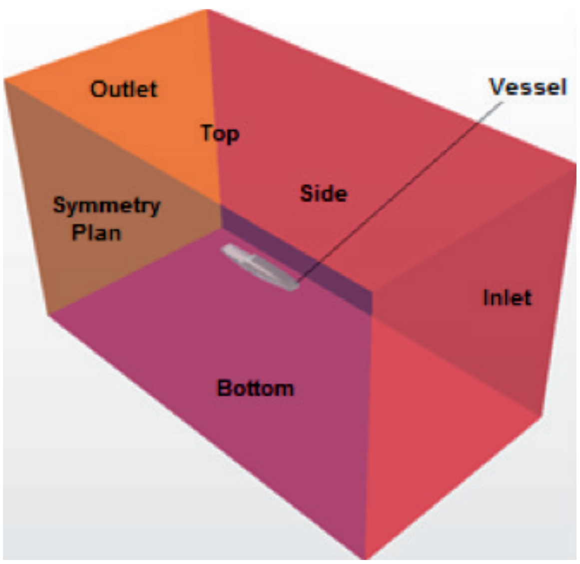

Meshing

A mesh has been configured for the validation case of approximately 1.8 million cells with 6 control volumes, each with at least 2 levels of refinement, on the other hand, for the case study of the vessel OPVMKII, a mesh of approximately 2.1 million was configured with the same control volumes, except for the aft appendages, since the geometry of the model does not include them for this analysis.

Parameters for Bulbs design

The main objective of the bow bulbs is to reduce the height of the waves caused by the local disturbance of pressures that form in the bow of the ship during its progress as indicated in Fig. 3.

The applicability of the bulb is initially defined in a Froude number range for relatively high speeds:

Fig. 3. Wake attenuation by bow bulb

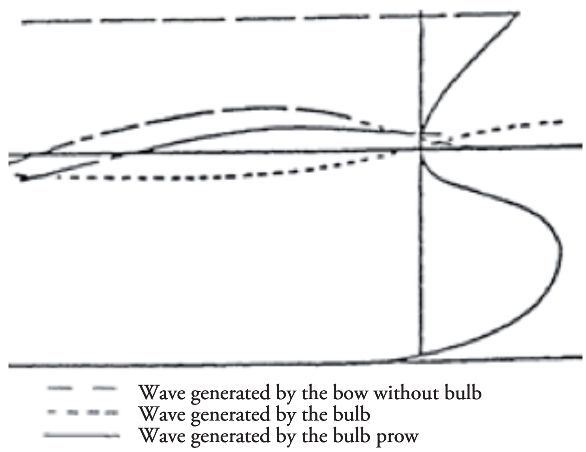

$$0,24 < Fn < 0,57 \tag{1}$$

But because the Fn range is very wide, other factors that can affect the adoption of a design bulb are estimated. The global tuning parameter of the vessel indicates that the bulb is not recommended if:

$$\frac{Cb.B}{Lpp} > 0,135 \tag{2}$$

Where:

Fn = Froude number
Cb = block coefficient
B = beam [m]
Lpp = length between perpendiculars [m]

The method to identify the dimensions of the bulb once the adoption of bulb is feasible is performed by linear parameters:

Fig. 4. Linear parameters for sizing the bulb

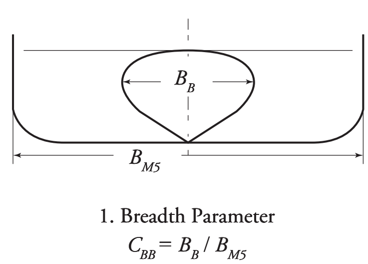

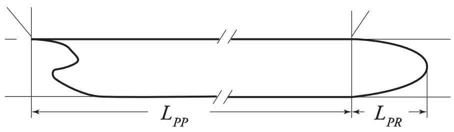

2. Lenght Parameter
$C_{LPR} = L_{PR} / L_{PP}$

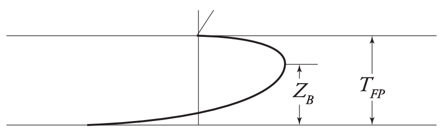

3. Depth Parameter
$C_{ZB} = Z_B / T_{FP}$

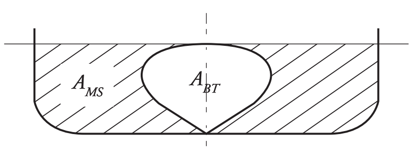

4. Cross-section Parameter
$C_{ABL} = A_{BL} / A_{MS}$

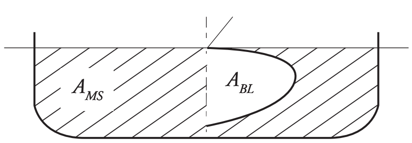

5. Lateral Parameter
$C_{ABL} = A_{BL} / A_{MS}$

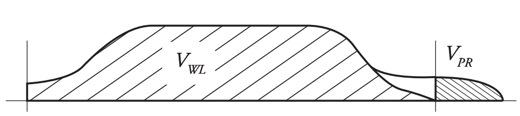

6. Volumetric Parameter
$C_{VPR} = V_{PR} / V_{WL}$

	Min	Max
C_{BB}	0.170	0.200
C_{LPR}	0.018	0.031
C_{ZB}	0.260	0.550
C_{ABL}	0.064	0.122
C_{ABL}	0.068	0.146
C_{VPR}	0.0011	0.00272

Fig. 5. Types of bulbs

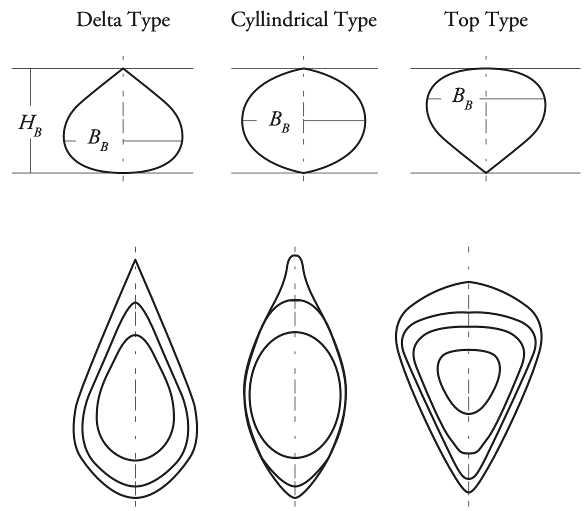

Bulb selected for OPVMKII

There are several types of bulbs such as those indicated in Fig. 5.

Not all the types of bulbs indicated in Fig. 5 are suitable for the OPV MKII project, since each one has a specific function, according to the hull shapes and type of service.

The research shows there are indications that the delta and cylindrical bulbs are more susceptible to suffering "slamming" due to their lower flat part and as a vessel with restricted navigation suitable for rough seas they would not be able to be used, therefore top type bulbs that maintain their fine entry angle and higher center of gravity will allow the boat to improve its performance at maximum load and make sure that the "slamming" water impacts are kept to a minimum as it is a vessel with a large number of people aboard.

With this type of bulb selection approach, three types of variations to the bulb type B1, B2 and B3 as indicated in Fig. 5 are analyzed, where basically it is based on varying the height ZB (see Fig. 3) of bulb bulge and to verify how the dissipation of the wave train generated by the hull improves.

Analysis

Validation of Model

The standard vessel used for the validation of the model is the first oceanic patrol boat built in Colombia by Cotecmar OPV 80 or *ARC 20 de Julio*, which is currently in service, of this vessel there are accurate data of the channel tests, for hull with appendices (without propellers) and with which the comparison was made.

Ship and model data:

Table 1. Real ship data and scale model

Determination of scale factor for CFD Model		
SHIP DATA		
L	74,4	m
B	13,00	m
D	6,5	m
d	3,9	m
Displacement	1800	M-Ton
V	18	knots
V	9,26	m/s
u	0,000001007	m^2/s
Re_Ship	684154324,5	
Frs	0,342829511	
MODEL DATA		
Lm	5,723076923	m
Bm	1,00	m
Dm	0,5	m
dm	0,3	m
Displacement	0,819299044	M-Ton
Vm	2,56825969	knots
u	0,0000010007	m/s
Re_model	14.596.174,54	m^2/s
Re_ideal	10.000.000,00	
Frm	0,34275961	
Scale (λ) = 13		

Model validation results

In the case of the wave map, it is necessary to compare the pattern with what is usually presented

Table 2. Boundary layer thickness of the model

THICKNESS CALCULATION OF BOUNDARY LAYER			
Data	**Value**	**Unity**	**Note**
p	998,186	kg/m^3	
Cf	0,0028122		Formulation taken from ITTC
Tw	9,2578031	Pa	
U*	0,0963049	m/s	
y^+	26		Enter the Y+ that you need
y	0,0002719	m	
2*y	0,0005437	m	Value to Enter in Software

Table 3. Time Step of the simulation

ESTIMULATION OF THE TIME STEP IN THE SIMULATION		
Wavelenght of the wave model	0,10701114	m
Wave height	2,1	m
Wave model height	0,16153846	m
ΔZ-Wave	0,00807692	m
ΔX-Wave	0,00133764	m
CFL	0,5	
Δt	0,00157245	s

Fig. 6. Types of bulbs defined for model

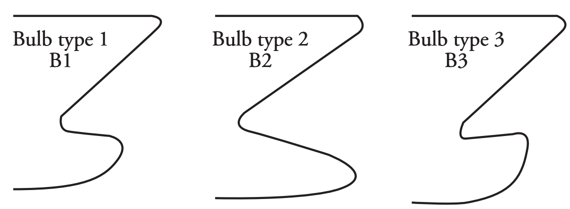

in the Kelvin wave pattern, where factors such as the angle of departure of the wave generated and the differentiation between the transversal and divergent waves are highlighted at the time of identifying computational errors of the simulation, this means that the physical phenomenon does not represent reality as it should.

As can be seen in Fig. 7 [1], the wave pattern thrown by the CFD analysis obeys the behavior

Fig. 7. Views and approaches of wave height map of vessel OPV 80

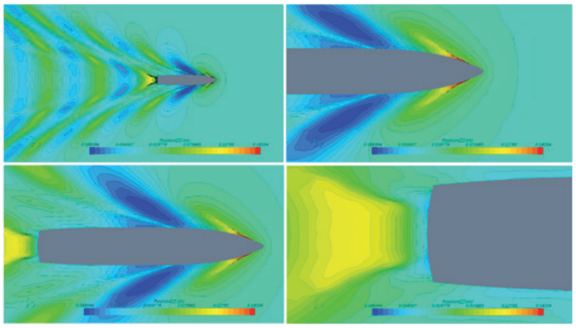

Fig. 8. Kelvin wave pattern

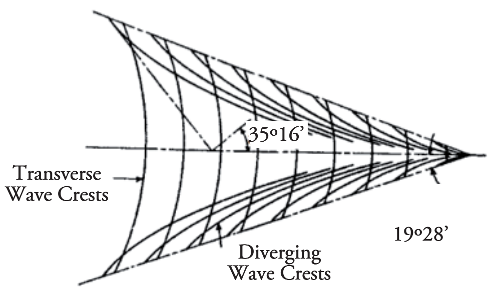

shown in Fig. 8, which shows that the analysis is adequately representing the physical phenomenon.

Fig. 9 shows a distribution of hydrostatic pressures in the hull of the vessel, which behave well, do not show high pressure concentration and no abrupt disturbances of the pressure lines are observed.

Fig. 9. Views and approaches of pressure distribution in the hull of the OPV 80 vessel

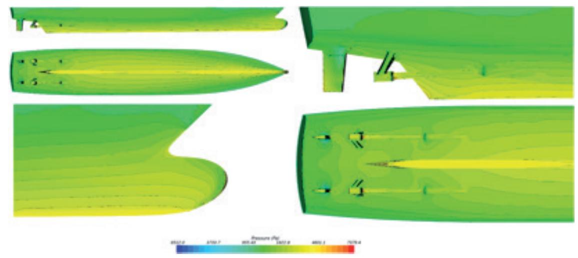

In the flow lines of Fig. 10 the most important thing is to appreciate that there is no turbulence in the middle of the flow through the hull, the height reached by the wave generated in the bow is of vital importance, because the objective of the analysis of the optimization of the resistance to the advance is to reduce as much as possible this effect to reduce the resistance to the advance of the ship.

Bare hull

The bare hull is the geometry of the appendix-free model and is the starting point of the analysis,

Fig. 10. Views and approaches of the OPV 80 ship's flow lines

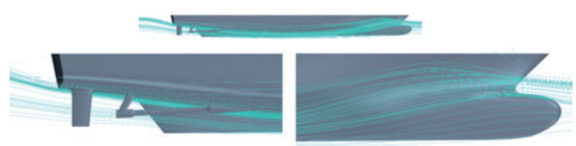

Fig. 11. Graph of resistance to the advance of OPV 80-Channel vs OPV80-CFD

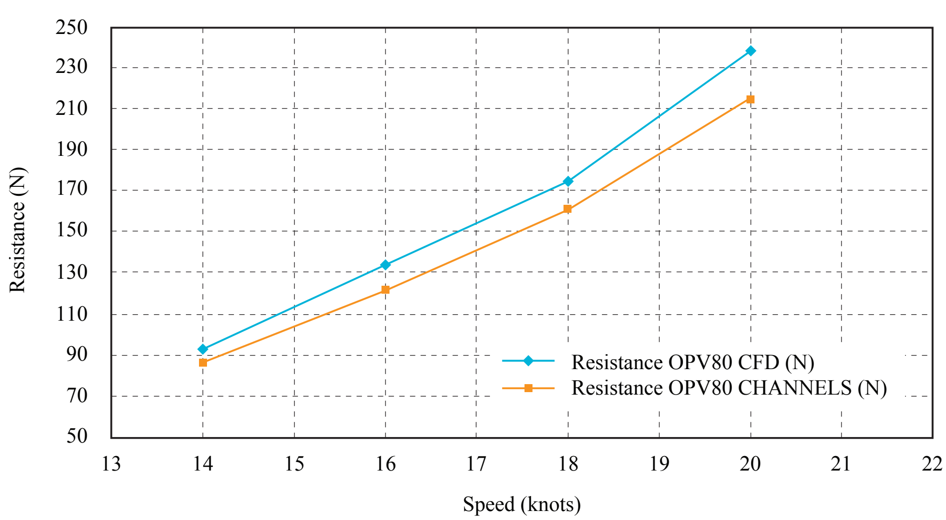

Table 4. OPV 80-channel and OPV80-CFD hull advance resistance values

Speed (knots)	Resistance OPV80 CFD (N)	Resistance OPV80 CHANNEL (N)	% Difference
14	93,11	86,29	7,32%
16	133,84	121,78	9,01%
18	175,33	160,99	8,18%
20	238,03	214,88	9,73%
Average			8,56%

since with this first simulation it will be possible to compare whether the use of a bow bulb is efficient and functional.

Fig. 12. Outline of bare hull

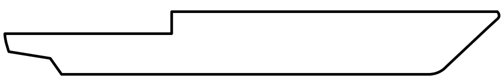

Fig. 13. OPVMKII helmet wave height map view

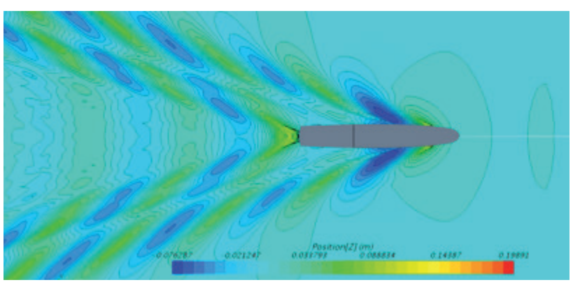

Fig. 14. View of OPV MKII flow lines

Fig. 15. View of pressure distribution in the OPVMKII helmet

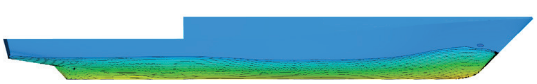

Bulb Design

Helmet with bulb type B1:

Fig. 16. Hull diagram OPVMKII B1

Fig. 17. View of the wave height map of the OPVMKII B1 hull

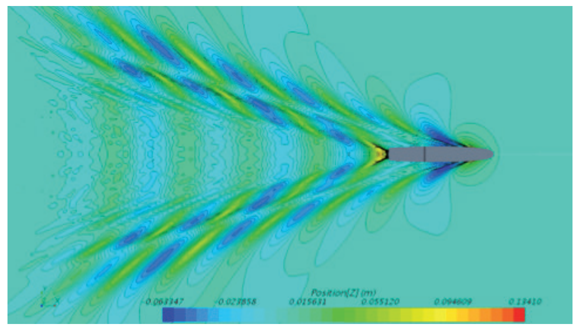

Fig. 18. View of hull flow lines OPVMKII B1

Fig. 19. Views and approaches of pressure distribution in helmet OPVMKII B1

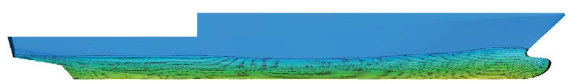

Helmet with bulb type B2:

Fig. 20. Hull diagram OPVMKII B2

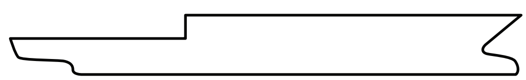

Fig. 21. View of the wave height map of the OPVMKII B2 hull

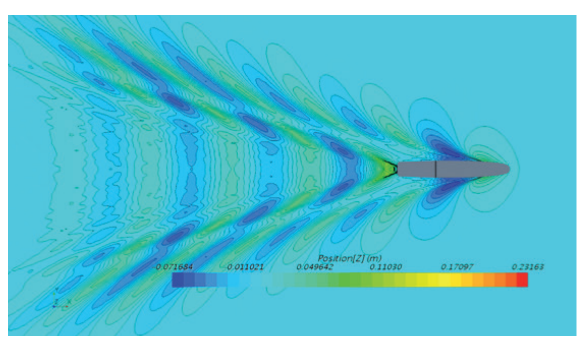

Fig. 22. View of hull flow lines OPVMKII B2

Fig. 23. Views and approaches of pressure distribution in the OPVMKII B2 hull

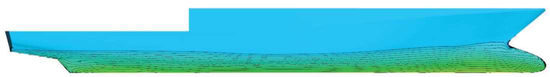

Helmet with bulb type B3:

Fig. 24. Hull diagram OPVMKII B3

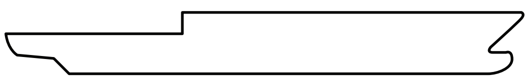

Fig. 25. View of the wave height map of the OPVMKII B3 hull

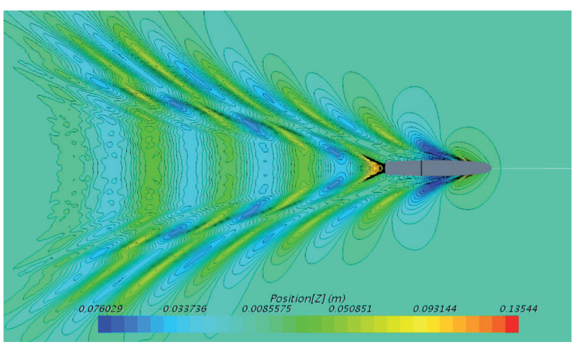

Fig. 26. View of hull flow lines OPVMKII B3

Fig. 27. Views and approaches of pressure distribution in helmet OPVMKII B1

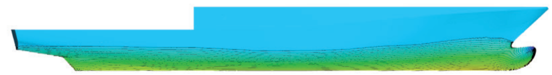

Analysis of the obtained results

After obtaining the results of the 4 cases studied, there are no cases or models with problems of flow distortion or pressure concentration, but to appreciate a little what happens between one bulb and another, we turn to the Fig. 28

It can be see that from one bulb to another the flow lines vary, the bare hull (to the upper left) presents a wave in the bow, this is because the flow is separated by the hull and tends to form a wave that starts what we know as kelvin wave pattern, which is the cause of a greater resistance to advance, so the bulbs tested should reduce this phenomenon and effectively they do so. Bulb 1, 2 and 3 reduce the wave formed in the bow, this is because this appendage causes the flow to separate before the water touches the hull, so that it no longer opens a high resistance to the advance and with each bulb there is a defined behavior, the important thing for this case was that there was a positive effect on the flow that passes through the hull and there are no vortices or turbulence due to the shapes of the appendages or the hull.

In Fig. 24 the gap between the curve of resistance to the advance of the bare hull and the 3 bulbs is notable, which denotes a clear need for the use of bow bulbs in the design of the OPVMKII hull. It can be seen that for the case of the bulbs the panorama of the

Table 5. Resistance values for bare-hull advance and 3 bulbs 1, 2 and 3

Speed (knots)	Resistance OPVMKII V1 CFD (N)	Resistance OPVMKII V1 B1 CFD (N)	Resistance OPVMKII V1 B2 CFD (N)	Resistance OPVMKII V1 B3 CFD (N)
12	38,93	37,76	40,41	37,71
15	71,02	60,63	62,22	62,87
18	131,78	110,44	107,05	112,62
19	150,86	125,81	122,50	127,35
20	167,44	147,72	143,54	148,94

Fig. 28. Pressures and flow lines in bulbs

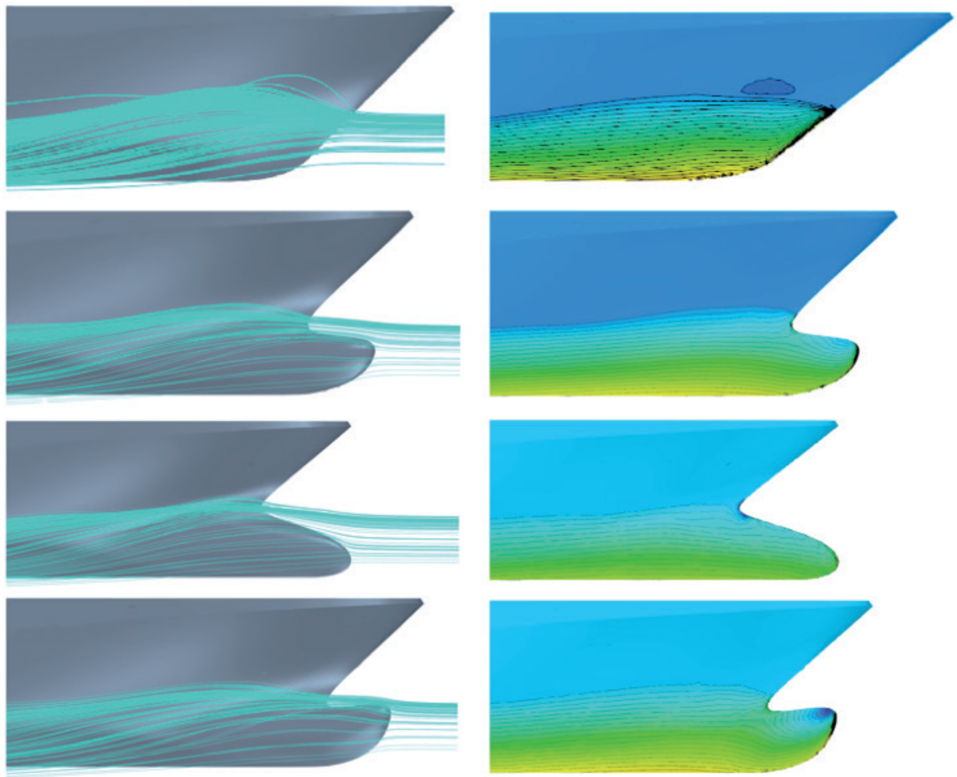

Fig. 29. Resistance graph

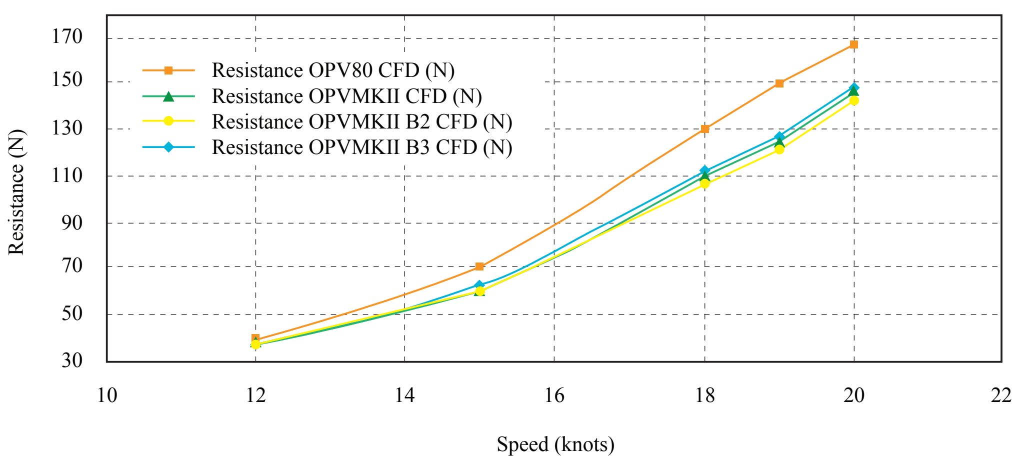

decrease in the resistance to the advance in the hull is closed, however there are considerations that can influence the use of one bulb and another, as is the case of the pitch of the vessel and the percentage of time in the life cycle that the ship will operate at certain speeds.

Conclusions

- Validation of the computational model was carried out, achieving a difference of less than 10% compared to the OPV80 hull channel tests, which allows us to make a qualitative analysis of the hydrodynamics of the OPVMKII hull.

- The influence of the bow bulb on the reduction of the resistance to the advance for this type of vessel was confirmed with results of around 16%.

- Comparing the 3 types of bow bulbs. The bulb that behaves best according to the graph of resistance to advance is the bulb type 2 for speeds over 18 knots, however the vessel will operate most of the time at 12 knots.

Future Tasks

- Optimization of the hull with the inclusion of stern appendages type interceptor or wedge using CFD methodology.

- Dimensioning and selection of the anti-casting systems from the roll decay test using the CFD methodology.

- Study of behavior in the sea and maneuverability using CFD methodology.

Bibliography

ODD M. FALTINSEN. Hydrodynamics of High-Speed Marine Vehicles. Norwegian University of Science and Technology. Cambridge University Press, 2005.

INTERNATIONAL TOWING TANK CONFERENCE (ITTC): Practical guidelines for ship CFD applications. Proceedings of the 26th International Towing Tank Conference, Brazil, 2011.

JEFF W. HOYLE. A Bulbous Bow Design Methodolgy for High-Speed Ships. SNAME. Vol 94, 1986.

ALFRED M. KRACHT. Design of Bulbous Bows. SNAME. Vol. 86, 1978.

Effects of the Duct Angle and Propeller Location on the Hydrodynamic Characteristics of the Ducted Propeller

Efectos del ángulo de ducto y ubicación de la hélice en las características hidrodinámicas de la hélice con ducto

DOI: https://doi.org/10.25043/19098642.162

Mehdi Chamanara [1]
Hassan Ghassemi [2]
Manouchehr Fadavie [3]
Mohammad Aref Ghassemi [4]

Abstract

In the present study, the effect of the duct angle and propeller location on the hydrodynamic characteristics of the ducted propeller using Reynolds-Averaged Navier Stokes (RANS) method is reported. A Kaplan type propeller is selected with a 19A duct. The ducted propeller is analyzed by three turbulence models including the k-ε standard, k-ω SST and Reynolds stress model (RSM). The numerical results are compared with experimental data. The effects of the duct angle and the location of the propeller inside the propeller are presented and discussed.

Key words: Kaplan propeller, 19A duct, Turbulent models, Hydrodynamic analysis.

Resumen

En el presente estudio se reporta el efecto del ángulo de ducto y la ubicación de la hélice sobre las características hidrodinámicas de la hélice con ducto, usando el método RANS (Reynolds-Average Navier Stokes). Una hélice de tipo Kaplan es seleccionada con un ducto tipo 19A. La hélice con ducto es analizada por tres modelos de turbulencia, incluyendo k-ε standard, k-ω SST y el modelo de esfuerzo de Reynolds (RSM - Reynolds Stress Model). Los resultados numéricos son comparados con datos experimentales. El efecto del ángulo de ducto y la ubicación de la hélice son presentados y discutidos.

Palabras claves: Hélice Kaplan, ducto 19A, modelos de turbulencia, análisis hidrodinámico.

Date Received: April 17th 2017 - *Fecha de recepción: Abril 17 de 2017*
Date Accepted: October 13th 2017 - *Fecha de aceptación: Octubre 13 de 2017*

[1] Department of Maritime Engineering, Amirkabir University of Technology, Tehran, Iran. Email: Chamanara.m68@aut.ac.ir
[2] Department of Maritime Engineering, Amirkabir University of Technology, Tehran, Iran. Email: gasemi@aut.ac.ir
[3] Department of Maritime Engineering, Amirkabir University of Technology, Tehran, Iran. Email: fadavie@aut.ac.ir
[4] Department of Maritime Engineering, Amirkabir University of Technology, Tehran, Iran. Email: marefghassemi@gmail.com

Introduction

In recent year, considerable efforts have been made to improve the propulsive efficiency of the propeller on the ships. One of these propulsors is called a ducted propeller found as widespread application. The duct is generally used to obtain augment thrust, but it is also used to minimize cavitation and underwater noise or to protect the propeller from damage. There are two types of duct, the first type is called an acceleration duct or Kort nozzle and the second type is a deceleration duct. Fig. 1 shows both types of the ducted propeller. The Acceleration duct has a flat surface on the outside of the curve in the inner area. The outer surface is high-pressure surface and the inner surface is low-pressure surface (or suction). The suction allows more current to be directed into the duct and thus increase the flow rate. The increased inflow velocity causes a decrease in the thrust and torque of the propeller. At the same time, a circulation develops around the duct section resulting in an inward directed force which has a forward component, the duct thrust. The duct also has a drag directed aft. The efficiency of the ducted propeller is therefore greater than of the open propeller *(Ghose, Kogarn, 2004)*.

Fig. 1. Acceleration and Deceleration duct

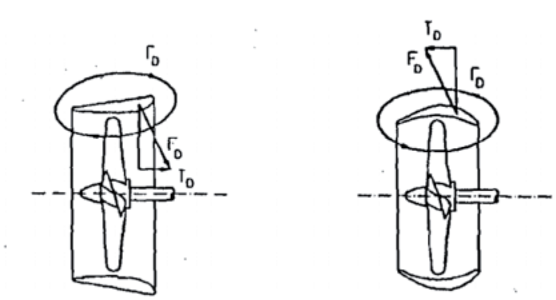

(a) Accelerating Duct
T < 1

(b) Decelerating Duct
T > 1

In recent years, computational fluid dynamics (CFD) have been extensively used for the analysis of marine propellers. Due to the complex shape, flow turbulence, flow separation and the possibility of cavitation, the analysis of marine propellers is a difficult task; however, some works have been done in the field of ducted propellers. For example, *(Taketani et al., 2009)* presented the advanced design method of a ducted propeller which has high bollard pull performance. A nozzle section shape and a propeller have been designed according to a parametric study of the numerical simulation in order to have higher performance than a conventional ducted propeller. The optimum arrangement between nozzle and propeller combination is also studied. The open water tests are carried out in a towing tank of Akishima Laboratories. *(Tadeusz et al., 2009)* have completed the design for ducted propellers using the new computer systems. In this paper, the performance of the five different ducts are compared and the result show that in most cases only the 19A duct was considered, and that this duct was designed for low speed and high bollard pull conditions. *(Celik et al., 2010, 2011)* presented a design methodology for the operation of ducted propellers in a non-uniform wake field. They also presented an investigation of optimum duct geometry for a passenger ferry. The numerical effect of duct shape on the propeller performance was presented by *(Caldas et al., 2010)*.

(Baltazar et al., 2012) predicted the thrust and torque of a ducted propeller using a panel method to improve the accuracy of the calculated shape of wake panels and the flow behavior in the tip gap region. The numerical analysis employed to the ducted propeller performance under open water test condition *(Yu et al., 2013)*. They also investigated the open water performance of the Ka-series propellers at various pitch and expanded area ratios in combination with the 19A duct by employing the panel method PAN-MARE and the RANSE code ANSYS-CFX. *(Krzysztof et al., 2014)* presented four different geometries ducts to get better thrust characteristics in medium and high advance velocity ratio. *(Xueming et al., 2015)* analyzed the hydrodynamic performance of the ducted propeller by different turbulent models. They presented the pressure distribution on the propeller surfaces, the pressure and the velocity vector distribution of the flow field around the ducted propeller. They showed that the Reynolds stress model (RSM) is better that the k-ε standard model.

The hydro-acoustic characteristics of the ship propeller in uniform and non-uniform flow were determined by *(Gorji et al., 2016)*. *(Majdfar et al., 2015 and 2017)* presented the numerical results of the hydrodynamic characteristics of a ducted propeller operating in oblique flow. Hydrodynamic characteristics of the Kort-nozzle propeller by different turbulence models carried out by *(Chamanara and Ghassemi, 2016)*.

Various studies have been done on a ducted propeller, but analyzing a ducted propeller by using different turbulence models and comparing them with each other, studying the effects of propeller position along the duct and duct angle relative to propeller on hydrodynamic characteristics have not been studied. In this paper, a Kaplan propeller with a 19A duct is used for CFD analysis. First, 19A duct data, especially data on the beginning and end of the duct which do not find in any references, are provided to model the duct geometry. Then, the ducted propeller is analyzed by using three different turbulence models including *k-ε* standard, *k-ω* SST and RSM and the results are compared with experimental data. Furthermore, the effects of the propeller position along the duct on hydrodynamic characteristics are investigated and the position in which the maximum thrust is produced will be determined. Finally, the effects of duct angle relative to propeller on hydrodynamic characteristics are studied.

Governing equations

In the present study, it is assumed that the fluid is incompressible. The governing equations consist of the mass and momentum conservations. Using the Reynolds averaging approach, the Navier–Stokes equations can be stated as:

$$\frac{\partial u_i}{\partial x_i} = 0 \qquad (1)$$

$$\frac{\partial}{\partial t}(\rho u_i) + \frac{\partial}{\partial x_j}(\rho u_i u_j) = \frac{\partial p}{\partial x_i} + \frac{\partial}{\partial x_j}\left(\mu \frac{\partial u_i}{\partial x_j} - \rho \overline{u_i' u_j'}\right) \qquad (2)$$

where $-\rho\overline{u_i' u_j'}$ is the Reynolds stresses.

In many important engineering flows, we deal with rotating or swivel flows. Rotating flows occur in turbo machinery, mixing tanks, marine propellers and a variety of other systems. Equations (1) and (2) are solved in a stationary coordinate system but sometimes it is useful to be solved in a moving coordinate system. When we are looking at moving parts from the stationary coordinate system, the flow zones result in a stability problem, but with a choice of rotating reference frame around the moving parts, the stability problem is solved. For simple problems, if we do not have any stationary zone, the single rotating reference frame (SRF) method can be used. For complex geometries, using the SRF is not possible. In this case, the problem is divided into several zones and two methods of MPM and MRF can be applied. The MPM method, despite being more accurate, due to the inclusion of interactions between the stationary and moving zones, requires a high computational time. In this paper, the MRF method is used, because not only does it need low computational time but it also has acceptable accuracy levels.

Geometric Modeling

The ducts are mostly used with 19A and 37 in ships with the Kaplan propeller. So, here we employed Kaplan propeller with a 19A duct for the analysis. The main dimensions of the ducted propeller are shown in Table 1. The duct section is shown in Fig.2. The three dimensional 19A duct model with a Kaplan propeller is created using CATIA software as shown in Fig. 3

Table 1. Main dimensions of the propeller and duct

Parameter	Value
Propeller Diameter	D=300mm
Number of blades	Z=4
Pitch ratio	P/D=1.2
Expanded area ratio	EAR=0.70
Rotational velocity	n=750 rpm
Length of duct (LD)	0.5D
Location of propeller	0.5LD
Clearance between duct and Propeller (m)	0.003 (0.01D)

Fig. 2. Duct section of 19A

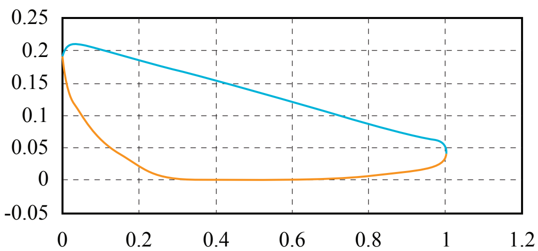

Fig. 3. Three dimensional ducted propeller

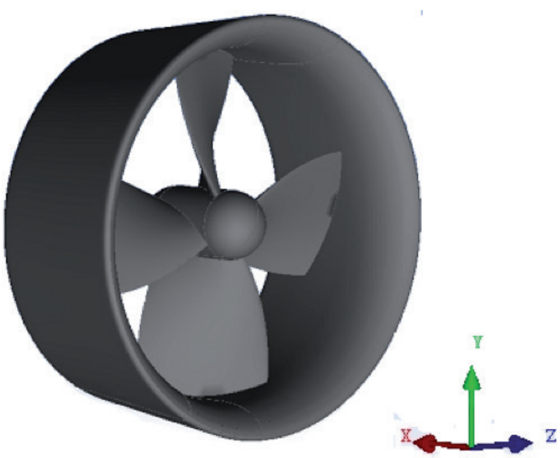

Mesh Generation and setting the boundary condition

The computational domain is required to be discretized to convert the partial differential equations into a series of algebraic equations. The ICEM software is used for mesh generation. Fig. 4 shows the computational domain of the ducted propeller. The upstream part is considered to be 3D (where D is diameter of the propeller) from the mid-point of the chord of the root section. The downstream part is considered at a distance of 6D. In radial direction, the domain is considered at a distance of 1.5D from the axis of the hub.

Fig. 4. Computational domain

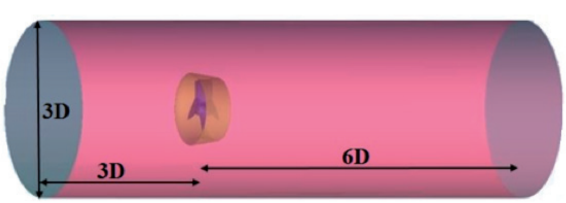

The method of tetra/mixed type is used for mesh generation in ICEM software. The maximum size of mesh elements is 0.2 and to make better meshing in the curved parts (such as the leading edge) it is necessary to enable curvature/proximity based refinement option and to set the minimum size limit at 0.00175. The blade section is an airfoil with a sharp edge so in order to preserve the airfoil form after the mesh generation, it is necessary to set the edge criterion value in the volume meshing parameters tab to 0.08. The split wall option of a rotating zone in the partial mesh setup should be checked to create an interface between the rotating and stationary zones.

Solver settings and boundary conditions

We used the MRF method which means that the computational domain is divided into two zones. The zone around the propeller is a rotational area and the other is a stationary area. The velocity inlet is changed to find the different advance coefficient. The inflow and outflow boundaries were set to velocity inlet and pressure outlet boundary conditions, respectively. The far field boundary was taken as the wall. The boundary conditions are shown in Fig. 5.

Fig. 5. Boundary conditions

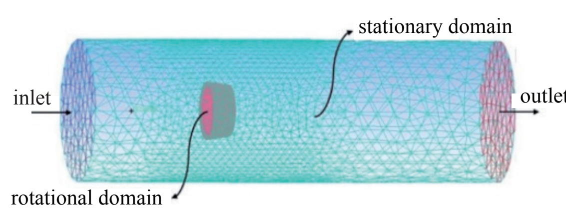

Calculations are carried out by the "Fluent software" to solve the three-dimensional viscous incompressible flow. The steady state pressure-based solver in a segregated mode was implemented using the MRF technique.

To find a proper turbulence model, the *k-ε* standard model, which has been used in most articles for ducted propeller analysis, is applied first. Then the results of this model are validated against the experimental results. In the next stage, the *k-ω* SST and RSM turbulence models are used and the

Table 2. Comparison of calculated results and experimental data of K_T, K_Q & η_0 with k-ε standard model

J	K_T CFD	K_T Exp.	$10K_Q$ CFD	$10K_Q$ Exp.	Effic. CFD	Effic. Exp.
0.201	0.531	0.562	0.619	0.655	0.275	0.275
0.300	0.468	0.504	0.600	0.636	0.372	0.378
0.402	0.404	0.445	0.576	0.606	0.450	0.471
0.499	0.346	0.389	0.545	0.572	0.505	0.540
0.600	0.287	0.325	0.504	0.526	0.544	0.588
0.698	0.229	0.258	0.453	0.474	0.561	0.607
0.797	0.170	0.179	0.394	0.408	0.545	0.558

results of these three models are compared. As a result of this comparison, the *k-ω* SST turbulence model is used as an appropriate model for investigating the effects of propeller position along the duct and also the effects of duct angle relative to propeller on hydrodynamic characteristics.

Results and discussion

Independence of the mesh

The number of mesh elements is checked to match the numerical results. In general, the mesh size should be small enough so that the results are not changed by increasing the number of elements. Finally, we observed that if the number of elements is equal to 2.5 million, the results will be independent of the mesh number.

Hydrodynamic characteristics

The open water characteristics of a propeller are usually given in terms of the advance coefficient (J), thrust coefficient (K_T), torque coefficient (K_Q) and open water efficiency Those coefficients are defined as follows:

$$\left\{\begin{array}{ll} K_T = \dfrac{T}{\rho n^2 D^4}, & K_Q = \dfrac{Q}{\rho n^2 D^5} \\ \eta = \dfrac{K_T}{K_Q}\cdot\dfrac{J}{2\pi}, & J = \dfrac{V_A}{nD} \end{array}\right. \quad (3)$$

Assuming constant rotational speed, advance velocity is changed until the advance coefficient of 0 to 1 is found and then, the hydrodynamic characteristics (K_T, K_Q, η) are calculated.

Firstly, we use the *k-ε* standard model for the analysis of ducted propeller. The trust coefficient, torque coefficient and efficiency are calculated and validated against the experimental. Table 2 is compared the calculated results and experimental data of K_T, K_Q & η_0 with the *k-ε* standard model.

Other turbulent models like the *k-ω* SST, *k-ε* standard and RSM are also employed. Table 3 compares the relative error of calculated efficiency with experimental data for three turbulent models. As can be seen, the relative error for RSM model is smaller than the two other models. The maximum relative error is less than 6%. The *k-ω* SST model is better than *k-ε* standard model. The *y+* value for all models is less than 30. It should be mentioned that very fine meshes are needed near the blades to achieve the less *y+*.

Table 3. Comparison of the relative error of calculated efficiency with experimental data

Advance coeff. (J)	RSM model	k-ω SST model	k-ε model
0.201	0.670697	0.187489	0.144466
0.300	0.685829	1.083604	1.544547
0.402	3.585964	3.873258	4.530412
0.499	5.192472	5.524279	6.583071
0.600	5.654494	6.055006	7.522543
0.698	4.73995	5.67678	7.557598
0.797	0.149689	1.805843	2.226791

Fig. 6. Comparison of open water characteristic with three turbulence models

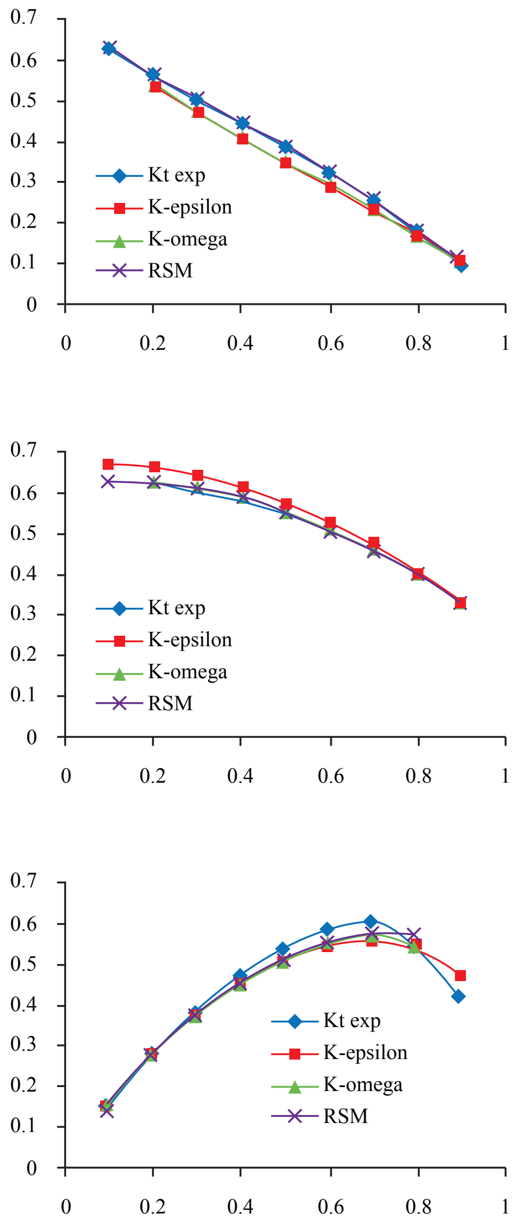

Effect of the propeller location

Here, the propeller is moved to the outlet direction as a percent of the duct length (*LD*%). The results of the thrust and torque are determined at various locations (0<*LD*%<7%). The thrust, torque and the percentage of the thrust is shown in Table 4. It is concluded that when *LD* is 3% the thrust increases about 2.148%. For other advance coefficients (when the *LD*% is 3), the results are given in Table 5. When the advance coefficient is 0.797 the efficiency is increased by approximately 1.05%.

Table 4. Increase of thrust with moving propeller

Moving propeller (percent of LD)	Thrust (N)	Torque (N.m)	Increase of thrust (%)
0	296.938	17.359	---
1	302.445	17.611	1.855
2	302.854	17.606	1.992
3	303.315	17.647	2.148
4	302.827	17.587	1.485
5	302.374	17.592	1.831
6	300.906	17.512	1.336
7	301.087	17.509	1.397

Table 5. Changes of the hydrodynamic characteristic with moving propeller (LD=3%)

Advance coeff. (J)	Increase of thrust (%)	Increase of torque (%)	Effi. (%)
0.300	1.418	2.375	-0.934
0.402	1.567	2.311	-0.727
0.499	2.071	2.847	-0.755
0.600	2.253	2.623	-0.360
0.698	2.096	1.939	0.154
0.797	***2.657***	***1.588***	***1.051***

Effect of duct angle

Another important point is the effect of the duct angle. The gap between the blade tip and the inner surface of the duct is 3 mm (0.001D where D is the propeller diameter) and a rotational zone is defined at this distance, so the duct or propeller cannot easily be rotated due to the duct angle. The maximum possible rotation of the duct relative to the propeller is 2 degrees counter-clockwise (CCW). Fig. 7 shows the duct angle with the propeller.

The results of the thrust and torque and their incremental are presented in Table 6. Thrust and torque are increased about 3 and 3.35% respectively. Efficiency is diminished about 0.25%.

Fig. 7. Duct angle with the propeller

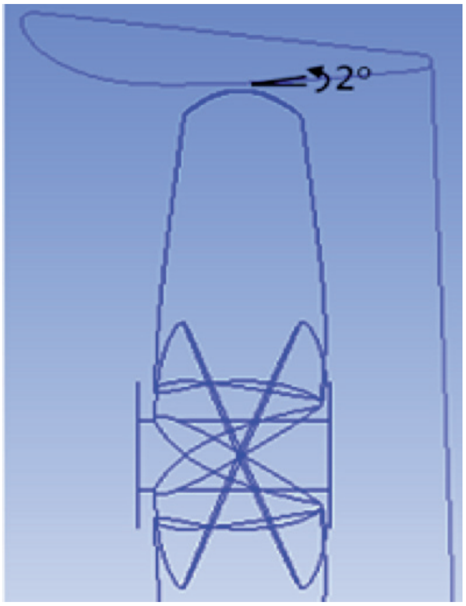

Table 6. Increase or decrease of the hydrodynamic characteristic with rotation propeller

Advance coefficient	**J=0.7**
Duct angle	2 [deg]
Thrust	306.11 [N]
Torque	17.9401 [N-m]
Increase of thrust%	3.08886
Increase of torque%	3.34818
Decrease of efficiency%	-0.2509

Conclusions

In this study, a Kaplan propeller with 19A duct was numerically analyzed using RANS solver. Three turbulent models were studied, and the effect of propeller location and duct angles were investigated. Based on the results, the following conclusions may be drawn:

- The ducted propeller was analyzed with three *k-ε* standard, *k-ω* SST and RSM models and the results were compared with experimental data. The error percentages showed that the RSM model has a lower error level compared to two other turbulent models.
- The propeller location is affected by the thrust and torque. According to our results, the best location is found when the LD is 3%, because of the higher thrust obtained.
- The effect of the duct angle by 2 degrees shows that efficiency decreases about 0.25% although thrust and torques are increased.

References

GHOSE J.P., GOKARN R.P.; *"Basic Ship Propulsion"*; Allied Publishers Pvt. Limited, 2004.

TAKETANI T., KIMURA K., ISHII N., MATSUURA M. and TAMURA T. *"Advanced design of a ducted propeller with high bollard pull performance"*, First International Symposium on Marine Propulsors smp'09, Trondheim, Norway, June 2009.

KORONOWICZ T., KRZEMIANOWSKI Z., and TUSZKOWSKA T., *"A complete design of ducted propellers using the new computer system"*; Polish Maritime Research, 2(60) Vol 16; pp. 34-39 10.2478/v10012-008-0019-3. 2009.

CELIK F., GUNERAND M. EKINCI S.; *"An approach to the design of ducted propeller"*; Transaction B: Mechanical Engineering Sharif University of Technology, Vol. 17, No. 5, pp. 406-417; October 2010.

CELIK F., DONGULAND A. ARIKAN Y.; *"Investigation of optimum duct geometry for a passenger ferry"*; IX HSMV Naples; May 2011.

CALDAS ALEJANDRO, MEIS MARCOS and SARASQUETE ADRIÁN; *"CFD validation of different propeller ducts on open water condition"*; 13th Numerical Towing Tank Symposium; Duisburg/Germany; October 2010.

BALTAZAR J., FALCÃO. DE CAMPOS and BOSSCHERS J.; *"Open-water thrust and torque predictions of a ducted propeller system with a panel Method"*; Hindawi Publishing

Corporation International Journal of Rotating Machinery; Article ID 474785, 11 pages doi:10.1155/2012/474785,2012.

YU L., GREVE M., DRUCKENBROD M., ABDEL-MAKSOUD M.; *"Numerical analysis of ducted propeller performance under open water test condition"*; Springer, J Mar Sci Technol, DOI 10.1007/s00773-013-0215-4; 24 February 2013.

KRZYSZTOF SZAFRAN, OLEKSANDR SHCHERBONOS, DARIUSZ EJMOCKI; *"Effects of duct shape on ducted propeller thrust performance"*; transactions of the institute of aviation; no. 4 (237), pp. 84-91, Warsaw 2014.

XUEMING HE, HECAI ZHAO, XUEDONG CHEN, ZAILEI LUO, YANNAN MIAO; *"Hydrodynamic performance analysis of the ducted propeller based on the combination of multi-block hybrid mesh and Reynolds stress model"*; Journal of Flow Control, Measurement & Visualization, 3, 67-74; April 2015 in Sci Res.

GORJI M., GHASSEMI H., MOHAMMADI J., *"Determining the hydro-acoustic characteristics of the ship propeller in uniform and non-uniform flow"*, International Journal of Engineering (IJE), Transactions A: Basics Vol. 29, No. 4, (April 2016).

CHAMANARA M., GHASSEMI, H., *"Hydrodynamic characteristics of the Kort-nozzle propeller by different turbulence models"*, American Journal of Mechanical Engineering, Vol. 4, No. 5, 2016, pp 169-172.

MAJDFAR S., GHASSEMI H., FOROUZAN H., *"Hydrodynamic Effects of the length and angle of the ducted propeller"*, Journal of Ocean, Mechanical and Aerospace -Science and Engineering-, Vol.25, 2015.

GHASSEMI H., MAJDFAR, S., FOROUZAN H., Calculations of the hydrodynamic characteristics of a ducted propeller operating in oblique flow, Ship Science & Technology, Vol. 10, no 20, (31-40) January 2017.

MAJDFAR S., GHASSEMI H., FOROUZAN H., ASHRAFI A., *"Hydrodynamic prediction of the ducted propeller by CFD solver"*, Journal of Marine Science and Technology, Vol. 25, No. 3, pp. 268-275, 2017.

Methodology for the Experimental Analysis of Offshore System in Deep and Ultra-Deep Waters in the Colombia Caribbean Sea

Metodología para el Análisis Experimental de Sistemas Offshore en Aguas Profundas y Ultra-profundas en el Mar Caribe Colombiano

DOI: https://doi.org/10.25043/19098642.163

Edgar Mulford [1]
Jairo Cabrera [2]

Abstract

Historically, different methodologies of experimental analysis of naval and oceanic structures oriented to the execution of controlled experimental tests in facilities capable of reproducing environmental conditions specific to their operating locations have been developed. These methodologies enable the efficient design of oceanic structures, the minimization of production costs and the generation of scientific knowledge. This article details the design of an experimental analysis methodology for semi-submersible offshore systems for deep and ultra-deep water fields, obtaining satisfactory results, and the validity of the procedure as an important contribution to the phases of semi-submersible platform design, a concept selected as appropriate for the areas of interest of the Colombian Caribbean.

Key words: Experimental analysis, offshore ocean structures, Semi-submersible, instrumentation, reduced scale model.

Resumen

Históricamente se viene desarrollando diversas metodologías de análisis experimental de estructuras navales y oceánicas orientadas a la ejecución de ensayos experimentales controlados en instalaciones capaces de reproducir condiciones ambientales propias de sus localizaciones de operación. Estas metodologías posibilitan el diseño eficiente de estructuras oceánicas, la minimización de costos de producción y la generación de conocimiento científico. En este artículo se detalla el diseño de una metodología de análisis experimental de sistemas offshore tipo semi-sumergibles para campos en aguas profundas y ultra-profundas, obteniéndose resultados satisfactorios, y de validez del procedimiento como un aporte importante a las fases del diseño de plataformas tipo semi-sumergibles, concepto seleccionado como el apropiado para las áreas de interés del Caribe Colombiano.

Palabras claves: Análisis experimental, estructuras oceanicas offshore, Semi-sumergible, instrumentación, modelo en escala reducida.

Date Received: June 8th 2017 - *Fecha de recepción: Junio 8 de 2017*
Date Accepted: September 30th 2017 - *Fecha de aceptación: Septiembre 30 de 2017*

[1] Escola Politécnica da Universidade de São Paulo, Brasil. Email: edgard.mulford@gmail.com
[2] Universidad Tecnológica de Bolívar, Faculty of Engineering, Cartagena, Colombia. Email: jcabrera@unitecnologica.edu.co

Introduction

The offshore industry, especially related to operations of exploration, extraction and production of oil and gas at sea, generates the need to have large oceanic structures. Colombia, as a developing country, is betting on the offshore oil industry through an aggressive exploration and production investment plan, focused mainly on increasing its reserves with new and renewed offshore exploration contracts.

This presents the need for investment in issues of technological development of the local industry through human capital, the adoption of technologies, creation of cooperation networks (university - industry - state) and increased infrastructure, among others.

In this scenario, it is especially important to strengthen local technological capabilities, encourage the transfer of knowledge and implement facilities such as tanks or experimental channels to evaluate operational restrictions according to the characterization of the physical-environmental conditions of the Colombian maritime environment in the areas of special interest.

The growing demand for the optimization of oceanic structures, whether for economic reasons (cost-benefit ratio), performance or viability, leads to the development of new experimental analysis techniques to determine their behavior, be it movements or efforts or any other phenomenon which structures are subject to. These experimental methods are used to verify theoretical predictions and / or evaluate physical conditions where mathematical approximations are very complicated.

The particularity of each naval or oceanic structure, depending on its geometric dimensions, the physical-environmental conditions of operation and the specific criteria established by norms and classification societies, makes the construction of prototypes and the development of real scale tests economically unfeasible.

Methodologies of the experimental analysis of naval and oceanic structures are being developed using reduced scale models, and scenarios able to reproduce the conditions of marine environments under controlled environments under the context of making the efficient design of structures viable, minimizing production costs and generating scientific knowledge.

Therefore, in order to prepare ourselves to face these challenges, to obtain the best advantage and future opportunities in the industry with the aim of contributing to offshore development in the country, this work focuses on the presentation of an experimental methodology such as a validation tool in the structural design of offshore ocean systems. A Semi-submersible floating platform is selected for validation purposes of the proposed methodology.

The challenge in Colombia

In recent years, the global trend of the development of the hydrocarbon exploitation industry has been shifting towards deep and ultra-deep waters. Situation that is not exempt to Colombia. According to recent findings, the Orca-1 Well (Tayrona Block) and Kronos-1Well (South Fort Block), in deep and ultra-deep waters respectively, (see figure 1), show the Colombian Caribbean as the newest and most promising exploratory boundary of hydrocarbons, but with great challenges *(Cabrera, 2016)*.

Fig. 1. Blocks of interest in the Colombian Caribbean (Source: ECP)

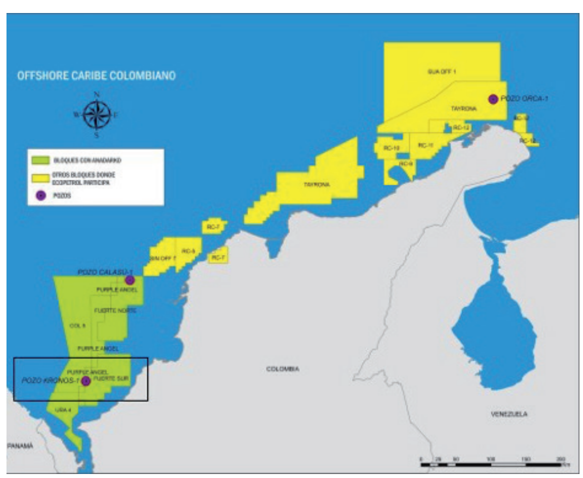

The development of offshore activities in deep and ultra-deep waters depends on a variety of physical and environmental conditions, representing a great challenge given the technological complexity of producing hydrocarbons in these depths.

One of the main implications of these exploratory fields is that for these regions of interest the installation of fixed platforms is technically and economically unfeasible, resorting to the need for floating production systems. The naval engineering competencies are the selection of the concepts and the design of the necessary infrastructure for these developments, giving special importance to systems of semi-submersible platforms and FPSO (Floating Production Storage and Offloading), among other alternatives.

The process of selecting the type of floating ocean platform to operate in these areas of interest in the Colombian Caribbean depends directly on the initially established functional requirements. Considering especially the physical-environmental conditions present and the operational restrictions that this area supposes, the selection of systems, subsystems and the definition of a matrix of influence and quality, where the physical factors of the structure are related to facilitate the perception of how these factors influence one another, and how they are influenced.

Through preliminary studies it has been concluded that in the Colombian Caribbean, and in deep and ultra-deep waters, a semi-submersible platform system would provide all the operational characteristics to cover the present needs in the areas and fields of interest. However, a detailed analysis is necessary to select the most efficient configuration for said application.

According to *(Chakrabarti, 2005)*, semi-submersibles consist of structures with one or more decks, supported by submerged columns and floats called "pontoons". This type of structure is also called a "stabilized column", which means that the center of gravity is above the center of flotation and stability is determined by the moment of restoration of the columns. An example of the various components of the structure of a conventional semi-submersible type platform is presented in Fig. 2 *(ABS, 2012)*.

Fig. 1. Typical semi-submersible platform configuration [ABS, 2012]

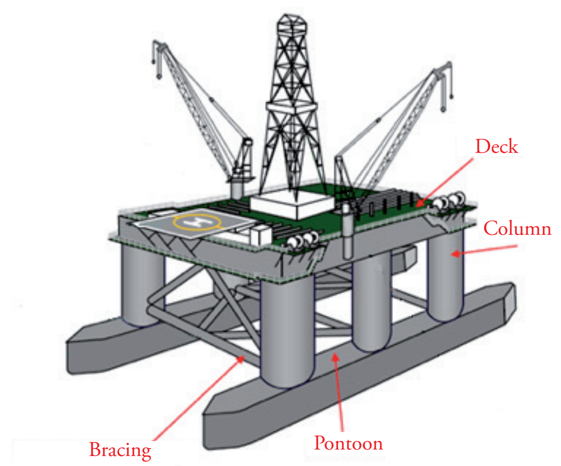

Independent of the mission of the platform, there are two essential functions, which establish the size of the structure *(Chakrabarti, 2005)*:

- To provide stable support for the loads on the deck under the action of the waves;
- To present minimal movements under the action of waves.

Figs. 3 and 4 illustrate a series of typical arrangements of columns and pontoons. Just as the parallel and closed pontoon arrangements are currently used, the configurations of 3 columns and closed pontoon (triangular) are used in semi-

Fig. 3. Arrangements of columns in semi-submersible [CHAKRABARTI, 2005]

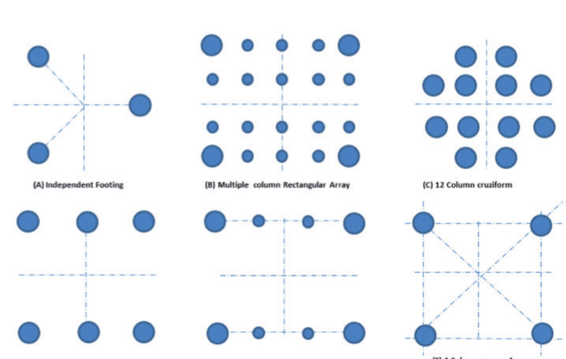

Fig. 4. Arrangement of pontoons in semi-submersibles [CHAKRABARTI, 2005]

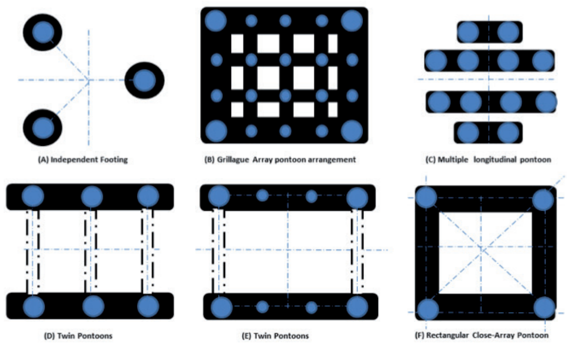

submersible applications offering a timely reduction of steel, but greater complexity in the roof.

The arrangement of closed pontoon or ring has greater resistance to the advance and therefore less push mobility, but is often preferred for a permanent fixed system, because it offers superior resistance. Follow the typical design methodologies for floating ocean systems below.

Design Methodologies

The method commonly used in the design of oceanic structures is based on concepts of synthesis, analysis and evaluation (see Fig. 5). Where the design requirements imposed by the client and the physical-environmental and operational conditions present in the area of action are defined. Based on these requirements, an initial hypothesis is proposed, to define the systems and subsystems inherent to the design process and the relationship between them. After a recommendation for solving the problem, an analysis is carried out where it is verified that the design object meets the imposed restrictions and rules (restrictive or acceptance criteria). Once the analysis process is finished, decisions are made to evaluate what was done according to the criteria established by the designers, where it is determined if the solution obtained can be improved or not, until reaching admissible values within the initial parameters of the project planned in a global evaluation.

Fig. 5. Design methodology

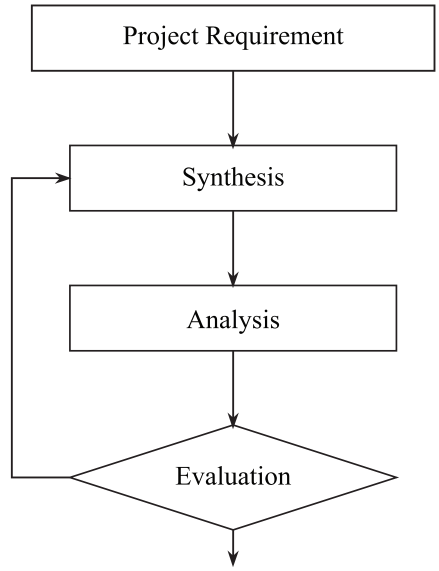

Similarly, the preliminary design of oceanic structures in many cases are based on the classical design spiral *(Evans, 1959)*, where criteria are presented in various phases that lead to the optimization of design in terms of costs especially. Although the sequence shown in Fig. 6 is based on the experience acquired through the design of oceanic platforms, it is not considered definitive. Depending on the type of project, the criticality of each phase can be different, causing the sequence to be altered so that the most critical and critical aspects are analyzed first.

Fig. 6. API Design Spiral for the TLP Project [Mercier, 1991]

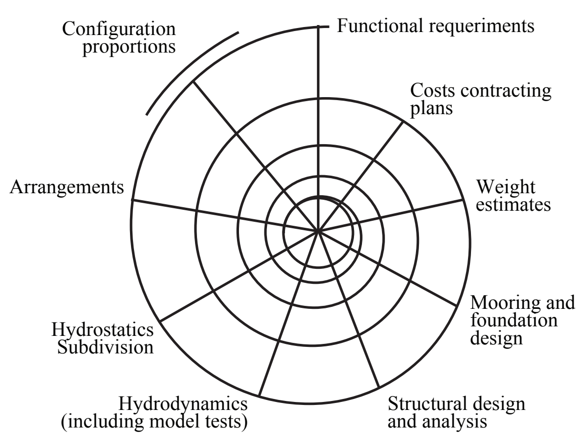

The design spiral is frequently used in the naval industry and allows an integrated and global vision of the project as a whole, highlighting the interconnections between the various phases, which has been adopted as an application model.

Proposed experimental analysis methodology

The experimental analysis of scale models (similar to real structures in terms of geometry and dynamics) during the design phase, in addition to allowing the reduction of costs when executing tests, in essence, allows the behavior of the original physical system to be predicted. This prediction is especially important in the operation in adverse environmental conditions, where the main natural agents (waves, wind and currents) act in a severe manner. Both *(Kure, 1981)* and *(Chakrabarti, 1994)*, proposed that the design of the structure be verified by testing the model in scale in a simulated oceanic environment.

Due to the costs of the experiments and the important decisions that derive from the experimental results, it is not advisable to look for solutions to a specific problem relying only on intuition. Therefore, the design of experiments allows a sequence of tests to be structured in the form of translating the pre-established objectives by the researcher and obtaining efficiency in terms of information. Thus, the planning of the design of experiments must be carefully schematized to minimize the time and costs of the test, while maintaining reliability *(Duarte, 2011)*.

Proposed Procedure

Referencing the works of *(Tachibana, 1994)*, *(Cardoza, 2002)*, and giving special emphasis to the research of *(Chakrabarti, 1994-1998-2005)* and *(Steen, 2014)*, due to its direct connection with naval and oceanic applications in wave tanks; a methodological proposal represented in the diagram shown in Fig. 7 was established.

Fig. 7. Proposed procedure [Mulford, 2014]

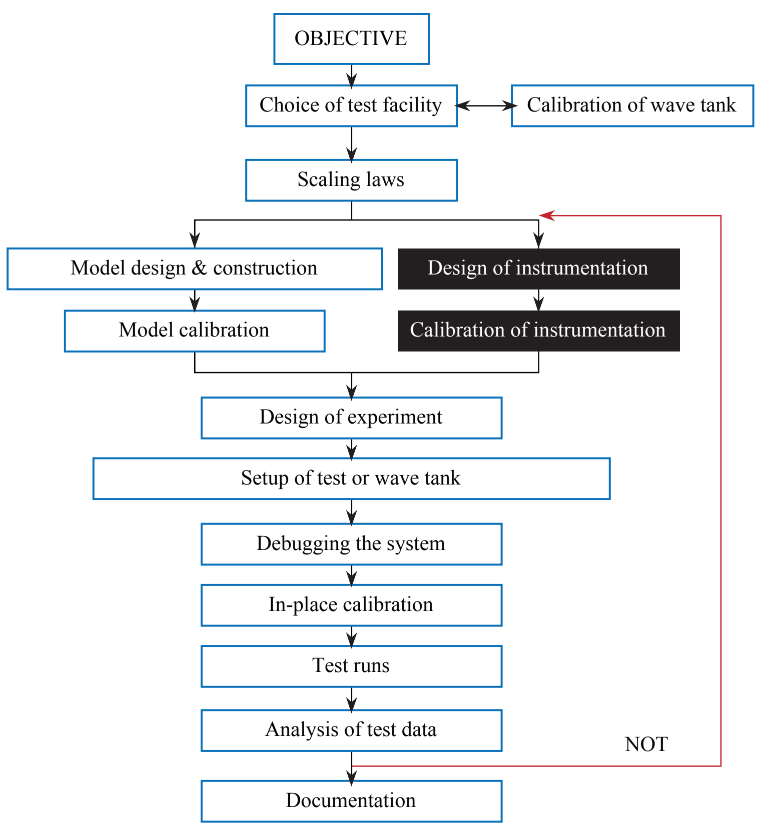

This proposal consists of a synthesis of recommendations, norms and rules established by authors, classification societies (DNV, ABS, BV), results of international conferences (ITTC, OTC) and research laboratories (NTNU, IPT), among others, which has been planned and coordinated efficiently and accurately to evaluate the objective problem.

The procedure consists initially of defining the type of structure (platform) and variable or physical phenomenon of interest to be evaluated.

The effective selection of the tank is based not only on the physical tank where the tests are executed. The facilities must cover different additional functions such as laboratories for building models, instrumentation, environmental simulation by computer, and also monitored data storage tools *(Steen, 2014)*.

Regardless of the type of tank, each laboratory has a programmed calibration program. Likewise, before the execution of an assay, calibrations are carried out to guarantee the quality of the results. In the case of wave calibration, consider not using the model to ensure that calibrated waves do not contain effects associated with the model / fluid interaction *(Steen, 2014)*.

The scale of the model is chosen as a compromise between the cost of the design and the technical requirements for similarity. In addition, the definition of the scale is directly associated with the infrastructure of the available test tank, seeking to avoid the problems of wave reflection in the walls of the tank and the blocking and repositioning of the model when carrying out the tests.

The selection of the scale factor starts from the definition of the laws of similarity, which quantify the response of the scale model in relation to the real structure. For the study of the phenomenon of fluids, there are three basic laws: Geometric, kinematic and dynamic similarity.

Scale factor

$$\lambda = L_F / L_M \tag{1}$$

Where the relationship between the scale model (L_M) and the real model (L_F) is constant *(Chakrabarti, 1998)*.

The Froude number is defined as follows:

$$Fr^2 = \frac{v^2}{gl^2} \rightarrow Fr = \frac{v}{\sqrt{gl}} \tag{2}$$

Where l is length parameter [m]; v is velocity parameter [m/s]; and g is the acceleration of gravity [m/s^2].

When it is not possible to recommend an optimal scale factor for a structure without investigating all the parameters of importance, a common scale factor used in effect of water waves in a tank is 1:50. For towing tanks a typical range of scales is between 1:10 and 1:100 *(Chakrabarti, 1994)*.

According to *(Harris, 1999)* the design of the model suggests:

- Define the scope of the problem; decide what is necessary for the model and what is not;
- Specify geometrical similarity requirements, materials and loads;
- Decide the size of the model and the level of reliability and precision requirement;
- Draw the plans (main views);
- Select the type of material to be used and establish the manufacturing plan.

Some typical materials used for the construction of these models are: paraffin wax, wood, foam, reinforced fiberglass.

Commonly additional internal reinforcements are used to ensure structural rigidity and behavior similar to that of the actual structure.

Within the model, weight is placed on lead or steel as a ballast method used for load monitoring. The exterior of the model is prepared and coated with high visibility inks *(Steen, 2014)*.

According to the same author, for dynamic tests where the model presents free movement and the forces of inertia are important, the distribution of mass must be appropriate. In practical termsthe following calibration requirements must be met:

- Total mass;
- Moment of inertia expressed in terms of the radii of rotation, rxx, ryy and rzz;
- Vertical and longitudinal position of the center of gravity;
- For stability effects, the mass distribution must be correctly modeled.

In cases where the elasticity is not important, the built model must be "sufficiently" rigid to avoid any artificial hydro-elastic effect on the structure.

In *(Malta, 2010)* and *(Steen, 2012)* the main instruments and measuring equipment used in laboratory tests are highlighted, for the structural analysis of different types of reduced scale models are used, such as: inductive transducers, angular and linear potentiometers, accelerometers, pressure gauges, extensometers, load cells, wave sensors (elevation), optical systems (cameras) for motion monitoring, etc.

Just as important as the careful planning of the test, is the appropriation of electronic tools and instruments for post-processing or manipulation of the data obtained in the tests.

In most simple applications the transducers are manufactured to have a linear relationship between the load and the output signal. The calibration of each transducer is carried out before the execution of the tests. It is advisable to perform a calibration review after the execution of the tests to ensure that the calibration factors do not have significant changes in the assemblies and to verify that all connections are correct.

The test matrix defines the formal plan constructed sequentially to conduct the experiments. Control factors are included in this matrix together with the levels and the treatment of the experiment *(Fraden, 2003)*.

International conferences such as the ITTC (International Towing Tank Conference) and the OTC (Offshore Technology Conference) present recommendations as experimental procedures that should be considered when carrying out the tests to guarantee the veracity of the results.

The instrumentation required to measure responses must be installed in the model. Instruments not associated with the model, as in the case of wave sensors, must be installed in the tank, calibrated and adjusted.

The environmental conditions must be calibrated in advance to guarantee the execution of the tests. The model must be positioned in the specific place for the test, in an area where the minimum reflection and distortion of the waves prevails. In addition, decay tests (free oscillation) must be carried out in the model, with or without anchoring, to determine natural frequencies.

Once the model is ballasted, instrumented, calibrated and adjusted in the position, the test matrix must be executed. The data should be stored digitally if possible. The sampling frequency must be high enough to capture the physical phenomenon analyzed.

In engineering applications the results must be presented in dimensional form. To evaluate the results and compare them with databases, it is advisable to present the answers in a dimensionless way.

The analysis procedure must be fully documented to ensure reproducibility

The ITTC (ITTC, 2014) provides recommendations for the development of uncertainties analysis and argues that most sources of error in model tests are in:

- Scale effects;
- Incorrect modeling of the structure (Geometry, mass distribution, etc.);
- Incorrect modeling of environmental conditions (period and height of the wave, physical limitations of the tank);
- Instrumentation and measurement error;
- Error in the analysis and interpretation of results.

It is important to document the results of the test to highlight important observations and present conclusions. The type of documentation depends on the requirements of the requestor and the characteristics of the tests.

Validation of the procedure through the development of a Prototype of a Semi-Submersible Platform

For validation purposes of the proposed methodology, the hydrodynamic study of the semi-submersible platform GVA 4000 was carried out, which is a four-column floating offshore structure in a square arrangement, with two parallel pontoons and a main deck (see Fig. 8).

Due to availability and costs, the wave tank (DENO-USP) was used, which has the following characteristics:

- Length: 21.61 meters.
- Width: 4.85 meters.
- Maximum depth: 1.78 meters.

This platform has a composite wave generator (with single tilting plate flap). The waves can be generated in a range of 0.5 to 3.0 Hz. (See Fig. 9).

Fig. 8. Semi-submersible study platform (Kallstrom, 1986)

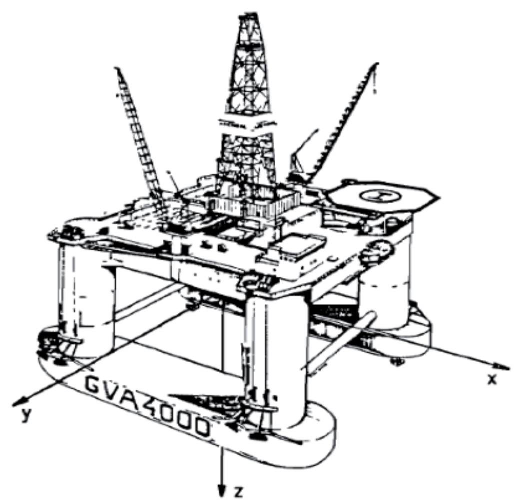

Fig. 9. Schematic diagram of the DENO-USP tank (Souza, 2003)

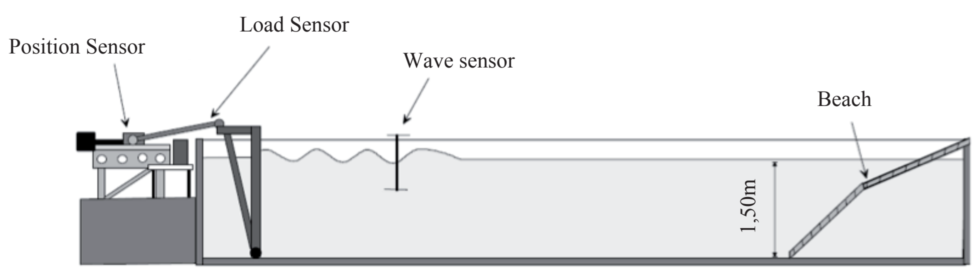

Fig. 10. Dimensional plan of the model of the platform in reduced scale

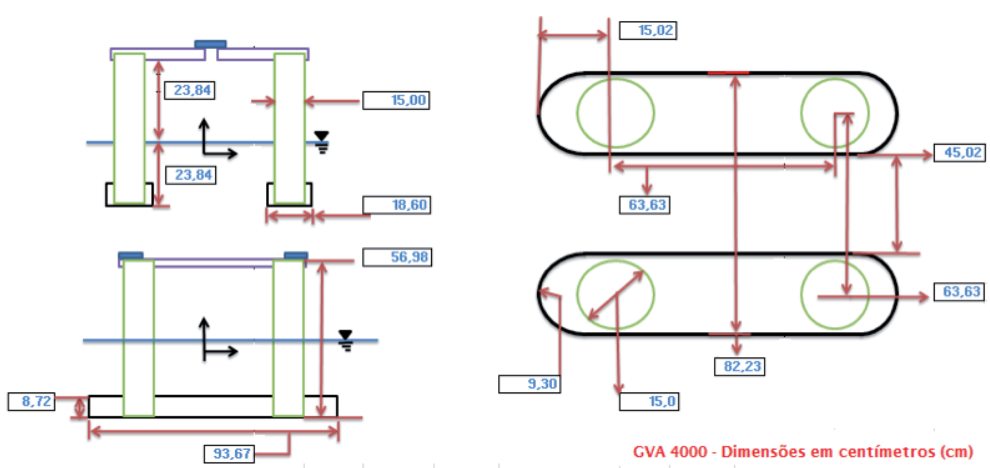

Considering the physical characteristics of the tank, a scale factor of the 1:86 model was established.

The model in dimensional plane (see Fig. 10) and in 3D was designed with the use of commercial computational tools (see Fig. 11) directly considering the main dimensions of the real structure given by the manufacturer.

Fig. 11. Model of the platform designed in 3D (Rhinoceros ®)

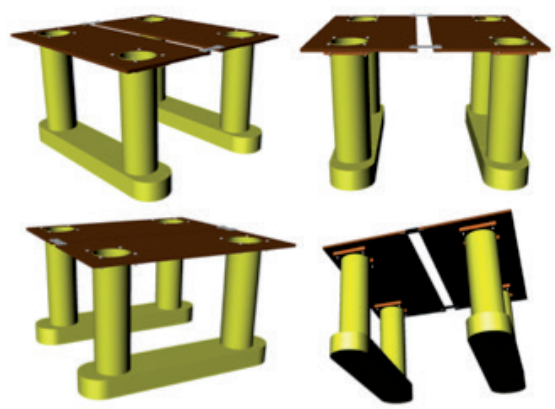

The pontoons and the columns were constructed with PVC and the deck with compensated wood. The use of epoxy resin and PVC reinforcements was crucial to give rigidity to the structure and guarantee the water tightness of the model once it is floating in the water (see Fig. 12).

Fig. 12. Construction of the model

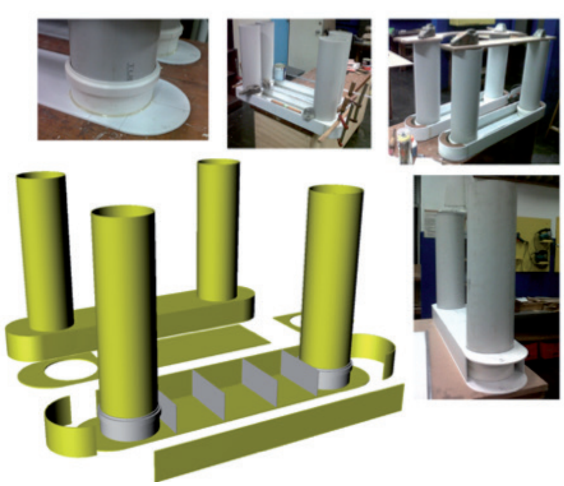

As a calibration process of the model, analytical calculations of static behavior (stability criteria) were carried out

$$GM = KB + BM - KG \tag{3}$$

where GM is the metacentric height, KB is the center of submerged volume (center of gravity), BM is the metacentric radius and KG is the center of gravity (see Fig. 13).

Fig. 13. Physical relationship between GM, KB, BM and GM

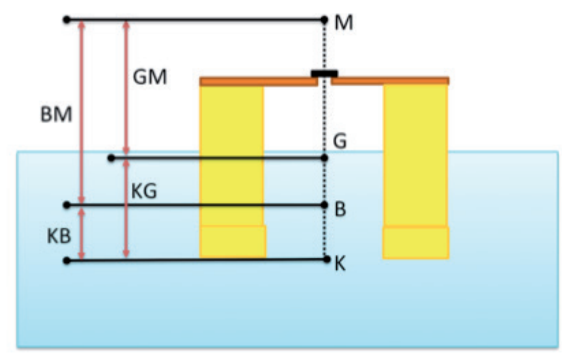

The dynamic calibration of the model began with the determination of the mass distribution, that is computationally simulated and experimentally validated, considering the center of mass in the geometrical center of the platform and the inertia of the radii of rotation (Kxx, Kyy and Kzz) given by the manufacturer of the real structure (see Fig. 14).

Fig. 14. Mass distribution (lastro) using ANSYS ™

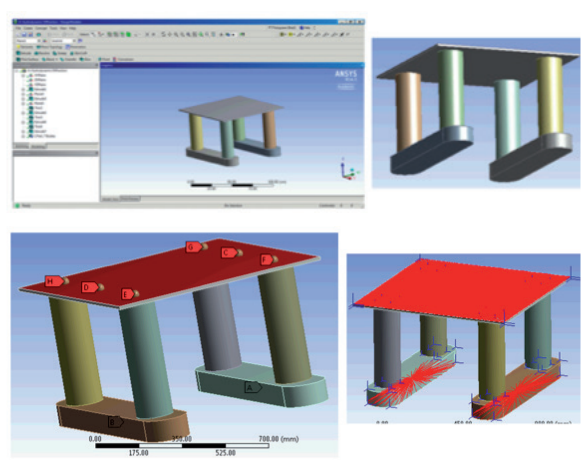

Fig. 15. Schematic of assembly and calibration of the model in the wave tank

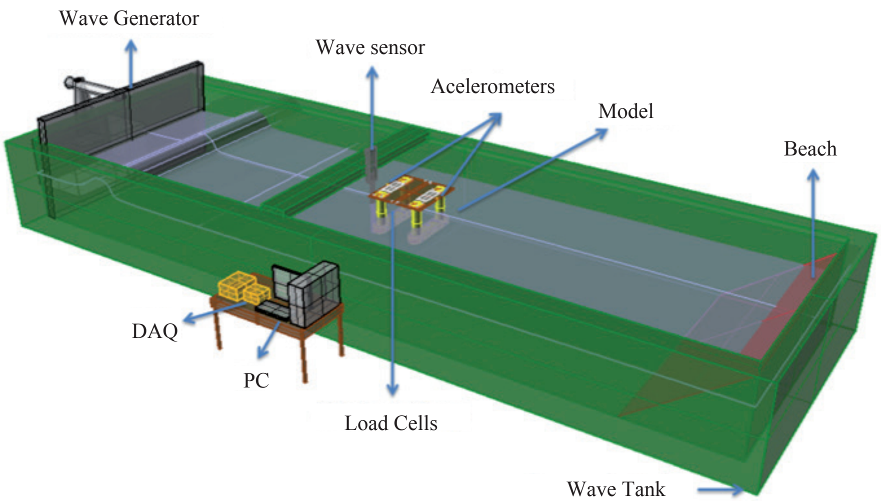

Figs. 15 and 16 shows a diagram of the assembly, positioning and calibration of the model in the wave tank and the final adjustment respectively.

Fig. 16. Adjustments and execution of the test matrix

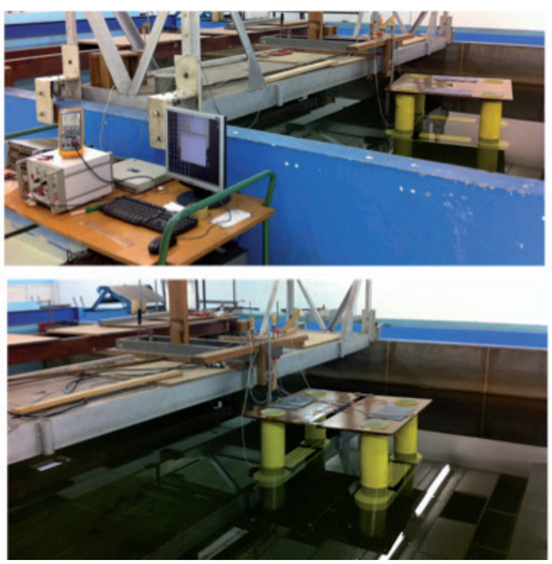

The computationally designed and simulated model for determining the natural frequency parameters of the structure and RAO response in the different degrees of free movement of the platform is represented in Fig. 17.

It is important to consider the peak frequency (see Fig. 18) best known as the natural frequency of the system, to avoid resonance effects by trying to keep the structure away from the oscillation frequency of the fluid medium.

Fig. 17. Adjustments and execution of the test matrix

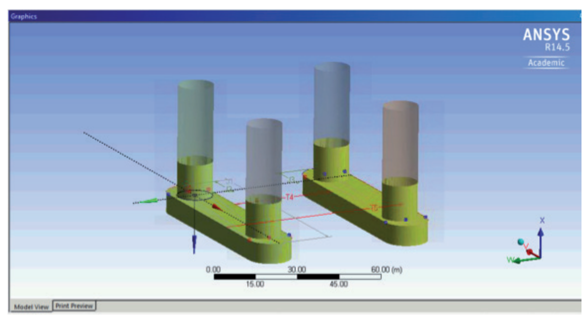

The experimental response of natural frequency obtained by the model is equivalent to approximately 0.4 Hz according to the analytical calculations (2.52 Rad / s ≈ 0.401 Hz) which represents concordance with the constructed physical model.

$$RAO_{heave} = \frac{A_{mov}}{A_{onda}} \quad (4)$$

This simplified form of obtaining RAO is only possible in tests with regular waves where the excitation frequency is approximately the same as the response.

Fig. 18. Heave ROA of the AQWA real-scale platform and the results of (Kim, 2010)

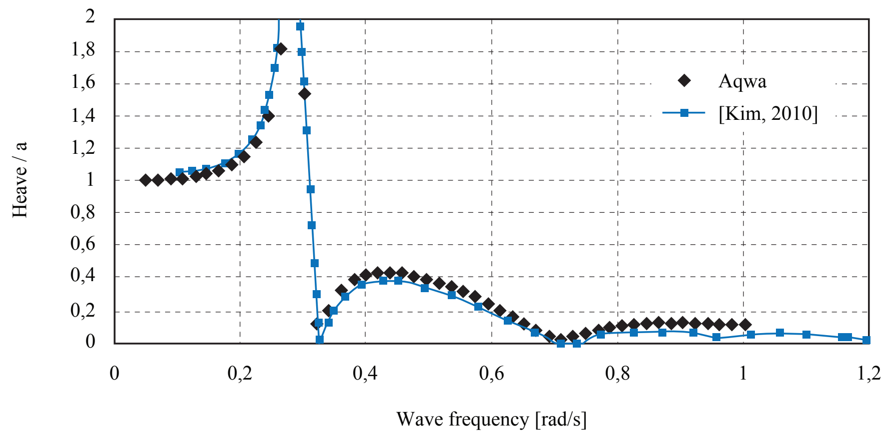

In Figs. 19 and 20 the constructed model validates the hydrodynamic behavior obtained in computational simulation, especially in relation to natural frequency.

In Fig. 21 it is verified that the highest Bending Moment experimentally measured on the deck is presented for the case of wave frequencies of 5.97 rad / s (0.95 Hz). Such that compared to the estimate of critical wave condition given by the DNV (2B = 6.1 rad/s), it is possible to validate the efficiency of the experimental procedure carried out.

Conclusions

The experimental procedure developed was validated through comparison with experimental results presented in the literature. Additionally, the experimental results were also used in the evaluation of the quality of the results obtained through computational simulation, usually used in the initial phases of the design and analysis of offshore floating platforms.

The proposed procedure always sought, as far as possible and due to the available equipment to

Fig. 19. Heave RAO of the reduced vs. simulated model (AQWA) in the direction of 180°

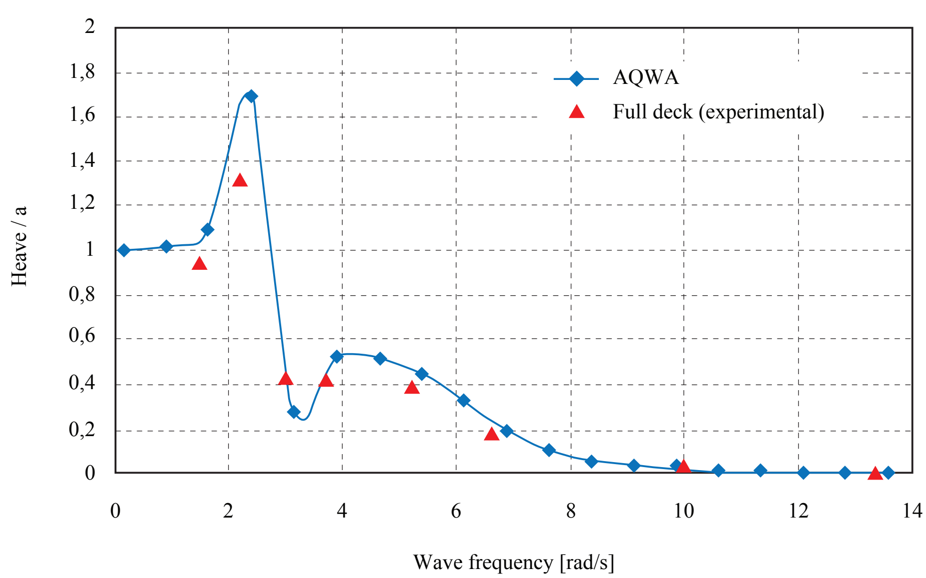

Fig. 20. Heave RAO of the reduced vs. simulated model (AQWA) in the direction of 90°

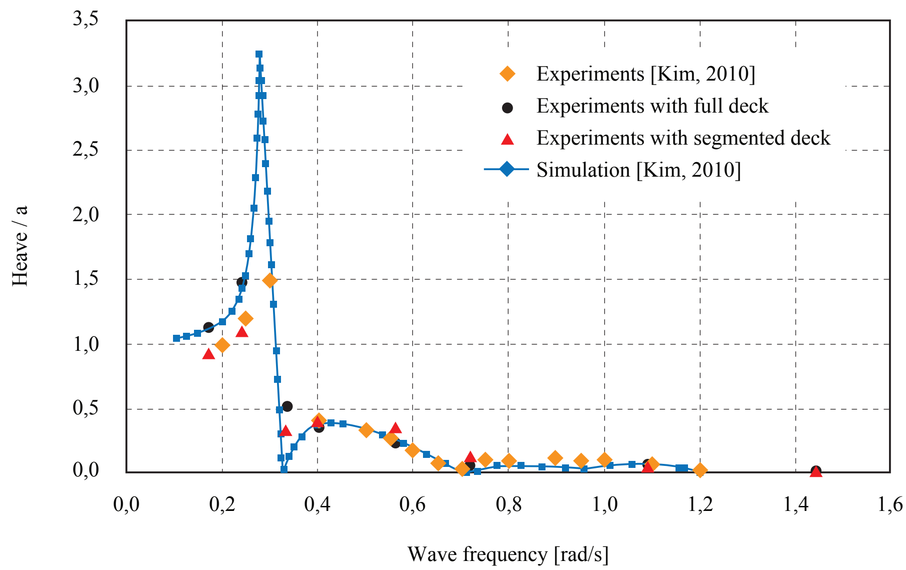

Fig. 21. Flector Moment acting on the cover of the reduced semi-submersible model in the direction of 90°

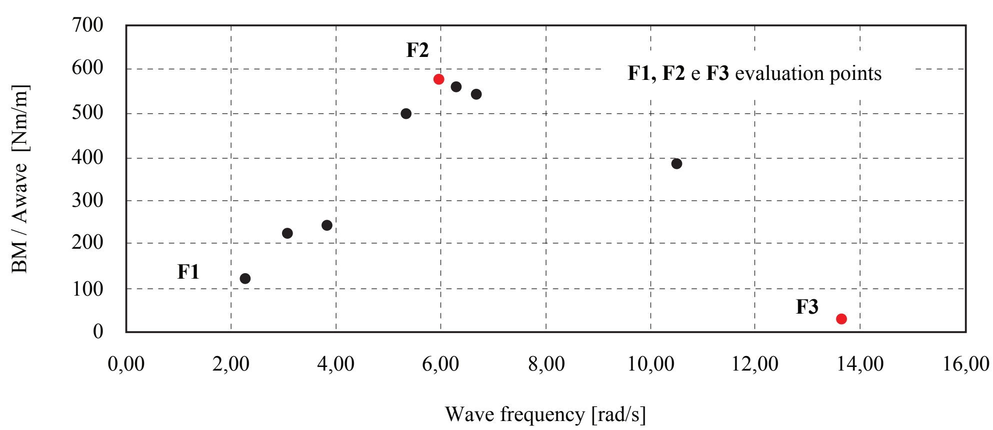

follow the recommendations and rules established by the literature.

In this sense a model capable of faithfully representing the hydrodynamic behavior of the real platform was successfully obtained. The geometric and dynamic similarity, especially with reference to the equilibrium criteria, was guaranteed.

References

API-RP 2T, *Recommended Practice for Planning, Designing, and Constructing Tension Leg Platforms, American Petroleum Institute*, April 1987.

CABRERA. J. – Nuevas fronteras y desafíos tecnológicos en aguas profundas y ultra-profundas en el caribe colombiano – DIMAR OFFSHORE CARIBE, Pag, 65 – 67, 2016

CARDOZA, E.V., *Aplicação das técnicas de planejamento e análise de experimentos na melhora da qualidade de um processo de fabricação de produtos plásticos*, 2002. Dissertação (Mestrado). Universidade de São Paulo, São Carlos. São Paulo. 2002. 121p.

CHAKRABARTI, S.K. *Offshore Structure Modeling, Advanced series on Ocean Engineering* – Volume 9, Chicago Bridge & Iron Technical Service Co., World Scientific, Plainfield, Illinois, USA. 1994. 470p.

CHAKRABARTI, S.K. *Physical Model testing of Floating Offshore Structures*. Marine technology Society, Dynamic Positioning Conference, October 13-14, 1998. 33p.

CHAKRABARTI, S.K. *Handbook of Offshore Engineering – Offshore Structure Analysis*, Inc. Plainfield, Illinois, USA. Elsevier Vol. 1 – Cap. 1,7,13. 2005. 1268p.

DUARTE, J. L. SCHWENGBER, *C. Série Monográfica Qualidade – Projeto de experimentos - Universidade Federal do Rio Grande do Sul, Escola de Engenharia - Programa de Pós Graduação em Engenharia de Produção Porto Alegre, RS*, Brasil. 2011

EVANS, J. H. *Basic Design Concepts, ASNE Journal, American Society of Naval Engineers*, 1959.

FRADEN, J., *Handbook of Modern Sensors – Physics, Designs, and Applications* – Cap 1 – Data Acquisition - Third Edition – Springer – San Diego, California USA. 2003. 608p.

HARRIS G., HARRY, S M., GAJANAM, *Structural Modeling and Experimental Techniques, Second Edition*, CRC Press LLC, USA. 1999. 808p.

ITTC, *Recommend Procedures and Guidelines, International Towing Tank Conference*, 2014.

KALLSTROM, C. G. AND BYSTROM, L. *Dynamic Positioning of a Semi-Submersible: Results of Scale Model Tests and Computer Simulations* - Society for Underwater Technology (Graham & Trotman. 1986) - SSPA Maritime Consulting AB, Goteborg, Sweden. 1986. 14p.

KIM, J., KIM, Y., SHIN S. *Experimental study of motion & wave load response on semi-submersible – Ocean Engineering Research Department*, MOERI/KORDI, Daejon, Korea. 2010. 4p

KURE, K. *Model tests with ocean structures* - Danish Ship Research Laboratory, Hjortekaersvej 99, DK-2800 Lyngby, Denmark. 1981. 6p.

MALTA, E.B. - *Métodos e processos para a análise experimental de sistemas oceânicos de produção de petróleo e gás*. 2010 – Dissertação (Mestrado) Universidade de São Paulo – São Paulo, Brasil. 2010. 218p.

MERCIER, J. A. *Tension Leg Platforms - Progress and Prospects*. Vol. 99; 1991; pp. 249-279

MULFORD, E. – *Dissertação (Mestrado), Procedimento para determinação experimental de carregamentos externo para o projeto estrutural de uma plataforma semi-submersivel – Escola Politecnica da Universidade de Sao Paulo – Departamento de Engenharia Naval e Oceânica*, 192p, 2014.

SOUZA, C.A.G. *Projeto, implantação e análise de um gerador de ondas - Departamento de Engenharia Naval e Oceânica, Escola Politécnica da Universidade de São Paulo – São Paulo – SP* – Brasil. 2003. 10p.

STEEN, S. *Experimental Methods in Marine Hydrodynamics – TMR7, Lecture notes – Faculty of Engineering Science and Technology – NTNU TRONDHEIM, Norwegian University of Science and Technology*. 2014. 183p.

TACHIBANA, T. *Método de avaliação do desempenho dinâmico de uma plataforma semi-submersível*, concurso livre-docência EPUSP, São Paulo, Brasil. 1994.

Development of Materials for Naval, Fluvial and Military Applications

Desarrollo de Materiales para Aplicaciones Marítimas, Fluviales y Militares

DOI: https://doi.org/10.25043/19098642.164

Fabio A. Suárez-Bustamante [1]
Orlando D. Barrios-Revollo [2]
Anderson Valencia [3]
Juan P. Hernández-Ortiz [4]

Abstract

A platform to design composite materials of a polymeric matrix, that are specifically for military applications on fluvial and naval navigation, has been developed using energy dissipation and storage mechanisms. Our composites are designed to generate synergy between the dissipation capacities of ceramics and high-performance fibers, which are used as the reinforced material in the lightweight laminates. The composite design is combined with processing tools and advanced characterization techniques that result in laminates with reliability, traceability and quality. The platform begins with the identification of energy dissipation mechanisms and the detailed characterization of the polymeric resin. It includes the Time – Temperature – Transformation Diagram (TTT- Diagram) that supplies the optimal processing conditions. Our designs open new paths for military applications including a wide spectrum of protective systems together with geometric versatility, high mechanical resistance and reliability.

Key words: Composite Materials, Materials Design, Military Applications, Impact Energy Dissipation Mechanisms, Naval and Fluvial Applications.

Resumen

Utilizando los múltiples mecanismos de disipación de la energía de impacto a alta velocidad, hemos desarrollado una plataforma de diseño de materiales compuestos de matriz polimérica, especiales para aplicaciones militares en navegación fluvial y marítima. Nuestros compuestos pretenden hacer sinergia entre las capacidades de disipación de cerámicos y fibras de alto desempeño, los cuales son utilizados como los elementos de refuerzo en los laminados de bajo peso. El diseño del material es combinado con herramientas de procesamiento y técnicas avanzadas de caracterización que resultan en laminados consistentes de alta repetibilidad, trazabilidad y alta calidad. La plataforma parte de la identificación de los mecanismos de disipación y de una caracterización detallada de la resina polimérica, el cual incluye un diagrama de Tiempo-Temperatura-Transformación que provee las condiciones óptimas de procesamiento. Nuestros diseños abren rutas novedosas para aplicaciones militares, los cuales incluyen amplios portafolios de protección, versatilidad geométrica, resistencia mecánica y confiabilidad.

Palabras claves: Materiales Compuestos, Diseño de Materiales, aplicaciones Militares, Mecanismos de Disipación de Energía de Impacto, Aplicaciones Navales y Fluviales.

Date Received: July 7th 2017 - *Fecha de recepción: Julio 7 de 2017*
Date Accepted: November 14th 2017 - *Fecha de aceptación: Noviembre 14 de 2017*

[1] Department of Materials, Faculty of Mines, Universidad Nacional de Colombia. Medellín, Colombia. Email: fasuarez@unal.edu.co
[2] Department of Materials, Faculty of Mines, Universidad Nacional de Colombia. Medellín, Colombia. Email: odbarriosr@unal.edu.co
[3] DynaComp S.A.S. Calle 80 Sur # 47 D163 - Bodega 1, Sabaneta, Colombia. Email: anderson.valencia@dynacomp.com.co
[4] Department of Materials, Faculty of Mines, Universidad Nacional de Colombia and Institute for Molecular Engineering, University of Chicago. Email: jphernandezo@wisc.edu

Ballistic Materials and Design Trends

From the beginnings of the human race, man has made elements for his personal protection. Leather, wood and some metals were used as materials to fabricate helmets, body-armor, shields and other items. Today, metals are used for these purposes and intensive research is done to improve their ballistic performance. Steel, aluminum and titanium alloys are widely used for these applications [1-11]. Nevertheless, metals are heavier than polymers and some ceramics, limiting their application for lightweight body and structural armors for land, air and water vehicles. In addition, metal processing requires large quantities of energy. Ceramics, polymers and composites have become the new option to avoid these restrictions [12-15]. However, each material and composite faces challenges due to the constant improvements in the development of projectiles and weapons and in the specific conditions of new applications.

According to Grujicic [16], fiber-based composites were used for the first time in body-armor in the Korean war. They were constructed with nylon fabric and E-glass fibers within an ethyl cellulose matrix composite. Currently, high performance polymeric fibers such as poly-aramids (Kevlar[17,18], Twaron [18,19], Technora [18, 20]), highly oriented and crystallized ultra high molecular weight polyethylene (UHMWPE) (Spectra [18, 21] and Dyneema [18, 22]), poly-benzobis-oxazole PBO (Zylon [18, 23]) and poly-pyridobisimi-dazole PIPD (M5) [18], are widely used for ballistic composites. Under tension, these materials differ significantly from the nylon fibers, having a high absolute stiffness, extremely high specific strength, and quite low (<4%) strains-to-failure. These fibers essentially behave in tension as rate-independent linear elastic materials. When they are subjected to transversal compression tests they show large plastic deformations similar to the strains measured for the nylon and without having significant losses in their tensile load capacity. This behavior radically differs from carbon and glass fibers, which tend to flake under a tensile load condition.

The ballistic performance of polymeric fibers is evaluated according to their capacity to absorb the kinetic energy from a projectile and how fast they can disperse that energy to their surroundings, avoiding local conditions for failure [16]. The last aspect is governed by the sound speed in the fiber $c = \sqrt{E/\rho}$ where E is Young's modulus and ρ the material density) [16,18].

UHMWPE and aramid fibers (like KEVLAR) had become popular reinforcement materials due to their high performance. They had replaced traditional ones like glass and nylon fibers [16]. However, in extreme applications, where a NIJ-III is required or IV protection levels, ceramic materials are preferred. Among them, alumina (Al2O3) is widely used due to its low manufacturing cost and the multiple options to process them, i.e. slip casting, pressing or injection molding. According to Medvedovski special and expensive equipment is not needed for their processing [12, 24-26]. These materials are characterized by good mechanical properties and a relative low density (3.95 g/cm^3 for the alumina; aluminum density is about 2.7 g/cm^3).

In this paper, we are describing a platform to design composite materials of polymeric matrix that are special for military applications. Our platform integrates lightweight laminar composite materials, designed from their impact energy dissipation and storage mechanisms, with state-of-the-art manufacturing process and material characterization techniques.

Energy Dissipation and Storage Mechanisms under Impact

There are multiple mechanisms that have been identified to stop a projectile. Some of them are associated to the energy absorption during the localized and progressive damage of the target material while projectile pass through it, *i.e.* matrix cracking, shear delamination, compression-cutting, tensile-cutting, hydrostatic compression, melting (Karamis' zones), adhesion and abrasion [27-32]. Other mechanisms are associated to the temporary energy storage, the elastic deformation and the movement of the cone [30, 33]. The presence and the incidence of all these mechanisms are conditioned by: the projectile and target materials [1, 18, 24-38]; the geometrical characteristics of the projectile nose [1, 37, 38]; the properties of the materials and the configuration of the composites (as laminar or layered structures, disperse particles in a matrix, oriented fibers in a matrix or porous mediums) [28, 30-33, 36-39]; impact angle and impact speed [1, 34] among others.

Polymer matrix composite materials with laminar structures are another kind of ballistic materials that combine a set of interesting mechanisms to stop a bullet. Gama and Gillespie [30-32] worked with a S-2 glass/SC15 composite and proposed a model based on a Quasi-Static Punch Shear Tests (QS-PST) to quantify and classify the energy dissipation into elastic and absorbed energies as a function of the penetration displacement and support span. The energy partition is based on the identification of the mechanisms that take place during the five phases of the bullet-penetration: (i) impact-contact and stress wave propagation; (ii) hydrostatic compression and local punch shear; (iii) shear plug formation under compression-shear; (iv) large deformation under tension-shear; and (v) end of penetration and structural vibration. Contrary to a dynamic ballistic impact, where typical bullets are engineered projectiles, flat nose cylinder projectiles were used, with the assumption that they are considered rigid bodies. Classical Ballistic Limit Analysis (CBLA) applies for rigid projectiles and establishes that the limiting velocity V_{50}, *i.e.* the velocity for which the probability that a projectile penetrates a target, is related with the impact velocity V_I, the residual velocity V_R and the projectile mass m_p:

$$\frac{1}{2}m_p V_I^2 - \frac{1}{2}m_p V_R^2 = \frac{1}{2}m_p V_{50}^2 + \frac{1}{2}m_E V_R^2 \qquad (1)$$

Equation (1) establishes that the transferred energy to the target by the projectile in case of whole penetration ($V_I > V_{50}$) equals the sum of the kinetic energy associated to V_{50} and the kinetic energy of an equivalent mass m_E that moves with residual velocity V_R. Consequently, V_R is defined as follows

$$V_R = \left(\frac{m_p}{m_p + m_E}\right)^{1/2} (V_I^2 - V_{50}^2)^{1/2}$$
$$V_R = \alpha\,(V_I^2 - V_{50}^2)^{1/2} \qquad (2)$$

This velocity can be estimated from the Lambert and Jonas equation [1] as

$$V_R = \beta\,(V_I^p - V_{50}^p)^{1/2}\ , \qquad (3)$$

where β and p are fitting parameters. Equations (1) and (2) with experimental data for impact tests using different V_I provide an estimation of the limiting velocity of a projectile-target system (see Fig. 1).

In the case where a complete projectile penetration occurs $V_I \rightarrow V_{50}^-$ and $V_R = 0$. Therefore, it is possible to separate the kinetic energy transmitted to the target as the sum of three components: (i) absorbed energy by the target by several failure mechanisms, $E_{absorbed}$; (ii) accumulated elastic energy, $E_{E\text{-}Acum.}$; and (iii) kinetic energy associated to cone movement, $E_{K\text{-}Come}$. The energy transmitted to the target, E_{50} is defined by,

$$E_{50} = E_{absorbed} + E_{E\text{-}Acum.} + E_{K\text{-}Come} \qquad (4)$$

Elastic and kinetic energies are dissipated after the impact by mechanisms of structural vibration and viscous damping (mechanisms (v)). Some authors [30-33] consider these energy components as part of the energy absorbed by the system; however, this approximation is not satisfactory because a great amount of energy that is initially transmitted to the target is then transmitted to the environment and is not fixed or permanently stored by the material [30].

To estimate each contribution in E_{50} , an identification of the active mechanisms is performed using ballistic punch shear tests (Ballistic-PST) and a relationship is established with those mechanisms observed in QS-PST for the same ballistic system (target-projectile) [30]. From a systematic study of set of curves obtained from the QS-PST, Gama and Gillespie's team developed a quasi-static ballistic

Fig. 1. Residual velocity V_R as function of the impact velocity V_I, for a S-2Glass/SC15 layered composite with a target thickness H_C = 13,2 mm and a flat nose cylinder projectile made of steel with mass m_p = 13,8 g and diameter D_p = 12,7 mm [30]

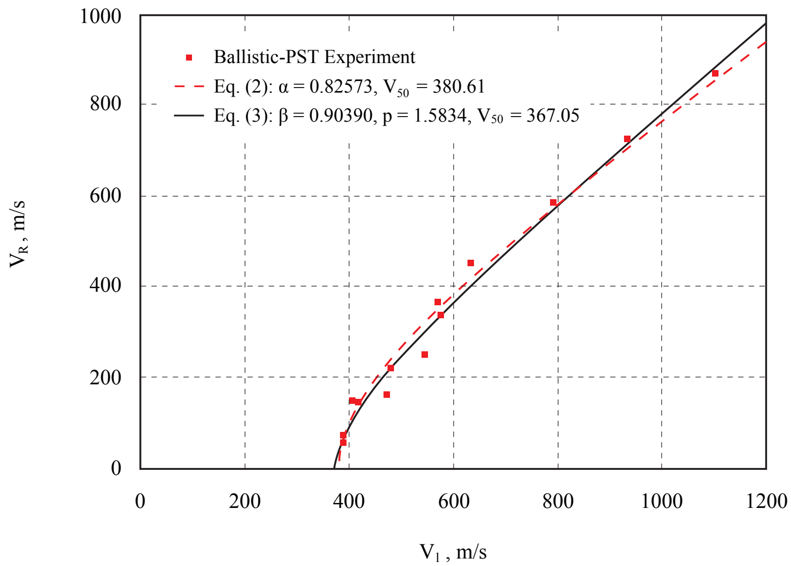

penetration model and a method to determine the ballistic limit V_{50} for laminar composite materials [30-32]. We currently are working to enhance the applicability of this model to laminar composite materials reinforced with hard ceramic particles.

In the case of ceramic materials of high alumina content (alumina-mullite AM, or alumina containing mullite, zirconia and zircon ZAS) and heterogeneous reaction-bonded ceramics, failure mechanisms are linked with brittle fracture [24-26]. On the rear face, the affected impact region is characterized by coaxial and radial cracks generated by tensile stress (because of bending associate to the bulging) that give this area a cone shape (Fig. 2). Spalling is also observed. The size of the generated fragments varies in an extremely wide range from extra-fine powders (on the nanometer scale) up to big parts of the order of several centimeters (mesoscale). *Sarva et al*. [35] have discovered that this fine powder is generated by an erosive mechanism that erodes the projectile reducing its kinetic energy. This resulting powder is the combination of the projectile and target material. This erosive mechanism that is accompanied by an ejected flow is very efficient to reduce the kinetic energy of the projectile and its effect could be enhanced to vastly improve the ballistic efficiency of ceramic tiles by judiciously restraining them with membranes of polymeric composites or metal sheets.

An application that has a close relation with our composite materials is the case of lightweight laminate metallic matrix composite reinforced with ceramic particles. The work of *Karamis at al*. is one of the best in the field from the descriptive point of view of the ballistic impact phenomenon [27-29]. They have designed some composites materials of this kind using an Al-matrix and alumina as a reinforcement element to defeat engineered projectiles (7,62 mm x 51 mm Armour Piercing, AP) shot by a G3 assault rifle with an average impact velocity of 710 m/s. Targets are 15 mm thick and can stop this kind of projectiles. The ballistic material was manufactured by the combination of a process of hot compression and squeeze casting. Fig. 3 shows details of the impact zones of ballistic tests carried out for two different configurations of their laminate, where multiple energy dissipation mechanisms are identified.

Our polymeric matrix composite is designed to generate synergy between the matrix, the

Fig. 2. Ceramic material. Energy Dissipation Mechanisms based in brittle fracture: spalling and radial and tangential cracking due to tensile stress. Projectiles are also deformed and their surfaces are abraded [24-26]

a) High content alumina and mullite ceramic (AM2). View of the rear face of the plate after being impacted by a projectil (NATO Ball FMJ 7.62x51mm). Backing material was removed

b) Biomophic ceramic (RBS) impacted by 7.62x63mm AP-M2 projectile

reinforcing fibers and ceramic particles. The mechanisms embedded in our composites are:

1. Elastic deformation of the main and secondary fibers in the impact zone.
2. Kinetic energy of the moving cone of the target.
3. Rupture or facture of fibers.
4. Cracking of the target matrix.
5. Delamination of the layers around impact zone.
6. Shear plug formation and compression of the layers in the contact zone just when projectile geometry is adequate.
7. Abrasion of the projectile surface (damage of the projectile skin).

Some of the individual contributions for these mechanisms have been estimated. We are currently working on the abrasive contribution of the particles. We are, however, able to provide a crude assessment of the energy involved in this complex phenomenon.

Fig. 3. Ceramic material. Energy Dissipation Mechanisms MMC - B Type Structure. Perforation left by projectile after its extraction [28]

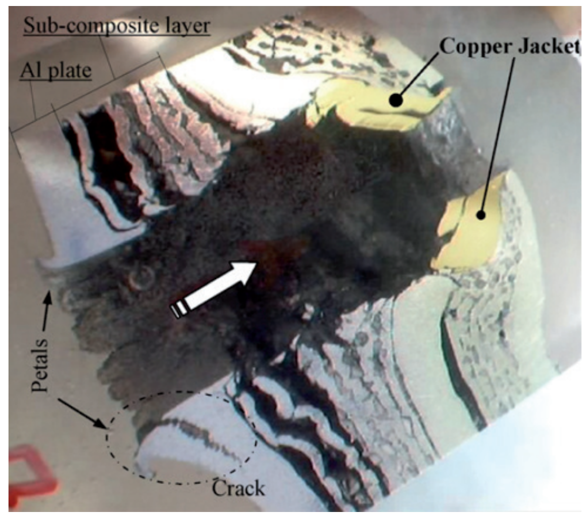

a) General view showing some failure mechanisms as petalling, swelling, delamination of layers, high strained regions by compression and shear, melting welding, bending and bulging

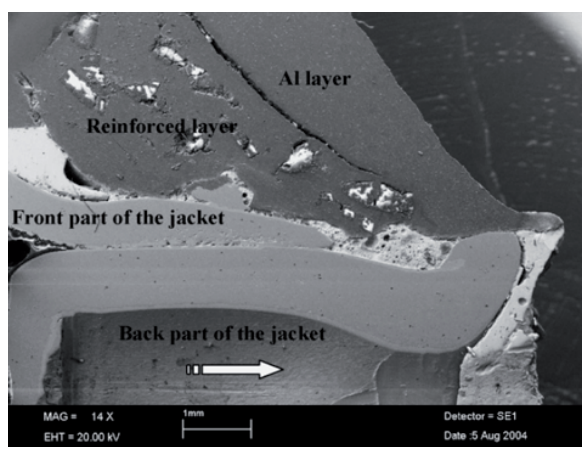

b) Detail of the projectile output: compressed and high-deformed layers, mixing regions, high deformation and geometrical changes of the peeling cap

Laminar Composites

We fabricated polymeric matrix composite materials reinforced with hard particles and high performance fibers using a state-of-the-art vacuum assisted infusion molding. Epoxy resins and a polyester based-resin are used as the polymeric matrices. Three kinds of high performance fibers were used as reinforcement: glass, Kevlar and carbon fibers. These fibers were provided as woven fabrics in four different configurations as shown in Fig. 4. Two kinds of hard particles are used as the additional reinforcement that provides abrasive and hardness characteristics to the composite. The laminates are thin tiles of laminar composites, are light and stiff and made with a thickness of approximately 1 mm. The infusion resulted in high reproducible laminates with a standard deviation of 0.3 mm in the thickness.

Fig. 5 shows details of some setups used to manufacture samples by vacuum assisted infusion techniques. Different configurations were used to explore how the vacuum line and the in/out points can affect the integrity of the manufactured samples. These types of experimental exercises have permitted the identification of the more relevant elements to be considered during the manufacture of the composites and how the assemblies can be simplified without affecting the quality of the products and reducing costs and the negative impact in the environment. Fig. 6 shows some samples manufactured by these techniques.

Fig. 4. Kinds of fabrics and fibers used as reinforcement

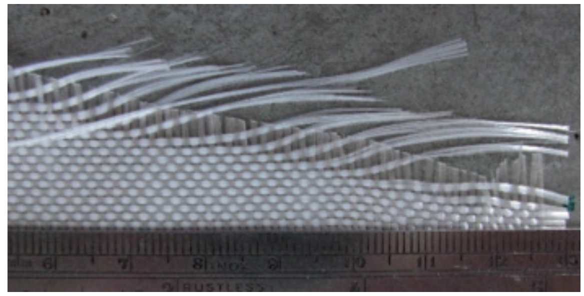

a) E-Glass Fiber fabric, density: 257 g/m^2

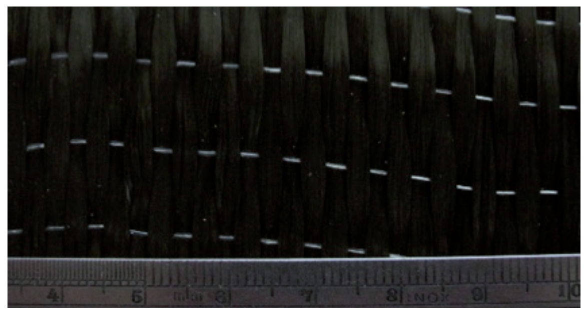

b) Unidirectional Carbon Fiber fabric

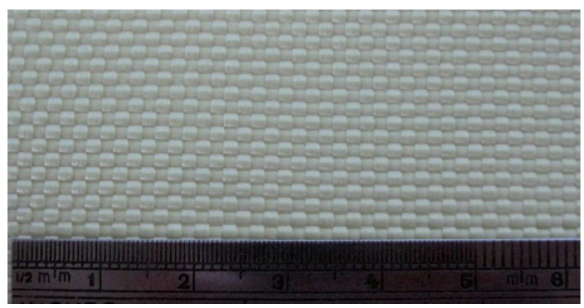

c) Kevlar woven fabric, density: 257 g/m^2

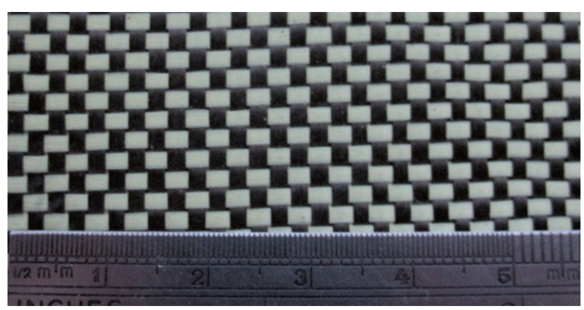

d) Mixed woven fabric: Kevlar and Carbon Fibers, density: 185 g/m^2

Characterization

Fig. 7 shows images obtained by a stereoscopic and optical microscopy of the cross section of four samples of laminar composites. These pictures reveal important details of their specific configurations: size and shape of the branches of fibers, fibers distribution, defects (as pores for instance), areal percentage of components, cross sections of the composite, spaces occupied by the matrix and composite homogeneity.

A primary characterization of some ballistic products was carried out at the Laboratorio de Caracterización de Materiales (Material Classification Laboratory) of the Universidad Nacional de Colombia using Scanning Electron Microscopy (SEM). Fig. 8 shows some geometrical characteristics of the fibers of the evaluated

Fig. 5. Examples of two Infusion Systems designed to evaluate the flexibility of the process and identify some of its relevant variables

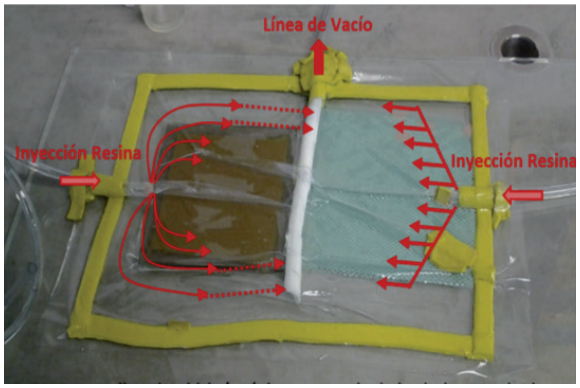

a) (left) 3 layers of Kevlar + Epoxy Resin; (right) 7 Layers of E-Glass fibers + Epoxy Resin

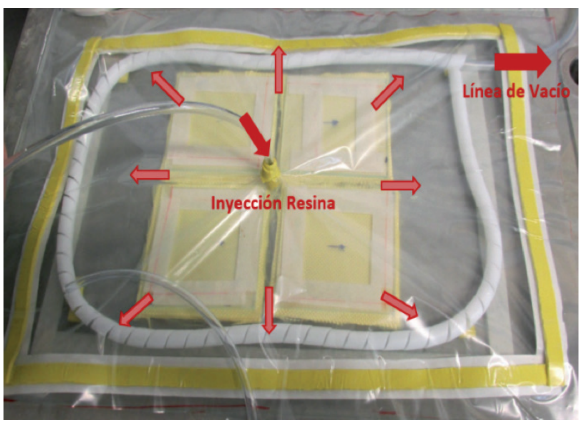

b) Infusion system to 4 samples manufacturing using a central feeding and a peripheral vacuum line: 3 layers of Kevlar + Epoxy Resin

materials: two samples of Spectra (HO-UHMW-PE) made by a Chinese manufacturer and one sample of Gold Shield (Aramid) manufactured by Honeywell (E.U.A). Table 1 shows some of the mechanical and physical properties of high performance fibers.

Notice that HMW-PE has the lowest density and an excellent combination between strength properties and toughness. The minimum diameters measured were around 13 μm (Table 2). It is important to consider the possibly negative effect of the "knot" found in the Spectra Shield II - Thick as a manufacture defect (see Fig. 7). Fibers of the Spectra SR121 and Gold Shield have a homogenous diameter. The Diameter of the fibers is an important variable considered in the models developed to assess the elastic energy storage and to consider the effect of weight and cost in a final product.

Nano-indentation Tests

This kind of test was carried out to assess the magnitude of the elastic module (E) of the fibers

Fig. 6. Samples manufactured by infusion systems of Fig. 5: epoxy resin reinforced by Kevlar and glass fibers

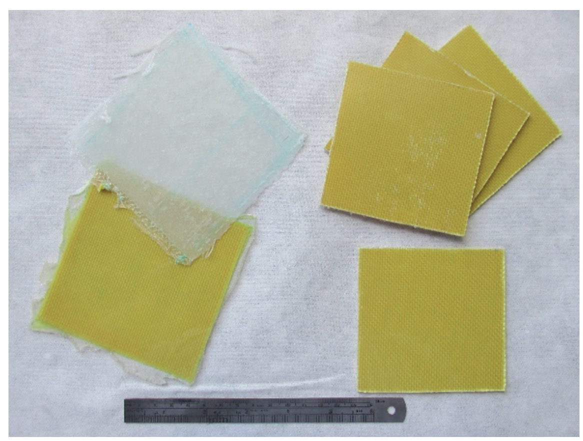

Table 1. Mechanical and physical properties of high performance fibres [16]

Fibre Type	Fracture Resistance, GPa	Fracture Strain, x1000	Axial Elastic Module, GPa	Density, kg/m^3
Aramid	2,8-3,2	15-45	60-115	1390-1440
HMW-PE	2,8-4,0	29.38	90-140	970-980
LPC	2,7-2,9	33-35	64-66	1400-1420
PBO	5,4-5,6	24-26	270-290	1540-1560
PIPD	3,9-4,1	11-13	320-340	1690-1710
Nylon	0,06-0,08	1500-2500	1,0-1,5	1070-1170
S-Glass	4,64-4,66	53-55	82-92	2470-2490

Fig. 7. Cross-sections of samples of several laminates for inspection and mechanical characterization

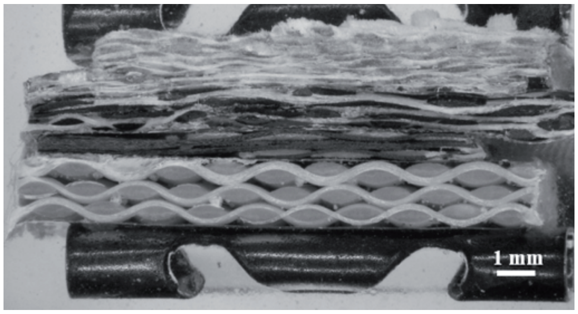

a) Laminate samples extracted for optical inspection and nanoindentation tests

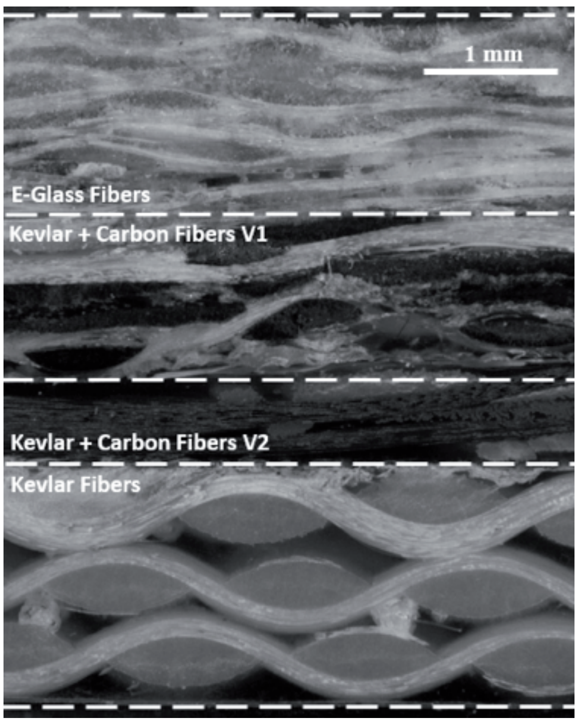

b) Stereo micrograph of a set of 4 samples of different configurations

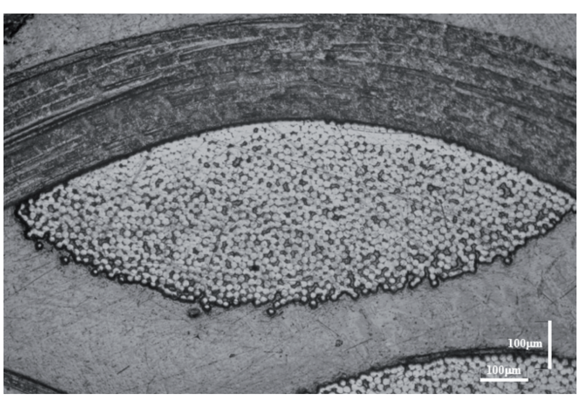

c) Detail of branches of Kevlar fibers (optical microscopy): longitudinal and cross views of fibers

Table 2. Average diameters of the analyzed fibers

Laminate	Fiber	D_{Fiber}, μm
Gold Shield® GV-2016	Aramid	**13,0**
Spectra Shield II – Thin	HMW-PE	**12,7**
Spectra Shield – Thick	HMW-PE	**26,0**

(upon their cross section) and its radial variation at the interface between fibers and matrix. Measurements were carried out using an IBIS Nanoindentation System with a Berkovich indenter. Results of these measurements were plotted in the graphs of Fig. 9 for composites with the three basic types of fibers used in the manufacture of laminar composites shown in Fig. 7. Results of the values measured for E are in agreement with those reported in specialized literature. The horizontal axis is the penetration depth (h_t).

Microhardness

The effect of the curing time and temperature time on the mechanical properties of a resin was explored using a polyester based resin prepared varying the weight percentage of its catalyst; see Fig. 10. Four days after the manufacturing of the samples microhardness was measured on the polished surfaces (red points); then, 24 days later the microhardness of the samples was measured (blue points). During this period the environmental temperature was between 21 to 28°C. Finally, 11 days later, the curing of the samples was accelerated by using a furnace at 80°C for 5 hours to guaranty a complete curing. Microhardness was then measured again (purple points).

From Fig. 10, significant and systematic increases in hardness can be seen such as curing time and temperature increase. The curing agent also has an important role on the microhardness of the tested samples (the microhardness of some samples has risen more than twice in regard their initial values, red points). The last two curves (blue and purple curves) have almost the same slope, showing a decrease in hardness as w% catalyst increases showing a different behavior of the hardness in regard to the initial curve (red points). It is important to bear in mind that for polymers the compressive yield stress can also

Fig. 8. Geometrical details of the analyzed fibers

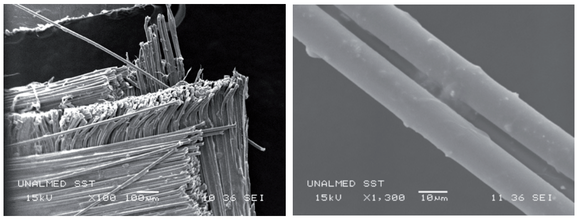

a) Aramid – Gold Shield

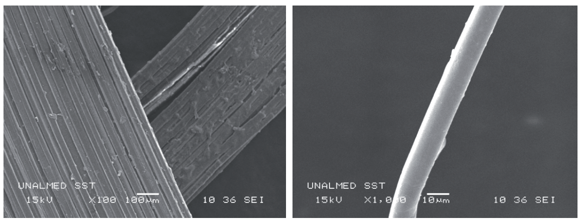

b) Spectra Shield II – SR1211 -Thin

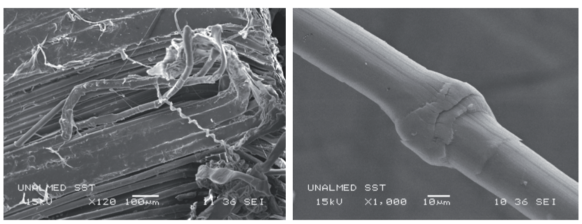

c) Spectra Shield II - Thick

be estimated from hardness measures (Y≈H/3, according to Tabor [40]).

We are currently obtaining extra-hard layers using alumina particles (Al_2O_3) and others. The goal is to place some hard layers on or near the impact face of the armors to promote the activation of some additional dissipative mechanisms as the projectile abrasion (projectile peeling), plastic deformation of the projectiles, fracture of hard particles and the flow of these hard particles into the polymeric matrix.

The hardness of Al_2O_3 is about 1170 (94% purity) to 1440 HV (99.5% purity). In our composites, microhardness values up to 940 HV have been measured in our samples using loads of 0.49 N (50 grams). These values correspond to the hardness of a mixture of alumina particles and polymeric resin; that is why the lower values were recorded because of the lesser hardness of the matrix.

Using a comprehensive characterization method, developed in our group, we measured reaction kinetics using differential scanning calorimetry. The dynamic and dynamic-isothermal DSC data is used in combination with a Kamal-Sourour model for the reaction kinetics and cure. The models are integrated to find the Time-Temperature-Transformation diagram of the resin (see Fig. 11). The TTT diagram provides the processability window for each resin and aids the processing design towards optimization and control.

Fig. 9. Elastic Module (E) of the transverse section of fibers and its surroundings of anti-depth penetration matrix (h_t).

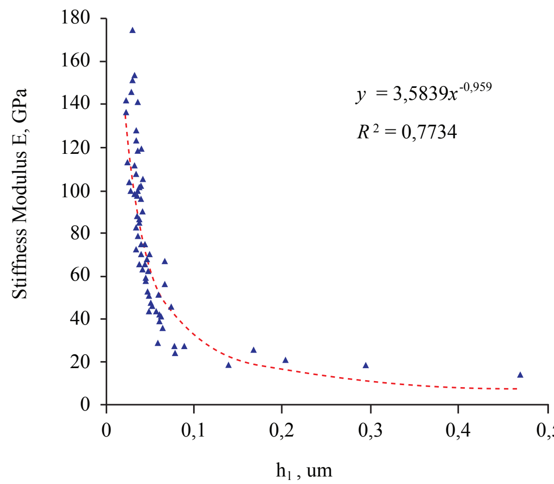

a) Sample B3: Carbon Fibers + Epoxy Resin

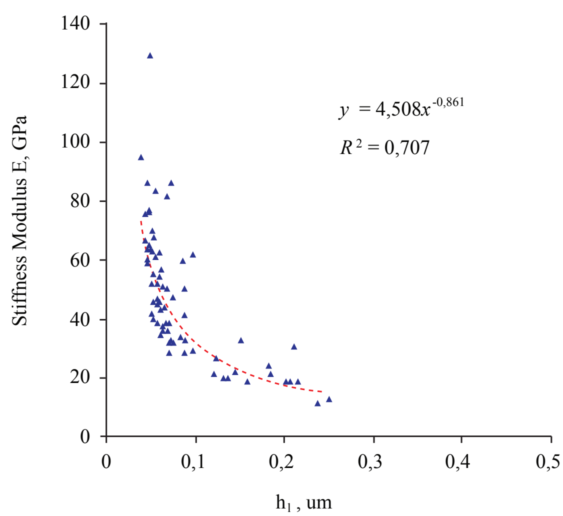

b) Sample B1: Glass Fibers + Epoxy Resin

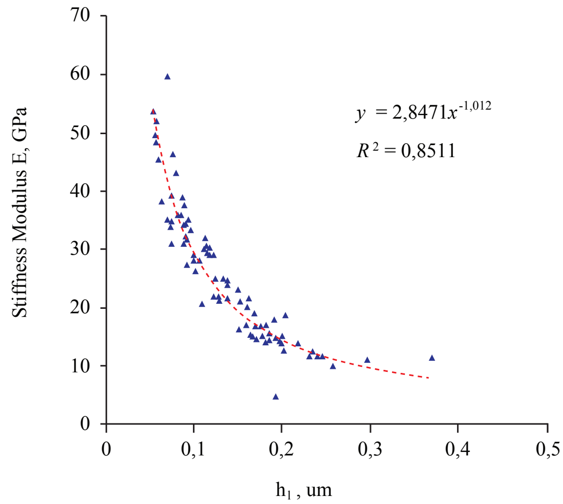

c) Sample B8: Kevlar Fibers + Epoxy Resin

Fig. 11. Time-Temperature-Transformation diagram of the Epoxy resin

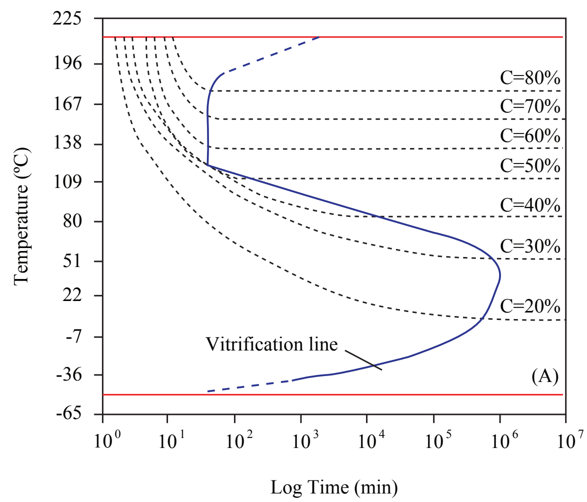

Conclusions

A platform to design composite materials of polymeric matrix that are specifically for military applications on (as) fluvial and naval navigation (among others) has been developed. The platform integrates laminar composite materials design based on impact energy dissipation and temporary storage mechanisms with their manufacturing process (vacuum assisted infusion) and characterization (physical, mechanical and ballistic properties, geometry and integrity of the components and materials).

Fig. 10. Effect of curing time and temperature on hardness of the matrix. For each tested condition, each plotted point represents the average value of five measurements

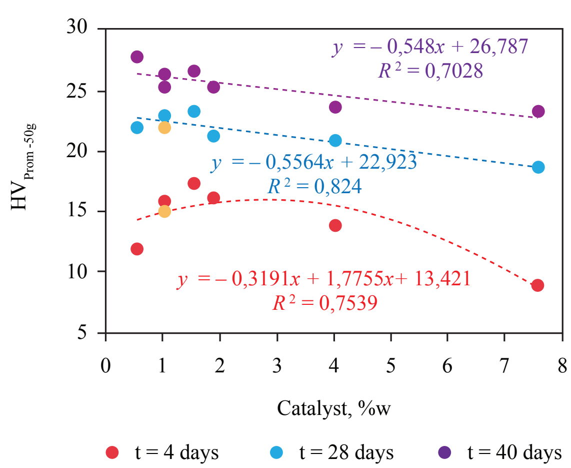

Acknowledgments

Authors want to thank Colciencias and Colfuturo (Convocatoria 528-2011) and Universidad Nacional de Colombia and Faro Tecnológico S.A.S. (Proyecto Hermes Nro. 27130) for its financial support. Also, they thank DynaComp S.A.S for the materials provided to manufacture some of the laminar composites for naval applications, the technical discussions and the assistance provided.

References

1. ZUKAS, J.A., NICHOLAS, T., SWIFT, H., GRESZCZUK, L.B., CURRAN, D.R. Impact Dynamics. John Wiley & Sons, USA 1982, 452p.

2. SRIVATHSA, B., RAMAKRISHNAN, N. (1999). Ballistic performance maps for thick metallic armour. Journal of Materials Processing Technology 96, 81-91.

3. DEMIR, T., UBEYLI, M., YILDIRIM, R.O. (2008). Investigation on the ballistic impact behavior of various alloys against 7.62 mm armor piercing projectile. Materials and Design 29, 2009–2016.

4. OZSAHIN, E., TOLUN, S. (2010). Influence of surface coating on ballistic performance of aluminum plates subjected to high velocity impact loads. Materials and Design 31, 1276–1283.

5. OZSAHIN, E., TOLUN, S. (2010). On the comparison of the ballistic response of coated aluminum plates. Materials and Design 31, 3188–3193.

6. BØRVIK, T., FORRESTAL, M.J., HOPPERSTAD, O.S., WARREN, T.L., LANGSETH, M. Perforation of AA5083-H116 aluminium plates with conical-nose steel projectiles – Calculations. International Journal of Impact Engineering 36 (2009) 426–437.

7. BØRVIK, T.,CLAUSEN, A.H., HOPPERSTAD, O.S., LANGSETH, M. Perforation of AA5083-H116 aluminium plates with conical-nose steel projectiles—experimental study. International Journal of Impact Engineering 30 (2004) 367–384.

8. DEY, S., BØRVIK, T., HOPPERSTAD. O.S., LANGSETH, M. On the influence of constitutive relation in projectile impact of steel plates. International Journal of Impact Engineering 34 (2007) 464–48.

9. DEY, S., BØRVIK, T., HOPPERSTAD. O.S., LANGSETH, M. On the influence of fracture criterion in projectile impact of steel plates. Computational Materials Science 38 (2006) 176–191.

10. UBEYLI, M., DEMIR, T., DENIZ, H., YILDIRIM,R.O., KELES, O. Investigation on the ballistic performance of a dual phase steel against 7.62mm AP projectile. Materials Science and Engineering A 527 (2010) 2036–2044.

11. MISHRA,B.,JENA,P.K.,RAMAKRISHNA, B., MADHU, V., BHAT, T.B., GUPTA, N.K. Effect of tempering temperature, plate thickness and presence of holes on ballistic impact behavior and ASB formation of a high strength steel. International Journal of Impact Engineering 44 (2012) 17-28.

12. MEDVEDOVSKI, E. (2001). Wear-resistant engineering ceramics. Wear 249, 821–828.

13. NAIK, N.K., SHRIPAO, P., REDDY, B.C.K. (2006) Ballistic impact behaviour of woven fabric composites: Formulation. International Journal of Impact Engineering 32, 1521–1552.

14. HOO-FATT M.S., SIRIVOLU, D. (2010). A wave propagation model for the high velocity impact response of a composite sandwich panel. International Journal of Impact Engineering 37, 117–130.

15. REYES, G., CANTWELL, W.J. (2004). The high velocity impact response of composite and FML-reinforced sandwich structures. Composites Science and Technology 64, 35–54.

16. GRUJICIC, M., ARAKERE, G., HE, T., BELL, W.C., CHEESEMANB, B.A., YENB, C.F., SCOTT, B. (2008). A ballistic material model for cross-plied unidirectional UHMWPE fiber-reinforced armor-grade composites. Materials Science and Engineering A 498, 231–241.

17. Technical Guide Kevlar - Aramid Fiber. DuPond, 32p: www.kevlar.com.

18. LANE, R. High Performance Fibers for Personnel and Vehicle Armor Systems-Putting a Stop to Current and Future Threats. AMPTIAC Rome, NY: http://ammtiac.alionscience.com/pdf/AMPQ9_2ART01.pdf

19. Tawron - a versatile high-performance fiber. TEIJIN, 7p: http://www.teijinaramid.com/aramids/twaron/

20. Technora. TEIJIN: http://www.teijinaramid.com/aramids/technora/

21. Honeywell Gold Shield® GV-2016: www.honeywell.com/spectra

22. Dyneema: http://www.dyneema.com/americas/applications/life-protection.aspx

23. POB Fiber Zylon. TOYOBO CO., LTD, 18p: www.toyobo.co.jp

24. MEDVEDOVSKI, EUGENE. Alumina–mullite ceramics for structural applications. Ceramics International 32 (2006) 369–375.

25. MEDVEDOVSKI, EUGENE. Ballistic performance of armour ceramics: Influence of design and structure. Part 1. Ceramics International 36 (2010) 2103–2115.

26. MEDVEDOVSKI, EUGENE. Ballistic performance of armour ceramics: Influence of design and structure. Part 2. Ceramics International 36 (2010) 2117–2127.

27. KARAMIS, M.B. Tribology at high-velocity impact. Tribology International 40(2007) 98-104.

28. KARAMIS, M.B., NAIR, F., CERIT, A.A. The metallurgical and deformation behaviours of laminar metal matrix composites after ballistic impact. Journal of Materials Processing Technology 209 (2009) 4880–4889.

29. KARAMIS, M.B.¸ CERIT, A.A., NAI, F. Surface characteristics of projectiles after frictional interaction with metal matrix composites under ballistic condition. Wear 261 (2006) 738–745.

30. GAMA, B.A., GILLESPIE, J.W. Punch shear based penetration model of ballistic impact of thick-section composites. Composite Structures 86 (2008) 356-369.

31. XIAO, J.R., GAMA, B.A., GILLESPIE, J.W. Progressive damage and delamination in plain weave S-2 glass/SC-15 composites under quasi-static punch-shear loading. Composite Structures 78 (2007) 182–196.

32. ERKENDIRCI, O.F., (GAMA) HAQUE, B.Z. Quasi-static penetration resistance behavior of glass fiber reinforced thermoplastic composites. Composites: Part B xxx (2012) xxx–xxx

33. MORYE, S.S., HINE, P.J., DUCKETT, R.A., CARR, D.J., WARD, I.M. Modelling of the energy absorption by polymer composites. Composites Science and Technology 60 (2000) 2631-2642.

34. Lightweight ballistic composites - Military and Law enforcement applications. Edited by Ashok Bhatnagar. Woohead Publishing Limited, Cambridge, England, 2006, 428p.

35. SARVA, S., NEMAT-NASSER, S., MCGEE, J., ISAACS, J. The effect of thin membrane restraint on the ballistic performance of armor grade ceramic tiles. International Journal of Impact Engineering 34 (2007) 277–302.

36. QUN WANG, ZHAOHAI CHEN, ZHAOFENG CHEN. Design and characteristics of hybrid composite armor subjected to projectile impact. Materials and Design 46 (2013) 634–639.

37. CORRAN, R.S.J., SHADBOLT, P.J., RUIZ, C. Impact Loading of Plates - An Experimental Investigation. Int. J. Impact. Engng. Vol 1 No. 1 (1983) pp3-22.

38. Dey, S., Borvik, T., Teng, X., Wierzbicki, T., Hopperstad, O.S. On the ballistic resistance of double layered steel plates: An experimental and numerical investigation. International Journal of Solids and Structures 44 (2007) 6701–6723.

39. HOCKAUF, M., MEYER, L.W., PURSCHE, F., DIESTEL, O. Dynamic perforation and force measurement for lightweight materials by reverse ballistic impact. Composites: Part A 38 (2007) 849 – 857.

40. FLORES, A., ANIA, F., BALTÁ-CALLEJA, F.J. From the glassy state to ordered polymer structures: A microhardness study. Polymer 50 (2009) 729-746.

Navantia's Shipyard 4.0 model overview

Vistazo general del modelo de Astillero 4.0 de Navantia

DOI: https://doi.org/10.25043/19098642.165

Ángel Recamán Rivas [1]

Abstract

Navantia finished the analysis of the concept Industry 4.0 in 2016 and its application to the naval shipbuilding industry, referred to herein as Shipyard 4.0. The implementation process has begun with several projects that involved various technologies. In order to incorporate them in the new project, for naval vessels and systems, special focus has been put in the future F-110 frigate.

This document aims to provide an overview of the Shipyard 4.0 model and a brief discussion regarding the projects launched for its implementation in Navantia. The initiative 4.0 is a key development vector across all the industrial sectors in the future and its expected outcomes match the ones established by the Government of Colombia in its "Plan de Transformación Industrial" (Plan of Industrial Transformation). In this context, the new frigate program (PES) is a unique opportunity to engage the local industry, in which Navantia offers its willingness to cooperate.

Key words: Industry 4.0, Shipyard 4.0, Navantia, Plan de Transformación Industrial

Resumen

Navantia finalizó el análisis del concepto Industria 4.0 en 2016 y su aplicación a la industria de la construcción naval, denominada Astillero 4.0. El proceso de implementación ha comenzado con algunos proyectos que involucraron varias tecnologías. Para incorporarlos al nuevo proyecto para buques y sistemas navales, se ha puesto especial énfasis en la futura fragata F-110.

Este documento tiene como objetivo proporcionar una visión general del modelo Astillero 4.0 y una breve discusión sobre los proyectos lanzados para su implementación en Navantia. La iniciativa 4.0 es un vector de desarrollo clave para todos los sectores industriales en el futuro y sus resultados esperados coinciden con los establecidos por el Gobierno de Colombia en su "Plan de Transformación Industrial". En este contexto, el nuevo programa de fragata (PES) es una oportunidad única para involucrar a la industria local, en la cual Navantia ofrece su disposición a cooperar.

Palabras claves: Industria 4.0, Astillero 4.0, Navantia, Plan de Transformación Industrial.

Date Received: June 3rd 2017 - *Fecha de recepción: Junio 3 de 2017*
Date Accepted: October 18th 2017 - *Fecha de aceptación: Octubre 18 de 2017*

[1] Engineering and Innovation Vice-President - NAVANTIA. Spain. Email: arecaman@navantia.es

Introduction

All developed countries are concerned with maintaining industrial and innovation capabilities as engines of their economies. After the economic crises of recent years, the contribution of Manufacturing to the GDP and the added value as a percentage of the GDP of most developed countries has fallen. Understanding that there is no sustained economic growth without a strong and innovative industry, there is a global approach to improve industry performances by leveraging new technologies, known as the Fourth Industrial Revolution.

If manufacturing productivity is to be increased and business costs reduced, reforms will have to be made. In shipbuilding, the Colombian Government has developed a plan to for the productive development of the key industrial sector for the Colombian economy, whose purpose is to enhance the competitiveness and productivity of the industry. That Plan is called "Plan de Transformación Productiva[1]" (Plan of Productive Transformation). In it, the Shipbuilding Industry is identified as one of the key industrial sectors.

In order to meet these requirements of improving productivity and reducing business costs, Navantia has implemented the Shipyard 4.0 model. This model aims to apply and optimise the Fourth Industrial Revolution technologies for shipbuilding applications and is being implemented at Navantia's Ferrol shipyard as part of the program to build the Spanish Navy's next-generation F110 frigates. By innovating in core business areas, the Shipyard 4.0 model provides the basis for optimisation of the shipbuilding processes.

Navantia's Shipyard 4.0 Model seeks to deliver the following outcomes

- Creation of a sustainable shipbuilding industry that will deliver the Navy´s future capability through an incremental low risk process;
- Modern facilities that will deliver internationally competitive products;
- Modern ICT (Information Communication Technologies) infrastructure that will support the ships' digital twins; and
- Creation of new skilled workforce able to face the new industrial challenges.

The Fourth Industrial Revolution: Industry 4.0

Throughout the western world new industrial paradigm has surfaced called the Factory of the Future. The Factory of the Future is enabled by the so-called Fourth Industrial Revolution, as a result of technological advances in digitalisation and connectivity.

The challenges originated by this revolution must be addressed without delay:

- standardisation and reference architecture;
- managing complex systems;
- comprehensive broadband infrastructure for industry;
- safety and security;
- work organisation and design;
- training and continuing professional development;
- regulatory framework; and
- resource efficiency.

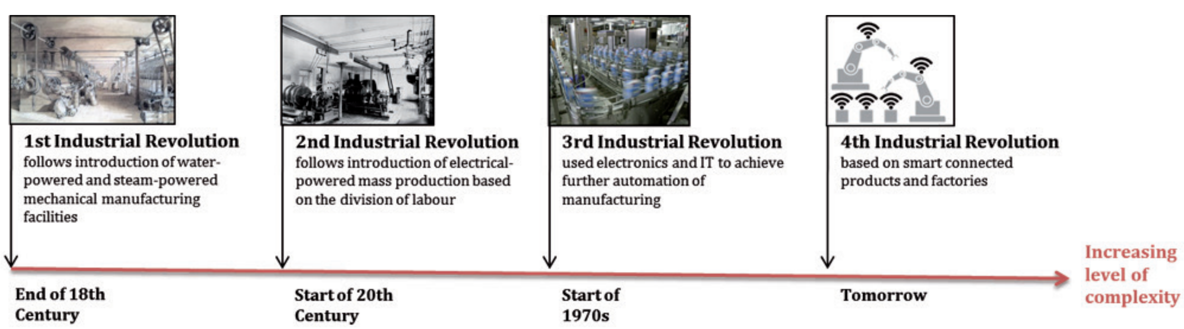

[1] https://www.ptp.com.co/portal/default.aspx

The 46th World Economic Forum in Davos in January 2016 focused heavily on the Fourth Industrial Revolution. In its report, the Forum emphasised the huge potential associated with the digital change, connectivity and the 'internet of things' for the development of society. Many developed countries have started to pursue this path with government policy being developed to harvest the potential of new digital technologies in order to revitalise the industrial economy of their respective countries, which has shrunk across all Europe (excluding Germany) and in the USA over the past two decades. To this aim, governments, industry, and all relevant stakeholders (universities, unions, media, etc.) have joined forces recognising that the magnitude of the challenge requires a coordinated effort. [1]

This industrial model, often termed Industry 4.0, has four axes:

- vertical integration in a modern factory, aiming to integrate the process from the workshop/deckplate to top management;
- horizontal integration with Customers and Vendors;
- end-to-end engineering to cover the complete value chain; and
- skilled personnel that respond to the new needs.

The Industry 4.0 doctrine is highly applicable to the naval shipbuilding industry, which combines heavy steel construction work with the most advanced electronics to produce technologically complex products. Naval vessels will benefit greatly from this innovative approach.

General Discussion of the Shipyard 4.0

Introduction

Navantia has recently completed the study and analysis of the Industry 4.0 model [2] for adaptation to shipbuilding. This adaptation has been termed "Astillero 4.0" - in English Shipyard 4.0 - and is currently being implemented. During this phase, projects are being executed to consolidate a range of different technologies with the aim of inserting them in the future ships and systems. Although it is a Navantia initiative, the main project targeted in this implementation phase is the Spanish Navy F110 Program.

The Shipyard 4.0 vision has been presented by Navantia to a range of different forums in Spain, including directly to the Spanish Navy. The vision is outlined in two elements: digitalisation, which is the technological driver of the vision; and the collaboration between all relevant stakeholders which this allows.

Key Elements

With transformative digital technologies, Navantia's Shipyard 4.0 will develop new processes for obtaining the hundreds of systems that compose our ships.

- *Digitisation of all the workshops' machinery* will enable vertical integration through information systems allowing optimisation of the machines' maintenance and energy consumption.
- *Collaborative robotics* will allow people and robots to work together. A range of tasks will be automated, from the more difficult and repetitive, to quality control, or even administrative work.
- *Additive manufacturing*, or 3D printing, will allow the manufacturing of complex component pieces from a 3D model with the same simplicity as printing on sheet of paper.
- *Virtual reality* will allow the development of a 'digital twin' or ship 0 to be created and fully explored ahead of physical construction.

Augmented reality will allow workers easy access to all of the information about any specific component.

- Data mining will allow the extraction of meaningful information from a large amount of data (*big data*) generated in the horizontal and vertical integration of Shipyard 4.0.
- The *Internet of Things* will connect all Shipyard 4.0 stakeholders: people, products, and facilities within the physical shipyard or around the world. This could include geographically disperse supply chains, or allow the connection of shipyards in Ferrol and Adelaide, for example.
- The *secure cloud* will remove the borders for storing, computing, and exchange existing information.
- *Cybersecurity* will ensure the protection of all information.
- *Virtual modelling* will optimise the ships and their systems' configurations in advance as well as simulating the production processes required for their fabrication. The digital twin will be the cornerstone of all the process along the whole lifecycle of the ships.
- All of these measures will directly translate into a significant improvement of personnel health and safety, environmental protection, and an optimisation of energy consumptions.

Technological Development

The use of these technologies will allow the full participation of the workshops, docks and different areas of the shipyard with the technicians and administrative personnel – vertical integration. The Shipyard 4.0 physical facilities will evolve alongside the information and communication systems, allowing connectivity between people, products, and machines, creating a cyber-physical space.

The use of on-line production processes sensors and insertion of specialised robots, as well as big data and data mining, will allow for the earlier identification of defects and errors to be corrected in advance. This will greatly improve quality assurance and reduce the risk inherent in complex programs.

In a similar manner, these new technologies will allow a continuous flow of information and materials between the shipyard (centre of gravity of the digital ecosystem) and its customers and

Fig. 1. Shipyard 4.0 Technologies

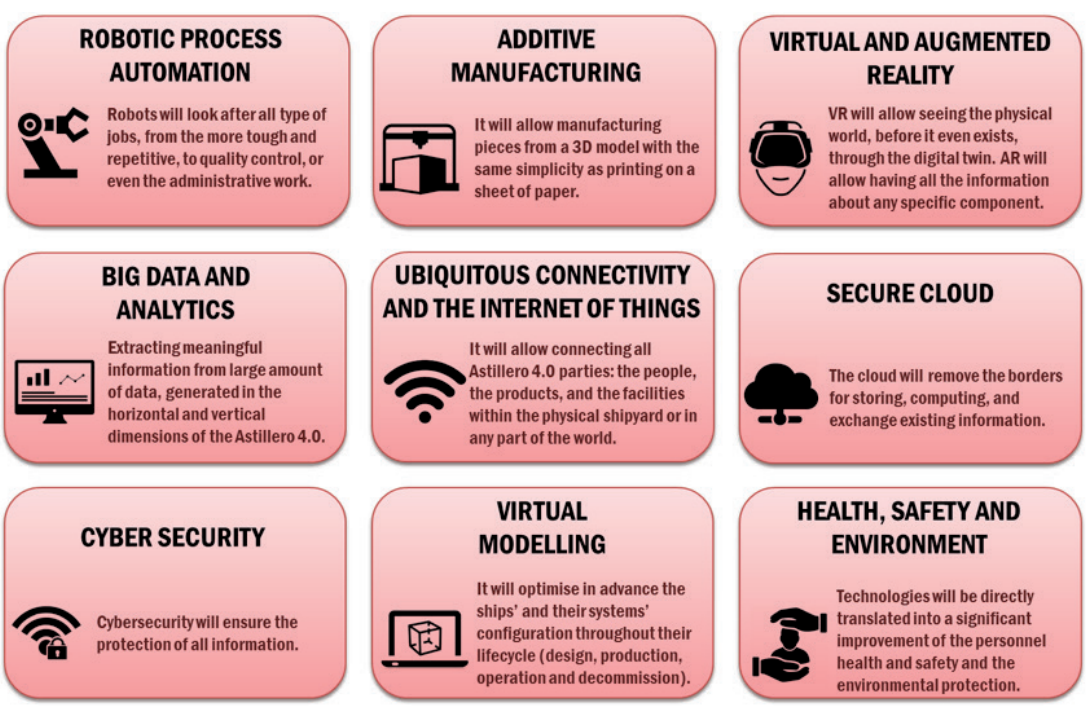

collaborators, including sub-suppliers. This integrates the value chain from the innovation phase, through to design and fabrication, and continuing through life support service.

This level of horizontal integration allows collaborators to have completely different engagement rules based on a previously unthinkable level of transparency and scope. This allows the incorporation of universities, and scientific and technological centres in addition to the more traditional vendor network.

As a direct consequence, Shipyard 4.0 will be very flexible in the make-control-buy[2] process, which could be adjusted based on the shipyard workload and the facilities capacity, while maintaining the integration function powered by the new digital technologies.

Effective application of the new technologies will require the contribution of engineering (End-to-End Engineering) in all aspects of the Shipyard 4.0, in the vertical and horizontal axes, and through the life of the ships. In this way, Systems Engineering will be used routinely as an integral part of the build process and the shipyard will evolve as a System of Systems.

Critically, all of the intelligence and connectivity on board the ships and their systems during their construction will be kept after delivery to the owners, allowing engagement between the *smart ship* and Shipyard 4.0 through their life by enabling *smart sustainment* and new business models.

The 'Digital Twin'

In this highly complex environment – for both the technical and management fields – the digital twin or ship zero will be the cornerstone of the Shipyard 4.0 concept. It will allow the simulation of new products and process developments in virtual work stations. This includes personnel considerations and the reduction of health and safety hazards. [3]

Fig. 2. Virtual Model Technologies

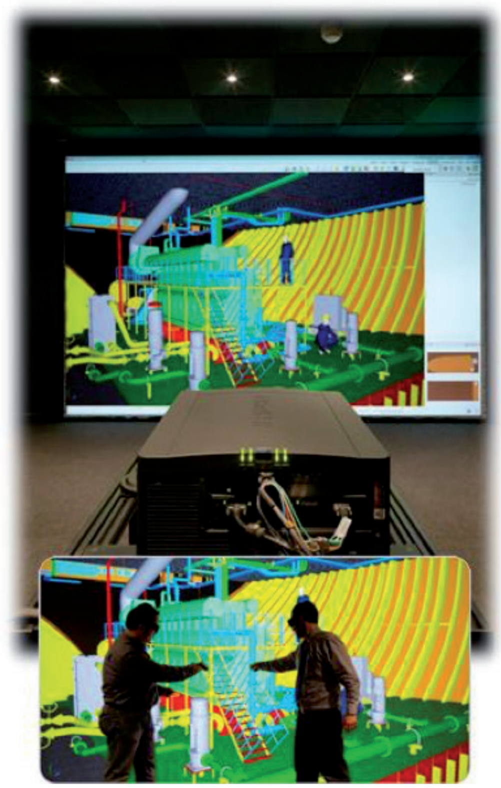

Moreover, the digital twin will be the key element for enabling the make-control-buy[3] strategy of the Shipyard 4.0. It will allow the different stakeholders to work simultaneously on the digital twin from two perspectives: that of the customer and that of the vendor. This work will happen throughout all product phases: innovation, design and construction, and through the vessel's life.

Obviously, in order to develop the potential of the digital twin and the massive amount of information gathered through the ship's life, it will be necessary to innovate in the rules of engagement between the shipyard, its vendors, and its customers. This innovation will start from the reference customer: the Spanish Ministry of Defence.

Implementation of Shipyard 4.0

Navantia is currently an international benchmark in the Naval shipbuilding industry because of the

[2] Make: fabricated at the shipyard

[3] Control: procured by the shipyard but with an increased oversight . Buy: procured by the shipyard

Fig. 3. Navantia´s Product Evolution Model

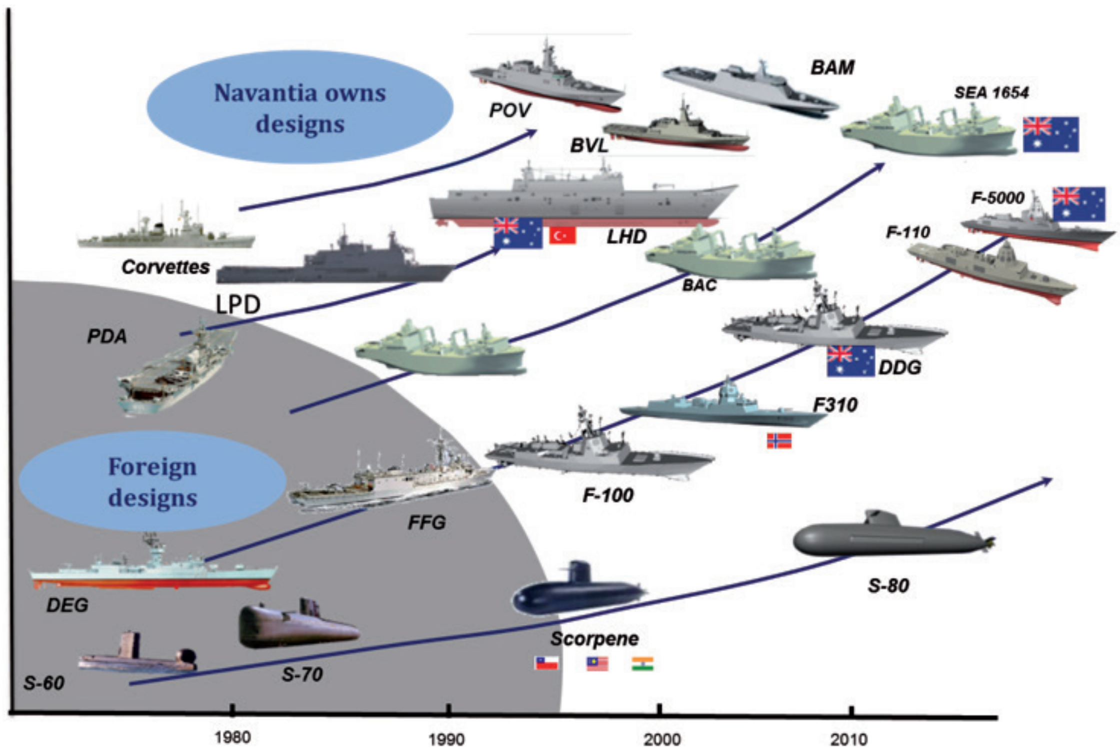

shipbuilding strategy defined and implemented in the 1960s when the Spanish Government started a program to obtain local capabilities. This strategy was performed through the selection of foreign partners; the United States for Surface Combatants, the Netherlands for Logistics and Amphibious ships and France for Submarine development. It was based on small but progressive steps towards a sovereign shipbuilding capability, which Spain achieved by the 1990s. Spain, through Navantia, is now a naval shipbuilding benchmark.

In a similar manner, the Shipyard 4.0 implementation plan must be based on a progressive plan in all Shipyard 4.0 axes (end to end engineering, vertical and horizontal integration and personnel). The materialisation of the concept requires real projects which consolidate the associated technologies and reveal the potential of the digital transformation of Navantia shipyards. [4]. Navantia is currently implanting the following specific projects:

- Modelling and simulation of the production process;
- Digital management of the shipyard plant;
- Additive manufacturing of ship components;
- Shipyard worker vital signs monitoring;
- Automation of the habitation modules fabrication line;
- Automation of the pre-outfit panels line;
- Wireless connectivity on board to reduce cabling;
- Cloud computing of production management processes;
- Factory floor control through Manufacturing Execution System tools; and
- Ship predictive maintenance based on data mining and big data.

These projects complement the R&D activities under the development at the UMI (University and Navantia Research Unit) located in Ferrol and will be added to the initiatives taken by the Advanced Manufacturing Centre in Cadiz (currently under development). The future Advanced Manufacturing Centre will develop projects associated to the following technologies:

- Additive manufacturing;
- Mobile robotics for limited access areas;

- Hybrid laser welding;
- Unmanned vehicles for dimensional control and inspection;
- Production processes and shipyard logistics modelling and simulation;
- Systems rapid prototyping in agile testing environments; and
- Technology demonstrators for transference to the supply chain.

Navantia and Ferrol Implementation

Naturally, fully realising the potential of digital technologies will require changes to physical facilities. For this reason, Navantia has begun a series of shipyard facilities improvement studies. Particularly notable is the Ferrol modernisation project to meet Shipyard 4.0 requirements for the Spanish Navy's F110 future frigate.

As a result of these studies, Navantia has defined a preliminary configuration for the Ferrol shipyard. Key features in this configuration are:

- Building a new dry dock which will allow the complete building of the ships; and
- Construction of the specialty workshops (piping, HVAC, etc.) next to the dock to

Fig. 4. Ferrol shipyard physical modernisation project

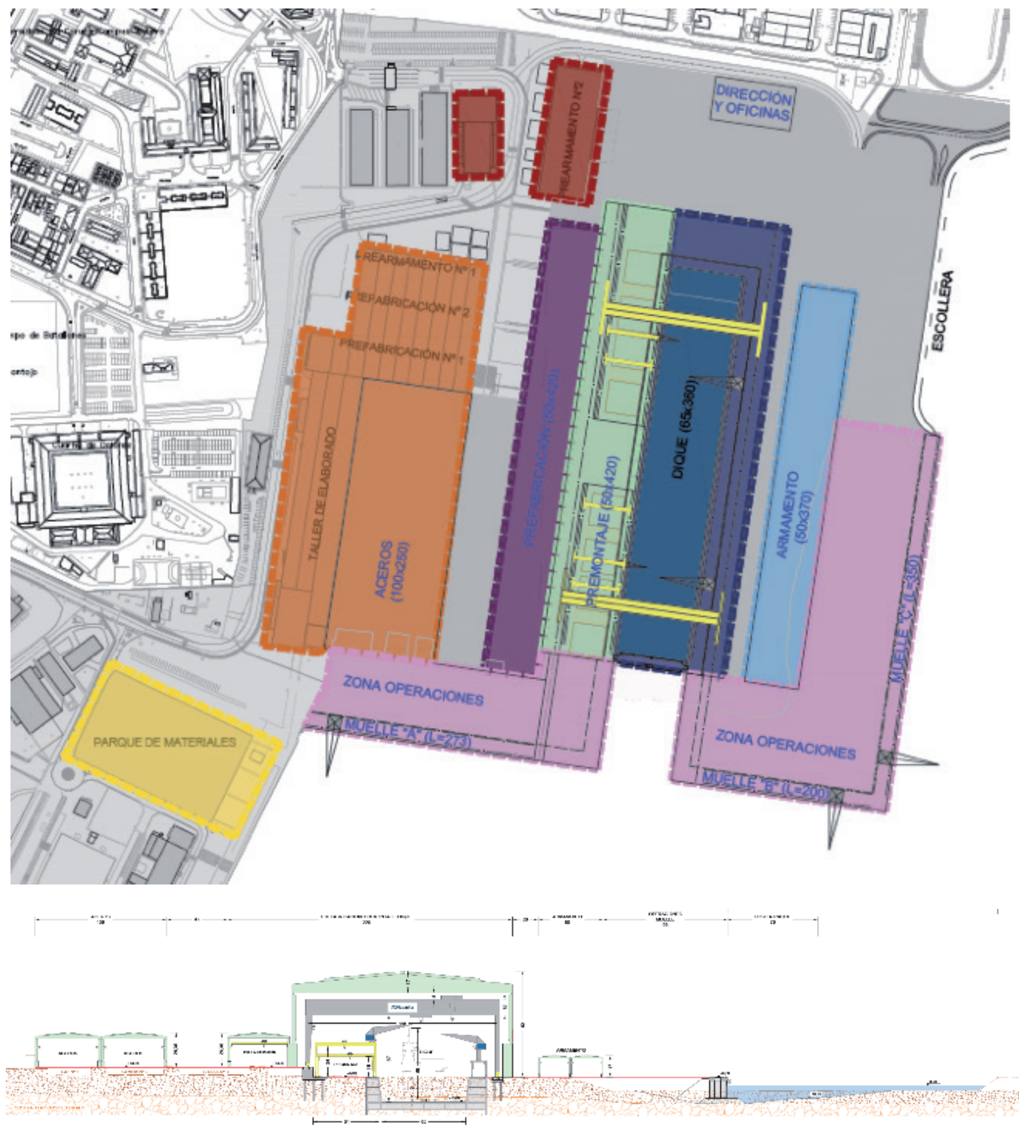

minimise distances and optimise the material flow.

The required surface to undertake the shipbuilding process will be reduced by 50%.

The new physical facilities will be enhanced with the most modern digital infrastructure, which will not only allow for monitoring of production within the shipyard facilities but also the vendors' production in their own plants. This will provide greater visibility to the shipyard, as well as greater transparency to the customer throughout the build process.

Navantia is working on the Information and Communication Technologies (ICT) architecture that will support this digital revolution.

Applicability to the Shipbuilding Industry in Colombia

Navantia's Shipyard 4.0 vision could be of great benefit to Colombia as well as Spain. As outlined in this document, this vision is currently being consolidated on specific programs (e.g. F110 in Spain – it could also be applied to Colombia future frigate program) but goes far beyond the ships themselves.

This initiative fits in the strategic view of the Government of Colombia as developed in the *Plan de Transformación Productiva*. The implementation of Shipyard 4.0 in Colombia would require an incremental approach in order to generate the benefits without unnecessarily increasing the inherent technological risks in naval shipbuilding. In this sense, a two batches approach to the shipbuilding program as planned by Colombia would allow significant benefits through a progressive implementation plan of Shipyard 4.0 ensuring that the shipyard, the supply chain, universities and technological centres remain tied to the program development inserting innovation all the way through the program.

In order for this vision to be realised in Colombia, the following will be required:

- A designer integrated with the shipbuilder to accommodate production and sustainment needs;
- A supply chain engaged in the innovation process by improving the connectivity of their products through each batch;
- A redesign of existing facilities to maximise the shipyard productivity levels, allowing them to reach or exceed international benchmarks;
- Defence Science and Technology Group (DSTG), universities and technological centres developing the key technologies that need to be inserted in the ships and in Shipyard 4.0; and
- ICT partners that will support the challenges of the vertical and horizontal integrations.

Fig. 5. Navantia´s vision of evolution from stand-alone Products to System of Systems

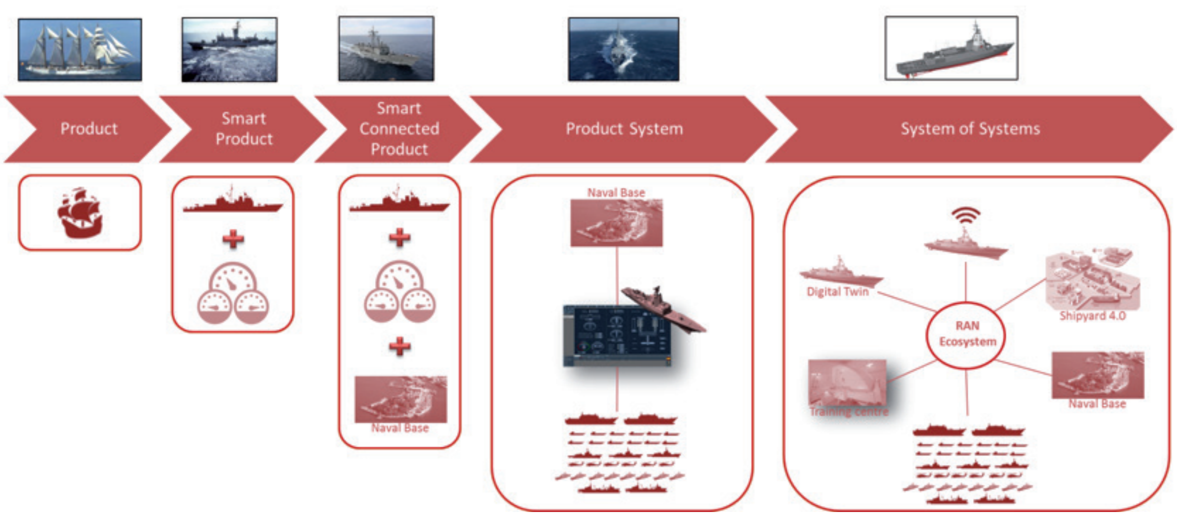

Conclusions

The following conclusions can be drawn:

1. Colombia is determined to develop the capacity of its shipbuilding industry. For that, strategic decisions regarding the development of the infrastructure, clustering of the industrial network, local supply chain engagement and cooperation with referenced shipbuilders through transfer of technology agreements are tools for the shipbuilding growth in the long term.
2. Spain commenced a shipbuilding enterprise reform plan in the 1980s, which has consolidated Navantia as a global leader in the shipbuilding industry. Navantia is ready and willing to assist Colombia now to implement its own plan.
3. In the pursuit of continuous improvement and innovation, Navantia has defined the Shipyard 4.0 Model that will enhance the company capabilities in the coming years. The model is holistic and is applicable to all relevant stakeholders. The Shipyard 4.0 implementation plan is collaborative and will be driven by specific innovative projects that will consolidate the Fourth Industrial Revolution in shipbuilding technologies.
4. Navantia is convinced that Shipyard 4.0 can be applied in the Colombian shipbuilding industry in its endeavour to develop an innovative and productive shipbuilding enterprise. This customisation process needs to be incremental to ensure that naval program outcomes are successfully delivered.

Acknowledgment

Thanks to my colleagues in Navantia, in Spain and Australia, who have contributed to this paper in all aspects.

The merits are really theirs.

References

[1] KLAUS SCHWAB, *"The Fourth Industrial Revolution"*, World Economic Forum, p.p. 11, 36.

[2] Office of the Industry-Science Research Alliance, "Recommendations for implementing the strategic initiative INDUSTRIE 4.0", ACATECH-National Academy of Science and Engineering.

[3] MICHAEL E. PORTER and JAMES E. HEPPELMANN, *"How Smart Connected Products Are Transforming Companies"*, Harvard Business Review, p.p. 6, 7.

[4] GEORGE WETERMAN, DIDAR BONET and ANDREW MCAFEE, *"Leading digital"*, Harvard Business Review Press, p.p. 109.

Editorial Guidelines for Authors

Thematic Interest

The *Ship Science and Technology* Journal accepts for publication original engineering contributions in English language on ship design, hydrodynamics, dynamics of ships, structures and materials, vibrations and noise, technology of ship construction, marine engineering, standards and regulations, ocean engineering and port infrastructure, as well as results of scientific and technological research. Every article shall be subject to consideration by the Editorial Council of The *Ship Science and Technology* Journal deciding on the pertinence of its publication.

Typology

The *Ship Science and Technology* Journal accepts to publish articles classified within the following typology (COLCIENCIAS 2006):

- *Scientific and technological research articles*. Documents presenting detailed original results of finished research projects. Generally, the structure used contains four important parts: introduction, methodology, results, and conclusions.
- *Reflection Articles*. Documents presenting results of finished research as of an analytical, interpretative, or critical perspective of the author on a specific theme, resorting to original sources.
- *Revision Articles*. Documents resulting from finished research in the field of science or technology in which published or unpublished results are analyzed, systemized, and integrated to present advances and development trends. These are characterized by presenting an attentive bibliographic revision of at least 50 references.

Format

All articles must be sent to the editor of The *Ship Science and Technology* Journal accompanied by a letter from the authors requesting their publication. Every article must be written in *Microsoft Word* in single space and sent in magnetic form.
Articles must not exceed 10,000 words (9 pages).
File must contain all text and any tabulation and mathematical equations.
All mathematical equations must be written in *Microsoft Word Equation Editor*. This file must contain graphs and figures; additionally, they must be sent in a modifiable format file (soft copy). Also, abbreviations and acronyms have to be defined the first time they appear in the text.

Content

All articles must contain the following elements that must appear in the same order as follows:

Title
It must be concise (no more than 25 words) with appropriate words so as to give readers an idea of the contents of the article. It must be sent in English and Spanish language.

Author and Affiliations
The author's name must be written as follows: last name, initial of first name . Affiliations of author must be specified in the following way and order:

- Business or institution (including department or division to which he/she belongs).
- Street mailing address.
- City (Province/State/Department).
- Country.

Abstract
A short essay of no more than one hundred fifty (150) words, specifying content of the work, scope, and results. It must be written in such a way so as to contain key ideas of the document. It must be sent in English and Spanish language.

Key Words
Identify words and/or phrases (at least three) that recover relevant ideas in an index. They must be sent in English and Spanish language.

Introduction
The text must be explanatory, clear, simple, precise, and original in presenting ideas. Likewise, it must be organized in a logical sequence of parts or sections, with clear subtitles to guide readers. The first part of the document is the introduction. Its objective is to present the theme, objectives, and justification of why it was selected. It must contain sources consulted and methodology used, as well as a short explanation of the status of the research, if it were the case, and form in which the rest of article is structured.

Body Article
It is made up of the theoretical framework supporting the study, statement of the theme, status of its analysis, results obtained, and conclusions.

Equations, Tables, Charts ang Graphs
All of these elements must be numbered in order of appearance according to their type and must have their corresponding legends, along with the source of the data.

Equations must be numbered on the right hand side of the column containing it, in the same line and in parenthesis. The body of the text must refer to it as "(Equation x)". When the reference starts a sentence it must be made as follows: "Equation x". Equations must be written so that capital letters can be clearly differentiated from lower case letters. Avoid confusions between the letter "l" and the number one or between zero and the lower case letter "o". All sub-indexes, super-indexes, Greek letters, and other symbols must be clearly indicated. All expressions and mathematical analyses must explain all symbols (and unit in which they are measured) that have not been previously defined in the nomenclature. If the work is extremely mathematical by nature, it would be advisable to develop equations and formulas in appendixes instead of including them in the body of the text.

Figure/Fig. (lineal drawings, tables, pictures, figures, etc.) must be numbered according to the order of appearance and should include the number of the graph in parenthesis and a brief description. As with equations, in the body of the text, reference as "(Fig. X)", and when reference to a graph is the beginning of a sentence it must be made as follows: "Fig. x".

Charts, graphs, and illustrations must be sent in modifiable vector file format (*Microsoft Excel, Microsoft Power Period*, and/or *Microsoft Vision*).

Pictures must be sent in TIF or JPG format files, separate from the main document in a resolution higher than 1000 dpi.

Foot Notes
We recommend their use as required to identify additional information. They must be numbered in order of appearance along the text.

Acknowledgment
Acknowledgments may be made to persons or institutions considered to have made important contributions and not mentioned in any other part of the article.

Bibliographic References

The bibliographic references must be included at the end of the article in alphabetical order and shall be identified along the document. To cite references, the Journal uses ISO 690 standards, which specify the mandatory elements to cite references (monographs, serials, chapters, articles, and patents), and ISO 690-2, related to the citation of electronic documents. We also use IEEE standard for the bibliographic references.

ISO 690

Quotations
They must be made in two ways: at the end of the text, in which case the last name of author followed by a comma and year of publication in the following manner:

"Methods exist today by which carbon fibers and prepregs can be recycled, and the resulting recyclate retains up to 90% of the fibers' mechanical properties" (*Davidson, 2006*).

The other way is:

Davidson (2006) manifests that "Methods exist today by which carbon fibers and prepregs can be recycled, and the resulting recyclate retains up to 90% of the fibers' mechanical properties".

List of References
Bibliographic references of original sources for cited material must be cited at the end of the article in alphabetical order and according to the following parameters:

In the event of more than one author, separate by commas and the last one by an "and". If there are more than three authors write the last name and initials of the first author and then the abbreviation "*et al.,*".

Books
Last name of author followed by a comma, initial(s) of name followed by a period, the year of publication of book in parenthesis followed by a comma, title of publication in italics and without quotation marks followed by a comma, city where published followed by a comma, and name of editorial without abbreviations such as Ltd., Inc. or the word "editorial".

Basic Form:
LAST NAME, N.I. *Title of book*. Subordinate responsibility (optional). Edition. Publication (place, publisher). Year. Extent. Series. Notes. Standard Number.

Example:
GOLDBERG, D.E. *Genetic Algorithms for Search, Optimization, and Machine Learning.* Edition 1. Reading, MA: Addison-Wesley. 412 p. 1989. ISBN 0201157675.

If a corporate author
Write complete name of entity and follow the other standards.

Basic form:
INSTITUTION NAME. *Title of publication*. Subordinate responsibility (optional). Edition. Publication (place, publisher). Year. Extent. Series. Notes. Standard Number.

Example:
AMERICAN SOCIETY FOR METALS. *Metals Handbook: Properties and Selection: Stainless Steels, Tool Materials and Special-Purpose Metals*. 9th edition. Asm Intl. December 1980. ISBN: 0871700093.

When book or any publication have as author an entity pertaining to the state, write name of country first.

Basic form:
COUNTRY, ENTITY PERTAINING TO THE STATE. *Title of publication*. Subordinate responsibility (optional). Edition. Publication (place, publisher). Year. Extent. Series. Notes. Standard Number.

Example:
UNITED STATED OF AMERICAN. EPA - U.S. Environmental Protection Agency. Profile of the Shipbuilding and Repair Industry. Washington D.C. 1997. P. 135.

Journal Article

Basic form:
Last name, N.I. Title of article, *Name of publication*. Edition. Year, issue designation, Pagination of the part.

Graduation Work

Basic form:
Primary responsibility. *Title of the invention*. Subordinate responsibility. Notes. Document identifier: Country or issuing office. *Kind of patent document*. Number. Date of publication of cited document.

Example:
CARL ZEISS JENA, VEB. *Anordnung zur lichtelektrischen Erfassung der Mitte eines Lichtfeldes. Et-finder*: W. FEIST, C. WAHNERT, E. FEISTAUER. Int. Cl.3 : GO2 B 27/14. Schweiz Patentschrift, 608 626. 1979-01-15.

Presentation at conferences or academic or scientific event

Basic form:
LAST NAME, N.I. Title of the presentation. In: Sponsor of the event. *Name of the event*. Country, City: Publisher, year. Pagination of the part.

Example:
VALENCIA, R., et al. Simulation of the thrust forces of a ROV En: COTECMAR. P*rimer Congreso Internacional de Diseño e Ingeniería Naval CIDIN 09*. Colombia, Cartagena: COTECMAR, 2009.

Internet

Basic form:
[1] LAST NAME, N.I. *Title of work*, [on-line]. Available at: http://www.direccion_completa.com, recovered: day of month of year.

Example:
[1] COLOMBIA. ARMADA NACIONAL. COTECMAR gana premio nacional científico, [web on-line]. Available at: http://www.armada.mil.co/?idcategoria=545965, recovered: 5 January of 2010.

IEEE

IEEE Publications uses Webster's College Dictionary, 4th Edition. For guidance on grammar and usage not included in this manual, please consult The Chicago Manual of Style, published by the University of Chicago Press.

Books

Basic form:
[1] J. K. Author, "Title of chapter in the book," in *Title of His Published Book*, *x*th ed. City of Publisher, Country if not USA: Abbrev. of Publisher, year, ch. *x*, sec. *x*, pp. *xxx–xxx*.

Example:
[1] B. Klaus and P. Horn, *Robot Vision*. Cambridge, MA: MIT Press, 1986.

Handbooks

Basic form:
[1] *Name of Manual/Handbook*, *x* ed., Abbrev. Name of Co., City of Co., Abbrev. State, year, pp. *xx-xx*.

Example:
[1] *Transmission Systems for Communications*, 3rd ed., Western Electric Co., Winston-Salem, NC, 1985, pp. 44–60.

Reports
The general form for citing technical reports is to place the name and location of the company or institution after the author and title and to give the report number and date at the end of the reference.

Basic form:
[1] J. K. Author, "Title of report," Abbrev. Name of Co., City of Co., Abbrev. State, Rep. *xxx*, year.

Example:
[1] E. E. Reber *et al*., "Oxygen absorption in the earth's atmosphere," Aerospace Corp., Los Angeles, CA, Tech. Rep. Angeles, CA, Tech. Rep. TR-0200 (4230-46)-3, Nov. 1988.

Conference Technical Articles
The general form for citing technical articles published in conference proceedings is to list the author/s and title of the paper, followed by the name (and location, if given) of the conference

publication in italics using these standard abbreviations. Write out all the remaining words, but omit most articles and prepositions like "of the" and "on." That is, *Proceedings of the 1996 Robotics and Automation Conference* becomes *Proc. 1996 Robotics and Automation Conf.*

Basic form:
[1] J. K. Author, "Title of paper," in *Unabbreviated Name of Conf.*, City of Conf., Abbrev. State (if given), year, pp. xxx-xxx.

For an electronic conference article when there are no page numbers:
[1] J. K. Author [two authors: J. K. Author and A. N. Writer] [three or more authors: J. K. Author et al.], "Title of Article," in [Title of Conf. Record as it appears on the copyright page], [copyright year] © [IEEE or applicable copyright holder of the Conference Record]. doi: [DOI number]

For an unpublished papr presented at a conference:
[1] J. K. Author, "Title of paper," presented at the Unabbrev. Name of Conf., City of Conf., Abbrev. State, year.

Online Sources

The basic guideline for citing online sources is to follow the standard citation for the source given previously and add the Digital Object Identifier (DOI) at the end of the citation, or add the DOI in place of page numbers if the source is not paginated. The DOI for each IEEE conference article is assigned when the article is processed for inclusion in the IEEE Xplore digital library and is included with the reference data of the article in Xplore. See The DOI System for more information about the benefits of DOI referencing.

The following sources are unique in that they are electronic only sources.

FTP

Basic form:
[1] J. K. Author. (year). Title (edition) [Type of medium]. Available FTP: Directory: File:

Example:
[1] R. J. Vidmar. (1994). *On the use of atmospheric plasmas as electromagnetic reflector*s [Online]. Available FTP: atmnext.usc.edu Directory: pub/etext/1994 File: atmosplasma.txt.

WWW

Basic form:
[1] J. K. Author. (year, month day). Title (edition) [Type of medium]. Available: http://www.(URL)

Example:
[1] J. Jones. (1991, May 10). Networks (2nd ed.) [Online]. Available: http://www.atm.com

E-Mail

Basic form:
[1] J. K. Author. (year, month day). Title (edition) [Type of medium]. Available e-mail: Message:

Example:
[1] S. H. Gold. (1995, Oct. 10). *Inter-Network Talk* [Online]. Available e-mail: COMSERVE@RPIECS Message: Get NETWORK TALK

E-Mail

Basic form:
[1] J. K. Author. (year, month day). Title (edition) [Type of medium]. Available Telnet: Directory: File:

Example:
[1] V. Meligna. (1993, June 11). *Periodic table of elements* [Online]. Available Telnet: Library.CMU.edu Directory: Libraries/Reference Works File: Periodic Table of Elements

Patents

Basic form:
[1] J. K. Author, "Title of patent," U.S. Patent x xxx xxx, Abbrev. Month, day, year.

Example:
[1] J. P. Wilkinson, "Nonlinear resonant circuit devices," U.S. Patent 3 624 125, July 16, 1990.

Standards

Basic form:
[1] Title of Standard, Standard number, date.

Example:
[1] IEEE Criteria for Class IE Electric Systems, IEEE Standard 308, 1969.

Theses (M.S.) and Dissertations (Ph.D.)

Basic form:
[1] J. K. Author, "Title of thesis," M.S. thesis, Abbrev. Dept., Abbrev. Univ., City of Univ., Abbrev. State, year.

Example:
[1] J. O. Williams, "Narrow-band analyzer," Ph.D. dissertation, Dept. Elect. Eng., Harvard Univ., Cambridge, MA, 1993.

Unpublished
These are the two most common types of unpublished references.

Basic form:
[1] J. K. Author, private communication, Abbrev. Month, year.
[2] J. K. Author, "Title of paper," unpublished.

Examples:
[1] A. Harrison, private communication, May 1995.
[2] B. Smith, "An approach to graphs of linear forms," unpublished.

Periodicals
NOTE: When referencing IEEE Transactions, the issue number should be deleted and month carried.

Basic form:
[1] J. K. Author, "Name of paper," *Abbrev. Title of Periodical*, vol. *x*, no. x, pp. *xxx-xxx*, Abbrev. Month, year.

Examples:
[1] R. E. Kalman, "New results in linear filtering and prediction theory," J. Basic Eng., ser. D, vol. 83, pp. 95-108, Mar. 1961.

References
NOTE: Use *et al*. when three or more names are given.

References in Text:
References need not be cited in the text. When they are, they appear on the line, in square brackets, inside the punctuation. Grammatically, they may be treated as if they were footnote numbers, e.g.,
as shown by Brown [4], [5]; as mentioned earlier [2], [4]–[7], [9]; Smith [4] and Brown and Jones [5]; Wood et al. [7]
or as nouns:
as demonstrated in [3]; according to [4] and [6]–[9].

References Within a Reference:
Check the reference list for ibid. or op. cit. These refer to a previous reference and should be eliminated from the reference section. In text, repeat the earlier reference number and renumber the reference section accordingly. If the ibid. gives a new page number, or other information, use the following forms:
[3, Th. 1]; [3, Lemma 2]; [3, pp. 5-10]; [3, eq. (2)]; [3, Fig. 1]; [3, Appendix I]; [3, Sec. 4.5]; [3, Ch. 2, pp. 5-10]; [3, Algorithm 5].

NOTE: Editing of references may entail careful renumbering of references, as well as the citations in text.

Acceptance

Articles must be sent by e-mail to the editor of The *Ship Science and Technology* Journal to otascon@cotecmar.com or in CD to the journal's street mailing address (COTECMAR Mamonal Km 9 Cartagena Colombia), accompanied by the "Declaration of Originality of Written Work "included in this journal.

The author shall receive acknowledgement of receipt by e-mail. All articles will be submitted to Peer Review. Comments and evaluations made by the journal shall be kept confidential. Receipt of articles by The Ship Science and Technology

Journal does not necessarily constitute acceptance for publishing. If an article is not accepted it shall be returned to the respective author. The Journal only publishes one article per author in the same number of the magazine.

Opinions and declarations stated by authors in articles are of their exclusive responsibility and not of the journal. Acceptance of articles grants The Ship Science and Technology Journal the right to print and reproduce these; nevertheless, any reasonable petition by an author to obtain permission to reproduce his/her contributions shall be considered.

Further information can be obtained by:
Sending an e-mail to sst.journal@cotecmar.com
Contacting Carlos Eduardo Gil De los Rios (Editor)
The Ship Science and Technology (Ciencia y Tecnología de Buques) office located at:
COTECMAR Bocagrande Carrera 2da Base Naval A.R.C. Bolívar
Cartagena de Indias – Colombia.
Phone Number: +57 (5) 653 5511

SHIP
SCIENCE & TECHNOLOGY
CIENCIA & TECNOLOGÍA DE BUQUES

Statement of Originality of Written Work

Title of work submitted

____

____

I hereby certify that the work submitted for publication in The Ship Science and Technology journal of Science and Technology for the Development of Naval, Maritime, and Riverine Industry Corporation, COTECMAR, was written by me, given that its content is the product of my direct intellectual contribution. All data and references to material already published are duly identified with their respective credits and are included in the bibliographic notes and quotations highlighted as such.

I, therefore, declare that all materials submitted for publication are completely free of copyrights; consequently, I accept responsibility for any lawsuit or claim related with Intellectual Property Rights thereof.

In the event that the article is chosen for publication by *The Ship Science and Technology journal*, I hereby state that I totally transfer publication and reproduction rights of such to Science and Technology Corporation for the Development of Naval, Maritime, and Riverine Industry - COTECMAR, which will be simultaneously subject to the **Creative Commons Attribution License (CC -BY)** that allows the license to copy, distribute, display and represent the work and to make derivative works as long as it recognizes and cites the work in the manner specified by the author or licensor.

In retribution for the present transfer I agree to receive two issues of the journal number where my article is published.

In witness thereof, I sign this statement on the ______ day of the month of _______________ of year ______________, in the city of _______________ .

Name and signature:

____

Identification document:

____

Level of Education:

____

Institutional Affiliation:

____

COTECMAR
COLOMBIA

Red Colombiana de Revistas de Ingeniería

Km. 9 Vía Mamonal - Cartagena, Colombia
www.shipjournal.co

Vol. 11 - n.° 22
January 2018

COTECMAR

www.shipjournal.co